

SIMULATION OF DEFECTS IN CRYSTALS
BY POINT FORCE ARRAYS

By

JEAN-PIERRE JACQUES GEORGES

A DISSERTATION PRESENTED TO THE GRADUATE COUNCIL OF
THE UNIVERSITY OF FLORIDA IN PARTIAL
FULFILLMENT OF THE REQUIREMENTS FOR THE DEGREE OF
DOCTOR OF PHILOSOPHY

UNIVERSITY OF FLORIDA

1972

ACKNOWLEDGMENTS

The author wishes to express his deep appreciation to Dr. C. S. Hartley, Associate Professor of Engineering Science, Mechanics and Aerospace Engineering, and chairman of the supervisory committee, for guidance and counsel during this research.

The author also wishes to express his appreciation to Dr. L. E. Malvern, Professor of Engineering Science, Mechanics and Aerospace Engineering, to Dr. M. A. Eisenberg, Associate Professor of Engineering Science, Mechanics and Aerospace Engineering, to Dr. J. J. Hren, Professor of Materials Science and Engineering, and to Dr. J. B. Conklin, Jr., Associate Professor of Physics, for serving on the supervisory committee. Special thanks are due to Dr. S. B. Trickey for his helpful assistance.

The author wishes to express his special gratitude to Dr. A. K. Head, Chief Scientific Officer at the Commonwealth Scientific Industrial Research Organization, Melbourne, Australia, for his very pertinent comments. Thanks are also due to Mrs. Edna Larrick for the typing of this manuscript.

This research has been sponsored by the National Science Foundation under the Grant GK 24360.

TABLE OF CONTENTS

	Page
ACKNOWLEDGMENTS	ii
LIST OF TABLES	v
LIST OF FIGURES	vi
KEY TO SYMBOLS	viii
ABSTRACT	xi
CHAPTER	
1 INTRODUCTION	1
2 BASIC CONCEPTS	4
Point Force	4
Double Force	7
Primitive Dislocation Loops	8
3 RECTANGULAR DISLOCATION LOOP IN SIMPLE CUBIC CRYSTAL	14
Displacement Field	14
Elastic Potential Energy	16
4 SCREW DISLOCATION IN SIMPLE CUBIC CRYSTAL	20
Displacement Field	20
Self-Energy of the Screw Dislocation	36
Single and Double Kinks in a Screw Dislocation	43
5 EDGE DISLOCATION IN SIMPLE CUBIC CRYSTAL CONSTRUCTED FROM AN ARRAY OF SHEAR LOOPS	64
Displacement Field	64
Self-Energy of the Edge Dislocation	82
Single and Double Kinks in an Edge Dislocation	91
6 EDGE DISLOCATION IN SIMPLE CUBIC CRYSTAL CONSTRUCTED FROM AN ARRAY OF PRISMATIC LOOPS	105
Displacement Field	105
Self-Energy of the Edge Dislocation	120

TABLE OF CONTENTS (CONTINUED)

CHAPTER	Page
7 CONCLUSIONS	124
BIBLIOGRAPHY	126
BIOGRAPHICAL SKETCH	128

LIST OF TABLES

Table		Page
1	Relative Displacement of Atoms Across the Slip Plane for a Screw Dislocation	26
2	Variation of Force Constant C_2 with the Atomic Positions in a Screw Dislocation	30
3	Atomic Displacements for a Single Kink in a Screw Dislocation	49
4	Atomic Displacements for a Double Kink of Length $2a$ in a Screw Dislocation	51
5	Atomic Displacements for a Double Kink of Length $4a$ in a Screw Dislocation	51
6	Atomic Displacements for a Double Kink of Length $6a$ in a Screw Dislocation	52
7	Relative Displacement Across the Slip plane for an Edge Dislocation	75
8	Relative Displacements and Force Constants C_2 at Singular Points for an Edge Dislocation	80
9	Atomic Displacements for a Single Kink in an Edge Dislocation	95
10	Atomic Displacements for a Double Kink of Length $2a$ in an Edge Dislocation	96
11	Atomic Displacements for a Double Kink of Length $4a$ in an Edge Dislocation	96
12	Atomic Displacements for a Double Kink of Length $6a$ in an Edge Dislocation	96
13	Displacements and Force Constants C_1 at Singular Points for an Edge Dislocation	116

LIST OF FIGURES

Figure		Page
1	Coordinate System to Evaluate the Core Region Around a Point Force	10
2	Prismatic Loop in Simple Cubic Crystal	10
3	Shear Loop in Simple Cubic Crystal	13
4	Shear Loop with Principal Axes	13
5	Rectangular Array of Shear Loops	15
6	Simulation of a Screw Dislocation	21
7	Relative Displacement Near the Core of a Screw Dislocation	27
8	Relative Displacement Between $-4a$ and $4a$ for a Screw Dislocation	28
9	Atomic Arrangement in Planes $x_3 = \pm \frac{a}{2}$ of a Screw Dislocation	32
10	Distribution Function of a Screw Dislocation	35
11	Region Where the Correction Energy Applies for a Screw Dislocation	37
12	Array of Forces for a Single Kink in a Screw Dislocation	44
13	Array of Forces for a Double Kink in a Screw Dislocation	44
14	Atomic Arrangement Around a Single Kink in a Screw Dislocation	48
15	Atomic Arrangement Around a Double Kink of Length $2a$ in a Screw Dislocation	53
16	Atomic Arrangement Around a Double Kink of Length $4a$ in a Screw Dislocation	54
17	Atomic Arrangement Around a Double Kink of Length $6a$ in a Screw Dislocation	55

LIST OF FIGURES (CONTINUED)

Figure		Page
18	Region of High Strain for a Double Kink in a Screw Dislocation	60
19	Atomic Relaxation for a Double Kink in a Screw Dislocation	60
20	Array of Forces Simulating an Edge Dislocation	65
21	Atomic Arrangement in $x_1 = 0$ Plane for an Edge Dislocation	73
22	Relative Displacement Close to the Core of an Edge Dislocation	76
23	Relative Displacement for an Edge Dislocation	77
24	Distribution Function for an Edge Dislocation	83
25	Region Where the Correction Energy is Computed for an Edge Dislocation	85
26	Array of Forces for Single Kink in an Edge Dislocation.	92
27	Array of Forces for Double Kink in an Edge Dislocation .	92
28	Atomic Arrangement for a Single Kink in an Edge Dislocation	98
29	Atomic Arrangement for a Double Kink of Length $2a$ in an Edge Dislocation	99
30	Atomic Arrangement for a Double Kink of Length $4a$ in an Edge Dislocation	100
31	Atomic Arrangement for a Double Kink of Length $6a$ in an Edge Dislocation	101
32	Array of Prismatic Loop in $x_2 = 0$ Plane	106
33	Array of Prismatic Loop in $x_1 = 0$ Plane	106
34	Relative Displacement of an Edge Dislocation	118
35	Atomic Arrangement in $x_2 = 0$ Plane of an Edge Dislocation	119

KEY TO SYMBOLS

A	Constant defined in Equation (72)
a	Lattice parameter
\vec{b}	Burgers vector
C_i	Force constant corresponding to a point force acting in the x_i direction
c_{ijkl}	Components of the elastic constant tensor
d	Constant defined in Equation (60)
$dV_{\vec{r}}$	Element of volume at the point \vec{r}
E_c	Correction energy
E_E	Energy of an edge dislocation
E_I	Energy defined in Equation (9)
E_S	Self-energy of a point force or energy of a screw dislocation
E_T	Total energy of dislocation loop
\vec{F}	General symbol for a point force
f	General symbol for any function
f_j	Component of a general force distribution
\vec{G}	General symbol for a point force
G_{ij}	Component of Green's tensor
g	General symbol for any function
\vec{h}	Vector separating points of application of the two point forces forming a double force

L	Dimension defined in Figure 5 or Figure 33
\vec{n}	Normal at \vec{r} of a surface
$P_{\ell k}$	Component of the dipole tensor
R	Dimension defined in Figure 5 or Figure 33
\vec{R}	Vector defined by $(\vec{r} - \vec{r}')$
\vec{r}	Point where the displacement field is computed
\vec{r}'	Point of application of a point force or a double force
r_0	Constant defined in Equation (6), Equation (93) or Equation (195)
r'_0	Constant defined in Equation (72)
r''_0	Constant defined in Equation (88)
\vec{u}	General displacement field
\vec{u}^j	J^{th} order when computing the displacement field \vec{u}
\vec{u}'	Perturbation of the displacement field due to the introduction of a general kink in the crystal
$\vec{u}'_{(\text{DK})}$	Perturbation of the displacement field due to the introduction of a double kink in the crystal
$\vec{u}'_{(\text{SK})}$	Perturbation of the displacement field due to the introduction of a single kink in the crystal
\vec{v}	Corrected displacement field between the planes of forces
W	Energy of the system of forces
W_F	Energy of the array of F forces in the simulation of an edge dislocation by primitive prismatic loops
W_{FG}	Interaction energy between the arrays of F and G forces in the simulation of an edge dislocation by primitive prismatic loops
W_G	Energy of the array of G forces in the simulation of an edge dislocation by primitive prismatic loops

W_{Int}	Energy defined in Equation (26)
W_{Row}	Energy defined in Equation (23)
w	Half-width for a screw or an edge dislocation
x_i	Component of the vector \vec{R}
x_i	Component of the vector \vec{r}
α_{21}	Distribution function for an edge dislocation
α_{22}	Distribution function for a screw dislocation
α_{ij}	K^{th} order term in the computation of the distribution function
	α_{ij}
Δu_2	Relative displacement across the slip plane
Δu_2^j	J^{th} order term in computation of the relative displacement Δu_2
δ_{ij}	Kornecker delta
$\delta(\vec{R})$	Dirac delta function
ϵ	Variable tending to zero
ϵ_i	Component defined on page 16
ξ	Peierls' symbol for the half-width of a dislocation
λ	Lamé's constant
μ	Shear modulus
ν	Poisson's ratio
σ_{ij}	Stress tensor component corresponding to the displacement field \vec{u}
τ_{ij}	Stress tensor component corresponding to the displacement field \vec{v}
θ	Angle defined in Figure 1

Abstract of Dissertation Presented to the
Graduate Council of the University of Florida in Partial
Fulfillment of the Requirements for the Degree of Doctor of Philosophy

SIMULATION OF DEFECTS IN CRYSTALS
BY POINT FORCE ARRAYS

By

Jean-Pierre Jacques Georges

December, 1972

Chairman: Dr. C. S. Hartley

Major Department: Engineering Science, Mechanics and Aerospace
Engineering

A new approach for analyzing dislocations and kinks in dislocations in simple cubic crystals is presented. The crystal is considered to be a continuum where defects are simulated by arrays of point forces acting on the centers of atoms in the immediate neighborhood of the defect. The magnitude of these forces is determined by the condition that they have the same displacement field as the corresponding defect in the ordinary continuum model. Infinitesimal prismatic and shear loops are constructed for simple cubic crystals and used to construct screw and edge dislocations. The arrangement of the atoms in the vicinity of the dislocation line is obtained and compared to Peierls' model. The self-energy of these dislocations is found to be of the correct form provided the force constants are correctly determined.

Atomic arrangements around kinks in screw and edge dislocations have been computed and are presented. The model developed promises to be of great value in studying atomic displacements in the vicinity of the dislocation.

CHAPTER 1

INTRODUCTION

A thorough comprehension of the nature of defects in crystalline materials and especially in metals is fundamental in order to explain many of the properties and the behavior of these solids. In particular, vacancies, interstitials and dislocations cannot be ignored when diffusion, mechanical behavior, electrical, optical and magnetic properties are studied.

The usual theory of lattice defects assumes a "local" continuum model. The matter concentrated in the atoms is supposed to be uniformly distributed over the whole space occupied by the crystal. The local atomic arrangement is ignored and the defect is replaced by a singular line, point or surface in a continuum body [1-3].

This model has proved to be extremely valuable for studying properties which are not sensitive to the atomic configuration in the vicinity of the defect, but it is limited by the discrete nature of the atomic array. Consequently, it is always necessary that expressions for the displacement field of the defect be terminated at some distance from it. Furthermore, since the continuum approximation ignores the local atomic arrangement around defects, it disregards the short range anisotropy of the displacement field.

To remedy these shortcomings, atomistic computations have been attempted. Atomic positions and interactions are considered explicitly

in the core region of the defect, with some laws defining the pairwise atomic potentials (see [4-13]). Further from the center of the defect, continuum theory is assumed to hold, so that the only atoms which need to be considered are those whose positions are necessary for calculations of energies for the core region. Such a method involves first the construction of a suitable interatomic potential, and, secondly, sums over a large number of lattice points which have to be carried out numerically. It is undoubtedly the best existing method of determining the local atomic arrangement around defects, but it is costly and very sensitive to the chosen size of the core region [14]. Furthermore, it involves convergence problems, and the manner in which boundary conditions are imposed is very delicate.

It is therefore worth exploring methods refining the ordinary continuum model by introducing the atomic arrangement of the crystal, but with a minimum increase in computational effort. In such a model, the atoms will be considered to be embedded in a continuum and the defect formed by the placement of suitable point forces at positions corresponding to atomic sites close to the defect [15]. The resulting displacement field is the sum of the displacement fields of all the point forces and is taken as the displacement field around the defect. Examples of such constructions by superposition of infinitesimal loops have been given by Koehler [16], Groves and Bacon [17] and Kroupa [18] for local continuum models.

In this present study, we shall concern ourselves in examining straight screw and edge dislocations in simple cubic crystals. First, a brief description of point forces and infinitesimal primitive loops

will permit us to analyze the displacement field and self-energy of dislocations. The screw dislocation will be constructed from an array of primitive shear loops, and the edge dislocation from an array of primitive shear loops and prismatic loops. Comparison will be made between both models in the case of the edge dislocation. Furthermore, calculations of atomic displacements around kinks will be attempted for both dislocations.

CHAPTER 2

BASIC CONCEPTS

Point Force

A point force \vec{F} is a highly localized body force distribution applied to a material point in a continuum.

$$F_j(\vec{r}') = f_j \int_V \delta(\vec{R}) dV_{\vec{r}} \quad (1)$$

where $\vec{R} = \vec{r} - \vec{r}'$ and $\delta(\vec{R})$ is the Dirac delta function. The displacement field at \vec{r} , $u_i(\vec{r})$, due to such a point force at \vec{r}' , can be obtained from the equilibrium equations of elasticity and Hooke's law [2] in the form

$$u_j(\vec{r}) = F_i(\vec{r}') G_{ij}(\vec{R}) \quad (2)$$

where for an infinite isotropic body

$$G_{ij}(\vec{R}) = \frac{1}{16\pi\mu} \left[\frac{3-4\nu}{1-\nu} \frac{\delta_{ij}}{|\vec{R}|} + \frac{1}{1-\nu} \frac{x_i x_j}{|\vec{R}|^3} \right] \quad (3)$$

$G_{ij}(\vec{R})$ is the Green's tensor response function for a point force. It is the component parallel to x_j of the displacement field at \vec{r}' due to a unit point force parallel to x_i at \vec{r} . It can be shown that the Green's tensor is symmetric.

As we see from the expression for $G_{ij}(\vec{R})$, this function is not defined for $\vec{R} = \vec{0}$ and we are unable to determine the displacement of

the point of application of the point force from Equation (2). To remove this mathematical divergence, we shall associate a finite displacement $u(\vec{r}')$ with the point of application of the point force. This value $u(\vec{r}')$ can be considered as being the average resultant displacement of points on a surface surrounding the point of application of the point force. This surface is determined such that $\vec{u}(\vec{r}')$ is the mean value of the vector displacements of two points symmetrical with respect to \vec{r}' . This vector is acting in the same direction as the point force.

$$\vec{u}(\vec{r}') = \frac{1}{2} \left[\vec{u}(\vec{r}' + \vec{r}) + \vec{u}(\vec{r}' - \vec{r}) \right]. \quad (4)$$

Using polar coordinates as shown in Figure 1, the absolute value of the displacement $u(\vec{r}')$ takes the following form.

$$|\vec{u}(\vec{r}')| = \frac{F}{16\pi\mu} \left[\frac{3-4\nu}{1-\nu} \frac{1}{r} + \frac{1}{1-\nu} \frac{\cos^2\theta}{r} \right]. \quad (5)$$

So, for a definite value of $|u(\vec{r}')|$ we can define a surface of revolution about the direction of \vec{F} , on which all the points have displacement components $|u(\vec{r}')|$ along \vec{F} . This surface surrounds a volume which can be considered as a core surrounding the point of application of the point force. The core can be interpreted as the volume where Equation (2) for the displacement field is no longer valid. The size of the core depends directly on the value of $|u(\vec{r}')|$ assigned.

It must be pointed out that the average value of the radius vector, $|\vec{r}|$, of the core is equal to the radius r_0 of the sphere on which the average displacement of its points is equal to $|u(\vec{r}')|$, that is

$$r_o = \frac{F}{24\pi\mu|\vec{u}(\vec{r}')|} \frac{5-6\nu}{1-\nu}. \quad (6)$$

On the other hand, $|\vec{u}(\vec{r}')|$ can be related to a force constant. By analogy with a discrete lattice model, such a point force applied on an atom causes an equal and opposite resisting force proportional to the displacement of the atom given by

$$|\vec{F}| = C|\vec{u}(\vec{r}')|. \quad (7)$$

C is known as a force constant, and is the force acting on an atom required to produce a unit displacement. In other terms, its inverse is the displacement of the atom caused by a unit force acting on it.

This force constant is the parameter we shall use in the following problems encountered. It will be determined for each special case by requiring that our mathematical model obeys certain physical imperatives. It will be straightforward to deduce $|\vec{u}(\vec{r}')|$ and the size of the core from the value of C.

The self-energy of a point force is defined as being the work done by this force against interatomic reaction forces when it is introduced into the continuum. So, using Equation (7)

$$E_S = \frac{1}{2} F|\vec{u}(\vec{r}')| = \frac{1}{2} \frac{F^2}{C}. \quad (8)$$

The interaction energy between two point forces $F_k^{(1)}(\vec{r}')$ and $F_m^{(2)}(\vec{r}')$ is

$$E_I = - F_k^{(1)}(\vec{r}) u_k^{(2)}(\vec{r}') = - F_k^{(1)}(\vec{r}) F_m^{(2)}(\vec{r}') G_{km}(\vec{r}-\vec{r}'), \quad (9)$$

where the sign is determined following Cottrell's convention for dislocation interaction energies, i.e., it is the work done by external forces when the second force is applied in the presence of the first, or vice versa. The total elastic potential energy of the system is the sum of the self-energies of the two point forces less the pairwise interaction between them.

Double Force

A double force is constructed from two equal and opposite point forces $\pm \vec{F}$ applied at points separated by a vector \vec{h} . If the forces are collinear, we have a double force without moment, otherwise with moment. The strength of a double force is defined as

$$P_{lk} = \lim_{\substack{|\vec{h}| \rightarrow 0 \\ |\vec{F}| \rightarrow \infty}} (h_l F_k). \quad (10)$$

The displacement field is obtained by superposition. If the separation distance between the forces is very small, we can expand the displacement field of each in a Taylor series about the midpoint of \vec{h} . Keeping only the first order terms, we are led to the displacement field mentioned by Kröner [2]

$$u_j(\vec{r}) = P_{lk}(\vec{r}') G_{kj,l}(\vec{r} - \vec{r}'). \quad (11)$$

As for a single point force, the displacement of the point of application is undefined, but this divergence can be removed in the same way as before by introducing the concept of a core surrounding a double force.

Primitive Dislocation Loops

Following Kröner's definition [2], an infinitesimal dislocation loop in a continuum is the boundary of a microscopic surface which separates regions in the continuum which have suffered a relative displacement \vec{b} . The Burgers vector of the loop is defined as the line integral of the elastic displacement \vec{u} around a circuit containing the dislocation. The displacement field, at a point \vec{r} , of such a loop of surface dS with normal vector \vec{n} and centered at \vec{r}' is found to be

$$u_m(\vec{r}) = b_i n_j c_{ijkl} G_{km,l} dS \quad (12)$$

where c_{ijkl} are the elastic constants.

The similarity between this expression and the displacement field of a double force (Equation (11)) leads us to consider the infinitesimal dislocation loop as a nucleus of strain with the fundamental double force tensor

$$P_{kl} = c_{ijkl} b_i n_j dS \quad (13)$$

or, for an isotropic continuum,

$$P_{kl} = \left[\mu (\delta_{ik} \delta_{jl} + \delta_{il} \delta_{jk}) + \lambda \delta_{ij} \delta_{kl} \right] b_i n_j dS \quad (14)$$

Up to this point, we have completely ignored the local atomic arrangement around the loop. In real crystals the interatomic reaction forces, developed when the atoms are displaced to form the defect, are the physical origin of the double force tensor characteristic of the dislocation loop. So it seems logical to construct such a loop by applying point forces in the continuum, but at points corresponding to atomic positions located immediately around the defect. The

displacement field of the loop is then the superposition of the displacement field of each point force. Each primitive loop has the character of a "unit cell" for the defect. These "unit cells" can be assembled to form a more complicated defect like dilatation centers or dislocations. So logically we can characterize the surface of the loop dS such that the produce $|b \cdot dS|$ equals one atomic volume in the crystal structure considered. This procedure will be analyzed more specifically for simple cubic crystals.

(a) Primitive prismatic loop in simple cubic crystals

The arrangement of the first neighbors of a vacancy loop in simple cubic crystal is shown in Figure 2. A primitive prismatic loop is constructed in the following steps. First a vacancy is created by removing an atom from the lattice. This vacancy is simulated by applying on its first neighbors forces of magnitude F directed towards the vacancy center. In the second step, two extra forces, $\pm G$, are applied in a direction normal to the $\{001\}$ plane, on the atoms in the $\langle 001 \rangle$ direction, towards the center vacancy in order to collapse the configuration onto the $\{001\}$ plane. In this manner, we have set up three double forces, all without moment, leading to the diagonal dipole tensor

$$P_{11} = P_{22} = 2Fa, \quad (15)$$

and

$$P_{33} = 2a(F + G),$$

where a is the lattice parameter of the simple cubic crystal.

Though each pair of forces is clearly separated by a distance $2a$, at distances from the loop large with respect to the interatomic

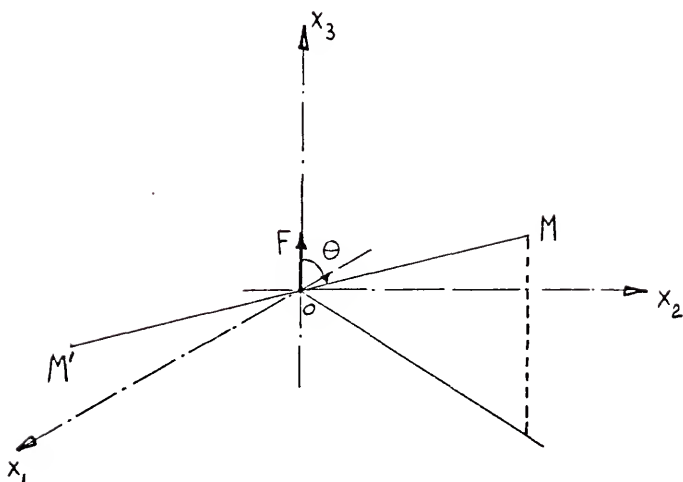


Figure 1. Coordinate System to Evaluate the Core Region Around a Point Force

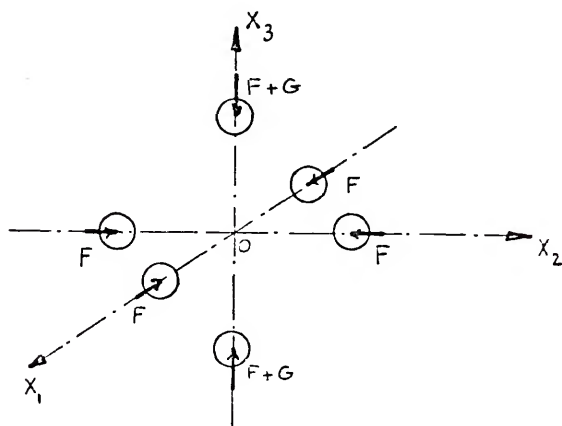


Figure 2. Prismatic Loop in Simple Cubic Crystal

distance they appear as three double forces which can be identified with a dislocation loop as described above. The Burgers vector of this loop must represent the collapse of the atoms in the $\langle 001 \rangle$ direction, whose relative displacement must be a in order to create a new regular arrangement of the atomic planes. As stated previously, the surface dS is chosen such that $|b \cdot dS|$ is equal to a^3 here. So, following Equation (14)

$$P_{11} = P_{22} = \lambda a^3$$

(16)

$$P_{33} = (\lambda + 2\mu) a^3,$$

and

The forces applied on the atoms can now be obtained by comparing Equations (15) and (16). The displacement field and the self-energy of the loop can easily be deduced.

(b) Shear loop in simple cubic crystal

A primitive shear loop in a simple cubic lattice (Figure 3) is constructed as follows. The forces F applied on the atoms impose the direction of the shear. Since the loop must be kept in equilibrium with respect to its center, additional forces G have to be applied, forming a couple whose moment about the center of the loop counterbalances that of the shear forces F . The Burgers vector of the loop is the smallest shift allowed by the atomic arrangement. By the same method as for the prismatic loop, it is found that the only nonvanishing components of the dipole tensor are

$$P_{12} = P_{21} = \mu a^3 = 2Fa = 2Ga, \quad (17)$$

so the magnitude of the forces has the value

$$F = G = \mu \frac{a^2}{2} . \quad (18)$$

The shear loop can be represented with respect to its principal axes \vec{x}'_1 and \vec{x}'_2 (Figure 4) leading to the dipole tensor

$$P'_{11} = 2aF = - P'_{22} , \quad (19)$$

which represents two double forces without moment, perpendicular to each other and acting in opposite senses.

(c) Conclusion

The primitive dislocation loops as described above are the basic elements for our process of simulating larger defects, especially dislocations. We shall see that a suitable array of shear loops can describe either an edge or a screw dislocation, but that an array of prismatic loops can only simulate an edge dislocation.

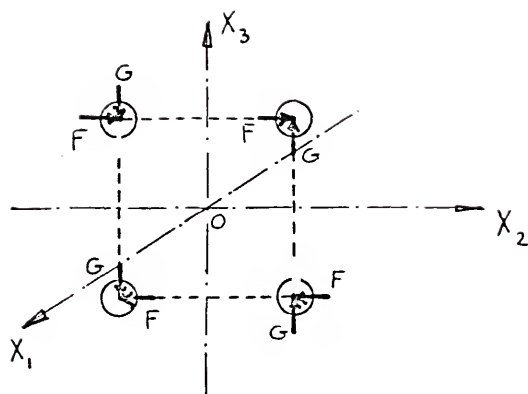


Figure 3. Shear Loop in Simple Cubic Crystal

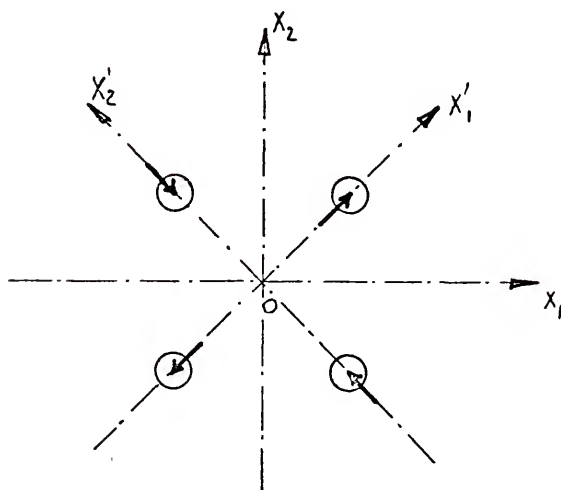


Figure 4. Shear Loop with Principal Axes

CHAPTER 3

RECTANGULAR DISLOCATION LOOP IN SIMPLE CUBIC CRYSTAL

A rectangular dislocation loop having a Burgers vector $a\langle 100 \rangle$ can be simulated by a rectangular array of primitive shear loops, stacked as shown in Figure 5. The dimensions of the array are considered to be very large compared to the atomic distance. The axes of reference are shown in Figure 5 with their origin at the center of the loop. In this chapter, we are only interested in obtaining properties of the rectangular dislocation loop related to our main interest, the displacement field and self-energy of the pure screw and edge dislocations.

Displacement Field

The displacement field at any points of this array is simply the sum of the displacement field of each point force

$$u_m(\vec{r}) = \sum_{i, \vec{r}'} F_i(\vec{r}') G_{im}(\vec{r} - \vec{r}'), \quad (20)$$

where $G_{im}(\vec{r})$ is defined in Equation (3). Developing this sum leads to the general expression

$$u_m(\vec{r}) = \mu \frac{a}{2} \sum_{p=-R/2}^{R/2} \left\{ \left(\sum_{q=-L/2}^{L/2} + \sum_{q=-(L/2-1)}^{L/2-1} \right) \left[G_{2m}(x_1 - pa, x_2 - qa, x_3 - \frac{a}{2}) - G_{2m}(x_1 - pa, x_2 - qa, x_3 + \frac{a}{2}) \right] \right\} -$$

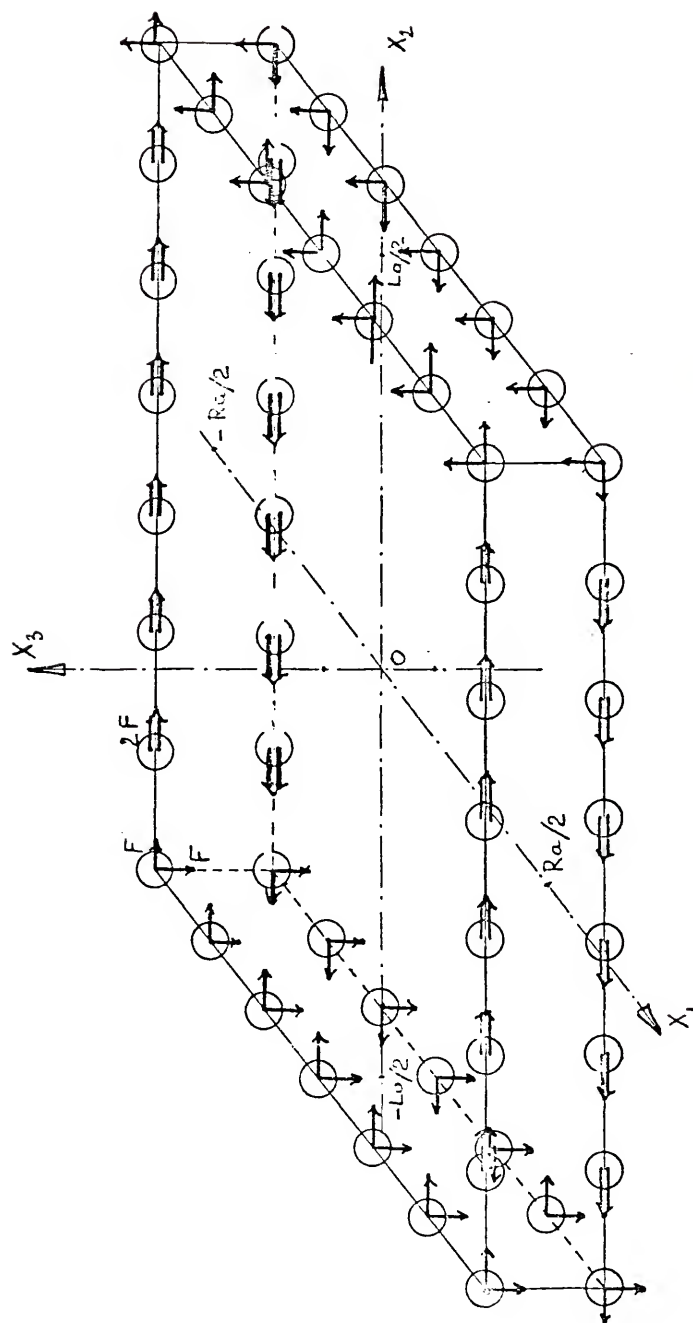


Figure 5. Rectangular Array of Shear Loops

$$\begin{aligned}
& - \left[G_{3m}(x_1 - pa, x_2 + \frac{La}{2}, x_3 - \frac{a}{2}) + G_{3m}(x_1 - pa, x_2 + \frac{La}{2}, x_3 + \frac{a}{2}) \right] \\
& + \left[G_{3m}(x_1 - pa, x_2 - \frac{La}{2}, x_3 - \frac{a}{2}) + G_{3m}(x_1 - pa, x_2 - \frac{La}{2}, x_3 + \frac{a}{2}) \right] \Bigg\}. \quad (21)
\end{aligned}$$

These equations for each component are valid everywhere in the continuum. They can be simplified for each particular region of the loop.

The regions of the continuum where a pure screw dislocation is simulated correspond to

$$\begin{cases} x_1 = -\frac{Ra}{2} + \epsilon_1 \\ x_2 = \epsilon_2 \end{cases} \quad \text{and} \quad \begin{cases} x_1 = \frac{Ra}{2} - \epsilon_1 \\ x_2 = \epsilon_2 \end{cases}$$

where ϵ_1 and ϵ_2 are small compared to Ra and La , respectively.

Similarly, regions where the loops have a pure edge character correspond to

$$\begin{cases} x_1 = \epsilon_1 \\ x_2 = -\frac{La}{2} \end{cases} \quad \text{and} \quad \begin{cases} x_1 = \epsilon_1 \\ x_2 = \frac{La}{2} - \epsilon_2 \end{cases}$$

where ϵ_1 and ϵ_2 are small compared to Ra and La , respectively.

Each particular case will be considered in the following chapters.

Elastic Potential Energy

The work done by the forces comprising the array, that is, the energy of the system, is the sum of the self-energy of each point force, minus the pairwise interaction energies, as defined by Equations (8) and (9). We call W_{Row} the energy of a row of forces, that is, two lines

of forces parallel to the x_2 axis for a given x_1 coordinate, and we call W_{Int} the interaction energy between two rows of forces, as defined above. Following these appellations, the total energy of the system has the form

$$W = (R+1)W_{Row} + \sum_{p=1}^R (R+1-p)W_{Int}. \quad (22)$$

W_{Row} and W_{Int} have the following expressions, respectively,

$$\begin{aligned} W_{Row} = & \frac{\mu^3 a^5}{2} \left[\frac{2L-1}{C_2} + \frac{1}{C_3} \right] + \frac{\mu^2 a^4}{2} \left[G_{33}(0,0,a) - (2L-1) G_{22}(0,0,a) \right] \\ & + \frac{\mu^2 a^4}{2} \left[G_{22}(0,La,0) - G_{22}(0,La,a) - G_{33}(0,La,0) - G_{33}(0,La,a) \right] \\ & + 2\mu^2 a^4 \sum_{q=1}^L (L-q) \left[G_{22}(0,qa,0) - G_{22}(0,qa,a) \right] \\ & - \mu^2 a^4 G_{23}(0,La,a) - 2\mu^2 a^4 \sum_{q=1}^L G_{23}(0,qa,a). \end{aligned} \quad (23)$$

$$\begin{aligned} W_{Int} = & \mu^2 a^4 (2L-1) \left[G_{22}(pa,0,0) - G_{22}(pa,0,a) \right] + \mu^2 a^4 \left[G_{33}(pa,0,0) + G_{33}(pa,0,a) \right] \\ & + \mu^2 a^4 \left[G_{22}(pa,La,0) - G_{22}(pa,La,a) - G_{33}(pa,La,0) - G_{33}(pa,La,a) \right] \\ & - 2\mu^2 a^4 G_{23}(pa,La,a) - 4\mu^2 a^4 \sum_{q=1}^L G_{23}(pa,qa,a) \\ & + 4\mu^2 a^4 \sum_{q=1}^L (L-q) \left[G_{22}(pa,qa,0) - G_{22}(pa,qa,a) \right]. \end{aligned} \quad (24)$$

Following Equation (22), W becomes

$$\begin{aligned} W = & \mu^2 a^4 (R+1)L \left\{ \frac{\mu a}{C_2} - G_{22}(0,0,a) + 2 \sum_{q=1}^L \left[G_{22}(0,qa,0) - G_{22}(0,qa,a) \right] \right. \\ & + 2 \sum_{p=1}^R \left[G_{22}(pa,0,0) - G_{22}(pa,0,a) \right] + 4 \sum_{p=1}^R \sum_{q=1}^L \left[G_{22}(pa,qa,0) \right. \\ & \left. \left. - G_{22}(pa,qa,a) \right] \right\} + \mu^2 a^4 (R+1) \left\{ \frac{\mu a}{2} \left(\frac{1}{C_3} - \frac{1}{C_2} \right) + \frac{1}{2} \left[G_{22}(0,0,a) + G_{33}(0,0,a) \right] \right. \\ & + \frac{1}{2} \left[G_{22}(0,La,0) - G_{22}(0,La,a) - G_{33}(0,La,0) - G_{33}(0,La,a) \right] \\ & \left. - 2 \sum_{q=1}^L q \left[G_{22}(0,qa,0) - G_{22}(0,qa,a) \right] \right\} \end{aligned}$$

$$\begin{aligned}
& - \sum_{p=1}^R \left[G_{22}(pa, 0, 0) - G_{22}(pa, 0, a) + G_{33}(pa, 0, 0) + G_{33}(pa, 0, a) \right] \\
& + \sum_{p=1}^R \left[G_{22}(pa, La, 0) - G_{22}(pa, La, a) - G_{33}(pa, La, 0) - G_{33}(pa, La, a) \right] \\
& - 4 \sum_{p=1}^R \sum_{q=1}^L q \left[G_{22}(pa, qa, 0) - G_{22}(pa, qa, a) \right] - G_{23}(0, La, a) \Big\} \\
& - 2 \sum_{q=1}^L G_{23}(0, qa, a) - 2 \sum_{p=1}^{R+1} G_{23}(pa, La, a) - 4 \sum_{p=1}^{R+1} \sum_{q=1}^L G_{23}(pa, qa, a) \\
& + \mu^2 a^4 L \left\{ - 2 \sum_{p=1}^R p \left[G_{22}(pa, 0, 0) - G_{22}(pa, 0, a) \right] \right. \\
& \left. - 4 \sum_{p=1}^R \sum_{q=1}^L p \left[G_{22}(pa, qa, 0) - G_{22}(pa, qa, a) \right] \right\} \\
& + \mu^2 a^4 \left\{ \sum_{p=1}^R p \left[G_{22}(pa, 0, 0) - G_{22}(pa, 0, a) - G_{33}(pa, 0, 0) - G_{33}(pa, 0, a) \right] \right. \\
& - \sum_{p=1}^R p \left[G_{22}(pa, La, 0) - G_{22}(pa, La, a) - G_{33}(pa, La, 0) - G_{33}(pa, La, a) \right] \\
& + 4 \sum_{p=1}^R \sum_{q=1}^L pq \left[G_{22}(pa, qa, 0) - G_{22}(pa, qa, a) \right] \\
& \left. + 2 \sum_{p=1}^{R+1} p G_{23}(pa, La, a) + 4 \sum_{q=1}^L \sum_{p=1}^{R+1} p G_{23}(pa, qa, a) \right\}. \quad (25)
\end{aligned}$$

The only mathematical difficulty in the computation of such a formidable expression lies in computing the single and double sums. The first terms are computed, up to a chosen integer N (usually $N=20$), and the rest of the terms are approximated by an integral. The following approximation follows:

$$\sum_{q=1}^L f(q) \approx f(q) + \frac{1}{2} f(N) + \frac{1}{2} f(L) + \int_N^L f(x) dx, \quad (26)$$

and for a double sum:

$$\begin{aligned}
\sum_{p=1}^R \sum_{q=1}^L f(p, q) & \approx \sum_{p=1}^{N-1} \sum_{q=1}^{N-1} f(p, q) + \frac{1}{2} \sum_{p=1}^{N-1} \left[f(p, N) + f(p, L) \right] \\
& + \frac{1}{2} \sum_{q=1}^{N-1} \left[f(N, q) + f(R, q) \right] + \sum_{p=1}^{N-1} \int_N^L f(p, y) dy
\end{aligned}$$

$$\begin{aligned}
& + \sum_{q=1}^{N-1} \int_N^R f(x, q) dx + \frac{1}{2} \int_N^L f(N, y) dy + \frac{1}{2} \int_N^R f(x, N) dx \\
& + \frac{1}{2} \int_N^L f(R, y) dy + \frac{1}{2} \int_N^R f(x, L) dx + \frac{1}{4} [f(N, L) + f(R, N) \\
& + f(N, N) + f(R, L)] + \int_N^L \int_N^R f(x, y) dx dy. \quad (27)
\end{aligned}$$

These approximations give the correct form of the divergence in R and L for divergent sums, and give an accuracy of 1 part in 10^4 when the sum converges, which is sufficient for the model employed.

The final expression for $W/\mu a^3$ becomes

$$\begin{aligned}
\frac{W}{\mu a^3} = & \frac{(R+1)L}{4\pi} \left[4\pi \frac{\mu a}{C_2} + \frac{2.8545 - 2.3676\nu}{1 - \nu} \right] - \frac{R+1}{2\pi(1-\nu)} \ln \frac{2RL}{R + \sqrt{R^2 + L^2}} \\
& - \frac{L}{2\pi} \ln \frac{1}{L + \sqrt{R^2 + L^2}} + \frac{R+1}{4\pi} \left[2\pi \mu a \left(\frac{1}{C_3} - \frac{1}{C_2} \right) + \frac{1.2979 - .6458\nu}{1 - \nu} \right] \\
& + \frac{L}{4\pi} \left[\frac{1.6420 + .3580\nu}{1 - \nu} \right] - \frac{2(2-\nu)}{1 - \nu} \frac{\sqrt{R^2 + L^2}}{4\pi} + \left[2\pi \mu \left(\frac{1}{C_3} - \frac{1}{C_2} \right) - \frac{3.3903 - .6872\nu}{4\pi(1-\nu)} \right]. \quad (28)
\end{aligned}$$

W is not the energy of the physical dislocation loop. It contains an extra strain energy in the region bounded by the plane on which forces are applied and the boundaries of the array, which does not account for the relaxation of the atoms. In the way the forces have been applied, a relative displacement greater than $a/2$ has been created across most of the slip plane for the atoms reaching their final configuration. It is from this final configuration that the relative displacement procedure must be measured in order to calculate the actual strain energy stored between the planes of forces. Such a correction energy will be computed in each case, for the pure screw and pure edge dislocation.

We shall not examine all the properties of the dislocation loop here, since our purpose is to treat this loop as an intermediate step in simulating screw and edge dislocations.

CHAPTER 4

SCREW DISLOCATION IN SIMPLE CUBIC CRYSTAL

From the results found in the previous chapter, the displacement field, the relative displacement across the slip plane, and the self-energy of the screw dislocation in simple cubic crystal will be obtained.

Displacement Field

As seen previously, the regions of the dislocation loop having the characteristics of a pure screw dislocation correspond to

$$\left\{ \begin{array}{l} x_1 = -\frac{Ra}{2} + \epsilon_1 \\ x_2 = \epsilon_2 \end{array} \right. \quad \text{and} \quad \left\{ \begin{array}{l} x_1 = \frac{Ra}{2} - \epsilon_1 \\ x_2 = \epsilon_2 \end{array} \right.$$

where ϵ_1 and ϵ_2 are small compared to Ra and La , respectively.

Since both regions represent two identical dislocations, but of opposite signs, we shall only consider the first one, and translate the x_2 axis by an amount of $-Ra/2$ so that it becomes the boundary of the array. We shall keep the same symbols x_1 and x_2 for the new variables. (See Figure 6.)

The only change in the expression for the displacement field as written in Equation (21) is that p is now summed from zero to R . Since an analytical expression is desired for u_m , an approximation different

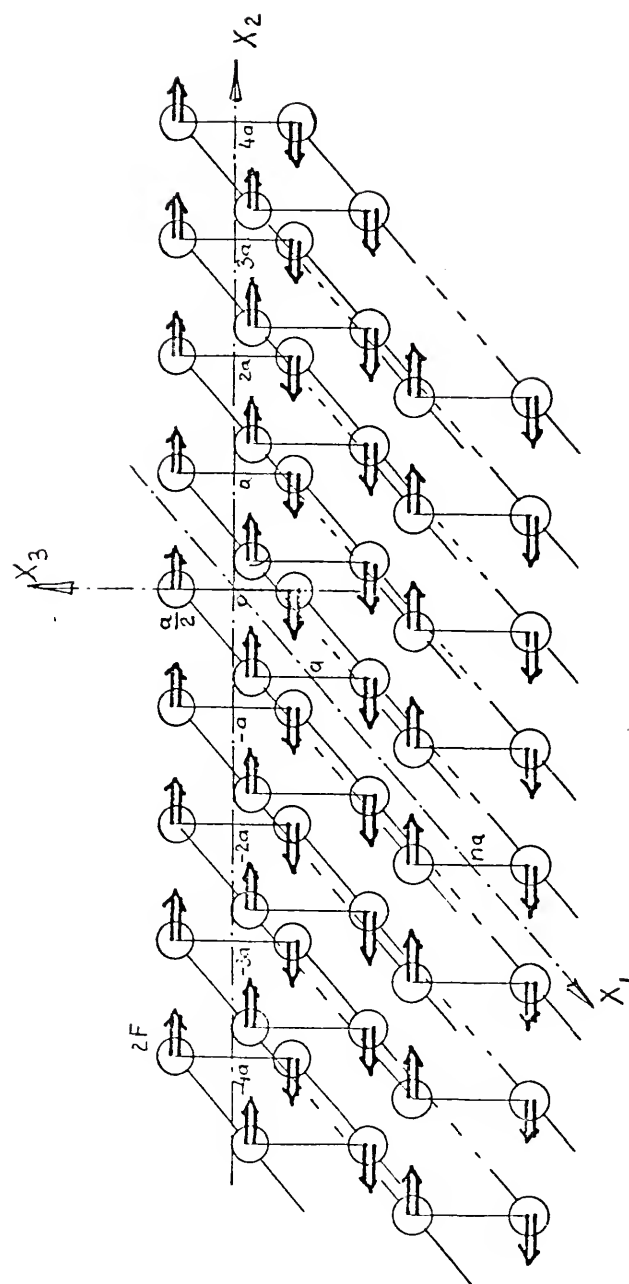


Figure 6. Simulation of a Screw Dislocation

from that given by Equation (26) will be employed to compute the discrete sums. Euler's formula [19] is most suitable for this case:

$$\begin{aligned} \sum_a^b f(p) = & \int_a^b f(x) dx + \frac{1}{2} [f(a) + f(b)] + \frac{1}{12} [f'(b) - f'(a)] \\ & - \frac{1}{720} [f'''(b) - f'''(a)] + \frac{1}{30,240} [f^{(5)}(b) - f^{(5)}(a)] \\ & + \dots \end{aligned} \quad (29)$$

The accuracy of the approximation depends on the number of terms used. The advantage of this method is that at most of the points where the displacement field is computed, the three first terms are sufficient for the accuracy required, i.e., a relative error of 10^{-3} is accepted.

The first summations which have to be computed are the two summations on q . These sums can be computed exactly because we always consider x_2 small with respect to L_a , or in other words, our range of interest is far from both ends of the dislocation line. So we shall have

$$\sum_{q=-L/2}^{L/2} f(q) = \sum_{q=-(L/2+1)}^{L/2-1} f(q) = \int_{-\infty}^{+\infty} f(x) dx \quad (30)$$

where f represents the whole expression to be summed. The following components of the displacement field have been found:

$$\begin{cases} u_1(x_1, x_2, x_3) = 0 \\ u_2(x_1, x_2, x_3) = \frac{a}{4\pi} \sum_{p=0}^R \varrho_p \frac{(x_1 - pa)^2 + (x_3 + \frac{a}{2})^2}{(x_1 - pa)^2 + (x_3 - \frac{a}{2})^2} \\ u_3(x_1, x_2, x_3) = 0 \end{cases} \quad (31)$$

We can already notice that some of the characteristics of the displacement field around a screw dislocation are displayed, that is, the components u_1 and u_3 are equal to zero, and u_2 is independent of x_2 .

Euler's formula can be applied a second time to obtain a final expression for u_2 , the accuracy depending on the number of terms retained. We shall label the different terms composing u_2 in the following way,

$$u_2^0(x_1, x_2, x_3) = \frac{a}{4\pi} \int_0^R g(x_1 - pa) \, dp \quad (32)$$

$$u_2^1(x_1, x_2, x_3) = \frac{a}{8\pi} \left[g(x_1) + g(x_1 - Ra) \right] \quad (33)$$

$$u_2^2(x_1, x_2, x_3) = \frac{a}{48\pi} \left[g'(x_1 - Ra) - g'(x_1) \right] \quad (34)$$

$$u_2^3(x_1, x_2, x_3) = -\frac{a}{2880\pi} \left[g^{(3)}(x_1 - Ra) - g^{(3)}(x_1) \right], \quad (35)$$

etc., where

$$g(x_1 - pa) = \ln \frac{(x_1 - pa)^2 + (x_3 + \frac{a}{2})^2}{(x_1 - pa)^2 + (x_3 - \frac{a}{2})^2}. \quad (36)$$

The computation of u_2^0 raises a mathematical problem, since we are integrating over a region where the integrand contains singular points for certain values of x_1 and x_3 ($x_1 = na$, $x_3 = \pm a/2$). For these points, the integral can be broken into two parts:

$$\int_0^{Ra} g(na - pa) \, dp = \lim_{\epsilon \rightarrow 0} \left[\int_0^{na-\epsilon} g(na - pa) \, dp + \int_{na+\epsilon}^{Ra} g(na - pa) \, dp \right]. \quad (37)$$

For this specific case

$$g(na - pa) = \ln \frac{(na - pa)^2 + a^2}{(na - pa)^2}. \quad (38)$$

Since

$$\int \ln (na-pa)^2 dp = -2 \left[(n-p) \ln (na-pa) - (n-p) \right], \quad (39)$$

the integral is equal to zero for $p=n$, and so

$$\int_0^{Ra} g(na-pa) dp = G(na-Ra) - G(na). \quad (40)$$

The integration makes all the singular points vanish, except for those at $x_1 = 0$ and $x_3 = \pm a/2$. So the final analytic expressions for u_2^i become

$$\begin{aligned} u_2^0(x_1, x_3) = & \frac{a}{4\pi} \left\{ \left[2\pi \frac{x_3}{a} \right] + \tan^{-1} \frac{x_1}{x_3 + \frac{a}{2}} + \tan^{-1} \frac{x_1}{x_3 - \frac{a}{2}} \right\} \\ & + 2x_3 \left\{ \tan^{-1} \frac{x_1}{x_3 + \frac{a}{2}} - \tan^{-1} \frac{x_1}{x_3 - \frac{a}{2}} \right\} + x_1 \ln \frac{x_1^2 + (x_3 + \frac{a}{2})^2}{x_1^2 + (x_3 - \frac{a}{2})^2} \Bigg\}, \end{aligned} \quad (41)$$

$$u_2^1(x_1, x_3) = \frac{a}{8\pi} \ln \frac{x_1^2 + (x_3 + \frac{a}{2})^2}{x_1^2 + (x_3 - \frac{a}{2})^2}, \quad (42)$$

$$u_2^2(x_1, x_3) = -\frac{a^2}{24\pi} \left[\frac{x_1}{x_1^2 + (x_3 - \frac{a}{2})^2} - \frac{x_1}{x_1^2 + (x_3 + \frac{a}{2})^2} \right], \quad (43)$$

and

$$u_2^3(x_1, x_3) = -\frac{a^4}{730\pi} \left\{ \frac{x_1 \left[3(x_3 - \frac{a}{2})^2 - x_1^2 \right]}{\left[x_1^2 + (x_3 - \frac{a}{2})^2 \right]^3} - \frac{x_1 \left[3(x_3 + \frac{a}{2})^2 - x_1^2 \right]}{\left[x_1^2 + (x_3 + \frac{a}{2})^2 \right]^3} \right\}. \quad (44)$$

Then, since $u_2(x_1, x_3)$ is the sum of $u_2^i(x_1, x_3)$ for every i ,

$$\begin{aligned} u_2(x_1, x_3) = & u_2^0(x_1, x_3) + u_2^1(x_1, x_3) + u_2^2(x_1, x_3) \\ & + u_2^3(x_1, x_3) + \dots \end{aligned} \quad (45)$$

Equation (41) takes three different forms, following the region where x_3 is computed: π corresponds to $x_3 > a/2$, $2\pi(x_3/a)$ to $-a/2 < x_3 < a/2$, $-\pi$ to $x_3 < -a/2$.

An asymptotic expression for u_2 can be obtained when x_2 and x_3 are considered large with respect to the atomic distance, but still far from the ends of the dislocation line.

$$u_2(x_1, x_3) = \frac{a}{2\pi} \left[\pm \frac{\pi}{2} + \tan^{-1} \frac{x_1}{x_3} \right]. \quad (46)$$

This is the well-known expression obtained from the Volterra solution for a screw dislocation [20].

The relative displacement across the slip plane is defined as

$$\Delta u_2(x_1) = u_2(x_1, \frac{a}{2}) - u_2(x_1, -\frac{a}{2}) = 2u_2(x_1, \frac{a}{2}). \quad (47)$$

It can be directly deduced from Equation (31) or Equation (42) to (45):

$$\Delta u_2(x_1) = \frac{a}{2\pi} \sum_{p=0}^{\infty} \ell\pi \frac{(x_1 - pa)^2 + a^2}{(x_1 - pa)^2}, \quad (48)$$

or

$$\Delta u_2(x_1) = \Delta u_2^0(x_1) + \Delta u_2^1(x_1) + \Delta u_2^2(x_1) + \Delta u_2^3(x_1) + \dots, \quad (49)$$

with

$$\Delta u_2^0(x_1) = \frac{a}{2\pi} \left[2 \tan^{-1} \frac{x_1}{a} + \pi + \frac{x_1}{a} \ell\pi \frac{x_1^2 + a^2}{x_1^2} \right], \quad (50)$$

$$\Delta u_2^1(x_1) = \frac{a}{4\pi} \ell\pi \frac{x_1^2 + a^2}{x_1^2}, \quad (51)$$

$$\Delta u_2^2(x_1) = \frac{a^2}{12\pi} \left[\frac{x_1^2}{x_1^2 + a^2} - \frac{1}{x_1} \right] \quad (52)$$

and

$$\Delta u_2^3(x_1) = \frac{a^4}{360\pi} \left[\frac{1}{x_1^3} - \frac{x_1(x_1^2 - 3a^2)}{(x_1^2 + a^2)^3} \right]. \quad (53)$$

The more and more precise expressions for $\Delta u_2(x_1)$ are plotted in Figures 7 and 8, and listed partially in Table 1. A remarkable precision is obtained for the regions where $|x_1| \geq a$ after evaluating only a few terms. On another hand, the only term which is not singular at $x_1 = 0$ is $\Delta u_2^0(x_1)$. It seems to deviate significantly from the correct curve for $\Delta u_2(x_1)$. However, the order of magnitude of the real relative displacement at x_1 can be obtained approximately by interpolation. So the relative displacement of atoms above and below the slip plane is known everywhere except at $x_1 = 0$.

TABLE 1. Relative Displacement of Atoms Across the Slip Plane for a Screw Dislocation

x_1/a	$\Delta u_2^0/a$	$\dots + \Delta u_1^1/a$	$\dots + \Delta u_2^2/a$	$\dots + \Delta u_2^3/a$
- ∞	.0000	.0000	.0000	.0000
- 5.0	.0316	.0347	.0349	.0349
- 4.0	.0394	.0442	.0446	.0446
- 3.0	.0521	.0605	.0614	.0613
- 2.0	.0766	.0943	.0970	.0968
- 1.0	.1397	.1948	.2081	.2074
- .5	.2243	.3524	.3949	.3890
+ .5	.7757	.9037	.8613	.8696
+ 1.0	.8603	.9155	.9022	.9033
+ 2.0	.9234	.9412	.9385	.9387
+ 3.0	.9479	.9563	.9554	.9554
+ 4.0	.9606	.9654	.9651	.9651
+ 5.0	.9684	.9715	.9713	.9713
+ ∞	1.0000	1.0000	1.0000	1.0000

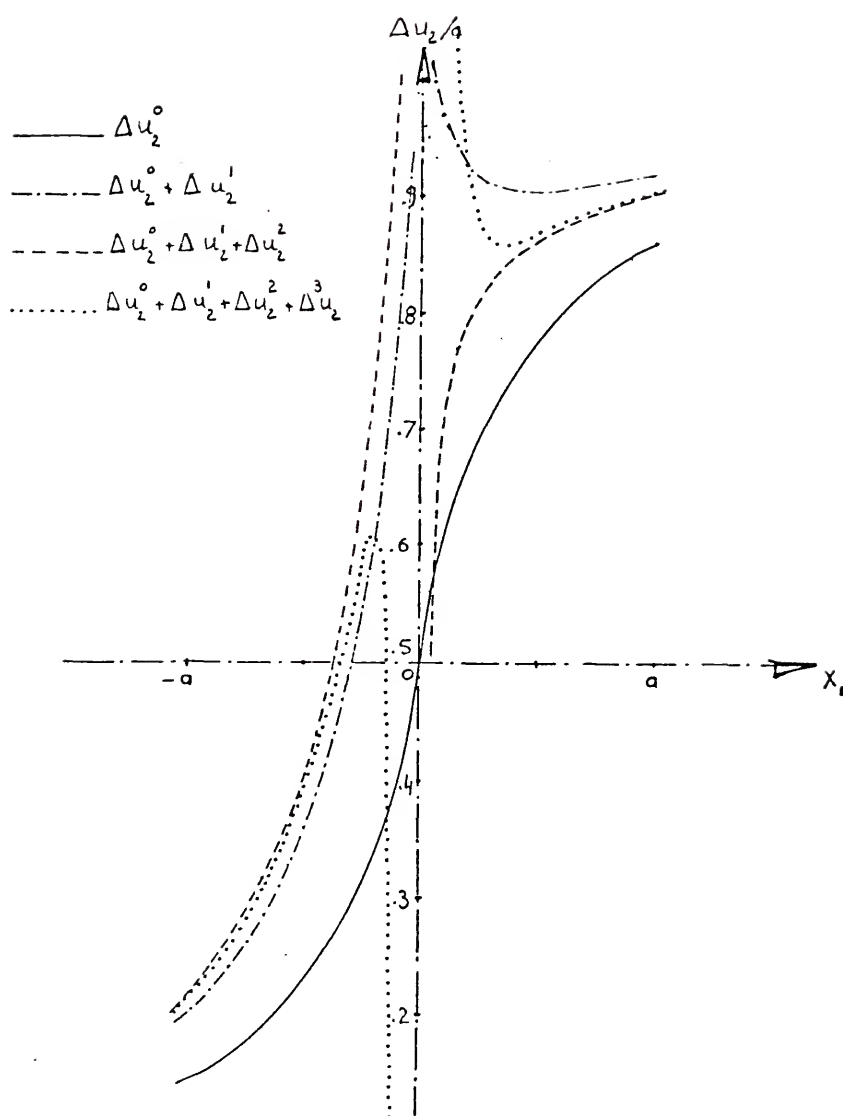


Figure 7. Relative Displacement Near the Core of a Screw Dislocation

- Δu_z^0
- - - $\Delta u_z^0 + \Delta u_z^1$
- - - $\Delta u_z^0 + \Delta u_z^1 + \Delta u_z^2$
- $\Delta u_z^0 + \Delta u_z^1 + \Delta u_z^2 + \Delta u_z^3$

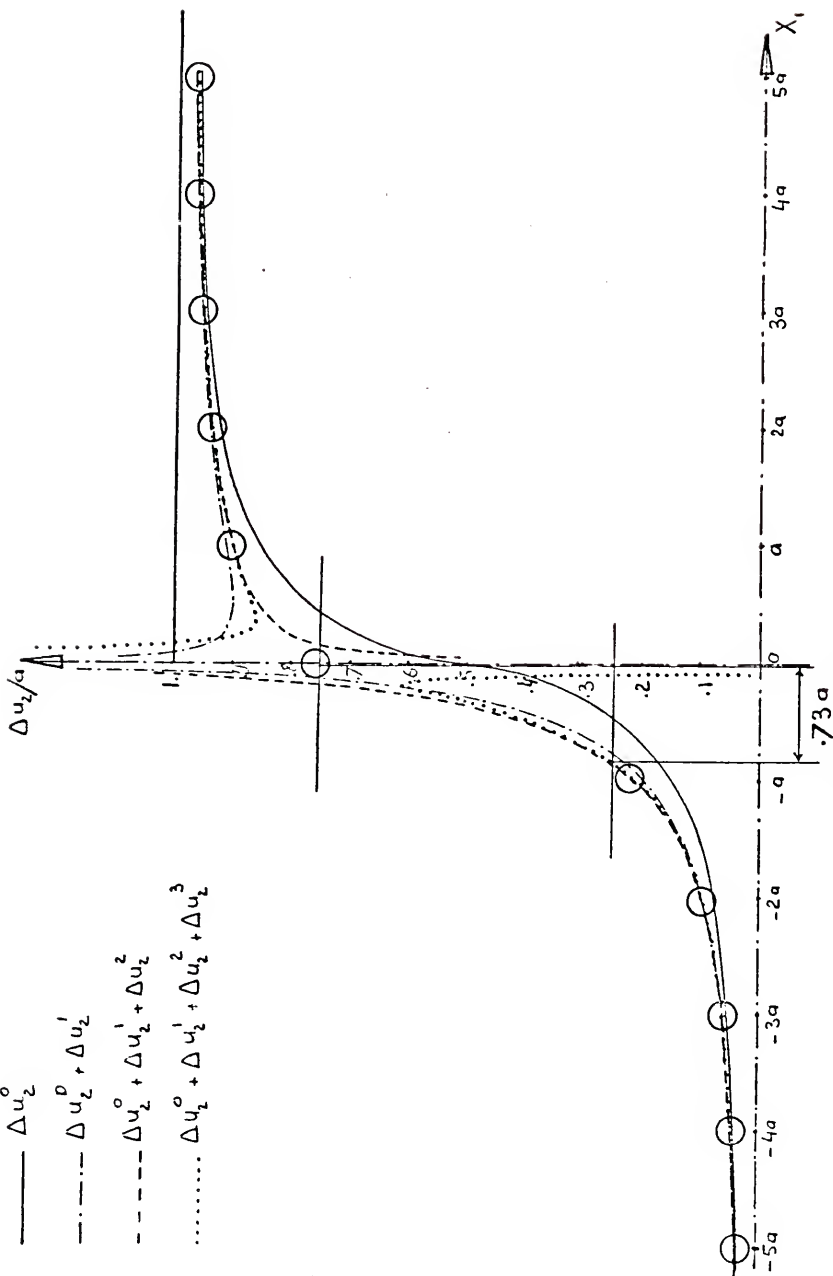


Figure 8. Relative Displacement Between $-4a$ and $4a$ for a Screw Dislocation

Another way of computing the relative displacement at atomic points is to go back to the definition of the displacement field by Green's functions.

$$\Delta u_2(na) = 2\mu a^2 \sum_{p=0}^{\infty} \sum_{q=-\infty}^{+\infty} \left[G_{22}(na-pa, qa, 0) - G_{22}(na-pa, qa, a) \right] \quad (54)$$

changing variables by setting $u = n - p$ changes Equation (54) into

$$\begin{aligned} \Delta u_2(na) = & 2\mu a^2 \left(\sum_{u=1}^n + \sum_{u=1}^{\infty} \right) \sum_{q=-\infty}^{+\infty} \left[G_{22}(ua, qa, 0) - G_{22}(ua, qa, a) \right] \\ & + 4\mu a^2 \sum_{q=1}^{\infty} \left[G_{22}(0, qa, 0) - G_{22}(0, qa, a) \right] \\ & + \frac{2\mu a^2}{C_2(n)} - 2\mu a^2 G_{22}(0, 0, a), \end{aligned} \quad (55)$$

where $C_2(n)$ is the force constant defined in Equation (7) for a point force acting on a point at a distance na from the origin. After computation of the sums as presented in Equation (26), $\Delta u_2(na)$ becomes

$$\Delta u_2(na) = \frac{2\mu a^2}{C_2(n)} + \frac{a}{2\pi} \left[\frac{2.866 - 2.368\nu}{1 - \nu} - \sum_{u=n+1}^{\infty} 2\pi \frac{u^2 + 1}{a^2} \right]. \quad (56)$$

For each value of n , a direct comparison can be made between the values of $\Delta u_2(na)$ from Equations (49) to (53) on one hand, and Equation (56) on the other hand. Since both ought to be identical, a value of $C_2(n)$ will be obtained for each value of n . Table 2 lists the different values of $\Delta u_2(n)$ and $C_2(n)$ for $n = 0$ to 5 and for $n = \infty$. The values of $C_2(n)$ are very nearly constant, and it seems reasonable to expect a value of $C_2(0)$ very close to $C_2(\infty)$. This extrapolation permits us to evaluate $\Delta u_2(0)$.

TABLE 2. Variation of Force Constant C_2 with the Atomic Positions in a Screw Dislocation

n	$\frac{\Delta u_2}{a}(n) - \frac{2\mu a}{C_2}$	$\frac{\Delta u_2}{a}(x_1)$	$C_2(n)/\mu a$
		$x_1 = na$	
0	.2885		
1	.3988	.9033	.3964
2	.4343	.9387	.3965
3	.4511	.9554	.3966
4	.4607	.9651	.3966
5	.4670	.9713	.3966
∞	.4957	1.0000	.3966

Replacing $C_2(n)$ by $C_2(\infty)$ in Equation (56) for any values of n and noticing that for large n

$$\Delta u_2(na) = a = \frac{2\mu a^2}{C_2(n)} + \frac{a}{2\pi} \frac{2.866 - 2.368\nu}{1 - \nu} \quad (57)$$

a very simple expression for the relative displacement across the slip plane for $n \geq 0$ is found:

$$\Delta u_2(na) = a - \frac{a}{2\pi} \sum_{n+1}^{\infty} \ell n \frac{u^2 + 1}{u^2} . \quad (58)$$

In particular for $n=0$, $\Delta u_2(na) = .794a$. This value fits very well on the interpolated curve for $\Delta u_2(x_1)$, as shown in Figure 8. For the atomic points corresponding to $x_1 = -na$, with $n > 0$, a direct transformation of Equation (48) leads to

$$\Delta u_2(-na) = \frac{a}{2\pi} \sum_n^{\infty} \ell n \frac{u^2 + 1}{a^2} . \quad (59)$$

It is striking to notice that the symmetry of the screw dislocation displacement field is preserved at the atomic points. The dislocation line, in the continuum sense, lies exactly at $x_1 = -a/2$. This result could have been guessed earlier by simply considering an oriented path around each loop. By adding the loops together, the only remaining part of the path would be a straight line at $x_1 = -a/2$. This method can be generalized for determining dislocation lines in more complicated cases. This symmetry does not appear in Equations (49) to (53) because of the divergence of these expressions at $x_1 = 0$.

A mapping of the atomic displacements in atomic planes immediately above and below the slip plane is shown in Figure 9.

The width of the screw dislocation is defined to be the region in which the relative displacement is comprised between $a/4$ and $3a/4$. Since the region where the relative displacement is equal to $3a/4$ cannot be known exactly, the value $2w = .73a$ for the width can be obtained by rough measurements on Figures 7 and 8.

The relative displacement described above can be compared to the results obtained by Peierls [20,21]. Fitting the expression for relative displacement obtained from the Peierls model to our results leads to the expression

$$\Delta u_2(x_1) = \frac{a}{2} + \frac{a}{\pi} \tan^{-1} \frac{x_1 + d}{w}, \quad (60)$$

where w is the half-width and d a translation parameter fixing the center of symmetry of Δu_2 . For large x_1 , this expression can be expanded in consecutive powers of $1/x_1$,

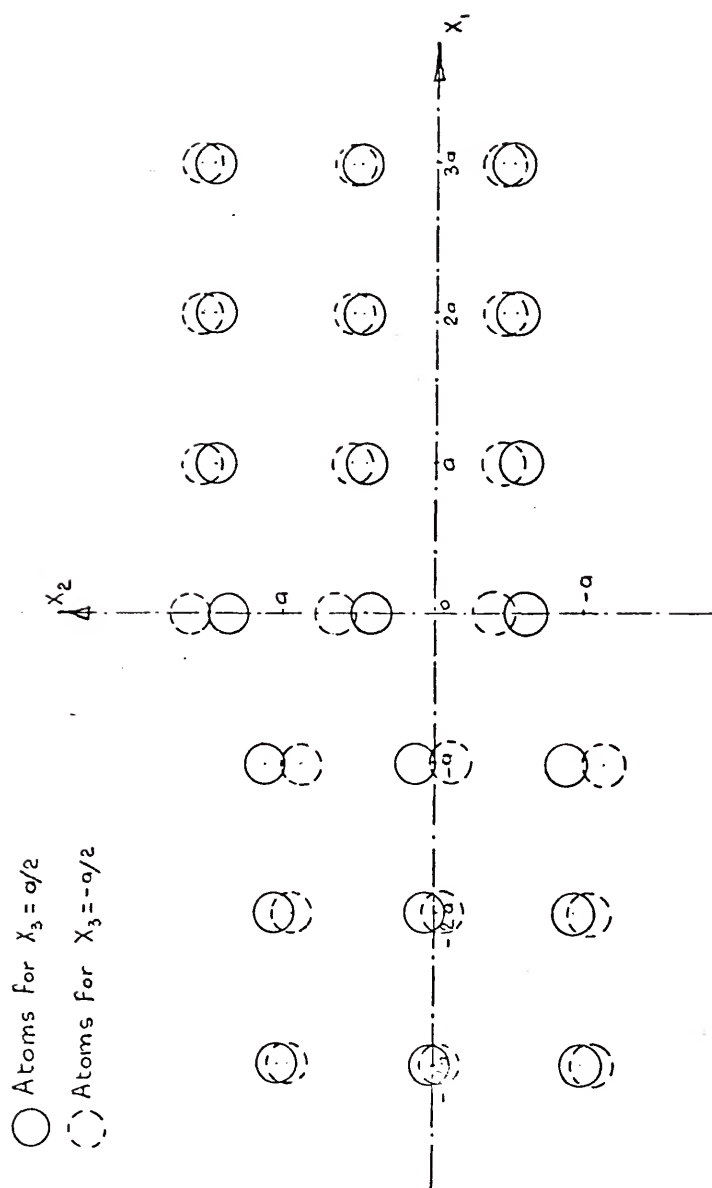


Figure 9. Atomic Arrangement in Planes $x_3 = \pm \frac{a}{2}$ of a Screw Dislocation

$$\Delta u_2(x_1) = a - \frac{a}{\pi} \frac{w}{x_1} + \frac{a}{\pi} + \frac{wd}{2x_1} - \dots \quad (61)$$

The same series expansion holds for Equations (49) to (53) and leads to

$$\Delta u_2(x_1) = a - \frac{a}{2\pi} \frac{a}{x_1} + \frac{a}{4\pi} \frac{a^2}{x_1^2} + \dots \quad (62)$$

By comparison of Equations (61) and (62), the half-width and the translation parameter are

$$w = \frac{a}{2} ; \quad d = \frac{a}{2} . \quad (63)$$

These values correspond to the Peierls' model when the origin is taken at $x_1 = -a/2$. Although the width of the dislocation in our model is slightly smaller than in Peierls' model, the two expressions for the relative displacement across the slip plane are exactly the same for large values of x_1 , as shown in Figure 8.

Finally, following Eshelby's suggestion [1], a distribution function for infinitesimal dislocations in the glide plane can be defined. Instead of being the result of a singularity concentrated on the x_2 axis, the straight screw dislocation is considered to be composed of a continuous distribution of infinitesimal dislocations. This distribution function is, in fact, the component α_{22} of the dislocation density tensor as defined by Kröner [2]. It is to be found equal to

$$\alpha_{22}(x_1) = \frac{d(\Delta u_2)}{dx_1} . \quad (64)$$

Differentiating Equations (49) to (53) with respect to x_1 leads to

$$\alpha_{22}^0 = \frac{1}{2\pi} \ln \frac{x_1^2 + a^2}{x_1^2}, \quad (65)$$

$$\alpha_{22}^1(x_1) = -\frac{1}{2\pi} \frac{a^3}{x_1(x_1^2 + a^2)}, \quad (66)$$

$$\alpha_{22}^2(x_1) = \frac{a^2}{12\pi} \left[\frac{x_1^2 - a^2}{x_1^2(x_1^2 + a^2)^2} \right] \quad (67)$$

and

$$\alpha_{22}^3(x_1) = \frac{a^4}{120\pi} \left[\frac{x_1^4 - 6a^2x_1^2 + a^4}{(x_1^2 + a^2)^4} - \frac{1}{x_1^4} \right]. \quad (68)$$

It can be easily verified that

$$\int_{-\infty}^{+\infty} \alpha_{22}^n(x_1) dx_1 = a. \quad (69)$$

A plot of the successive approximations is made in Figure 10, emphasizing the values of $\alpha_{22}(x_1)$ at the atomic positions. Symmetry of the distribution function at these points with respect to $x_1 = -a/2$ is evident.

In summary, we shall emphasize that this model is in perfect agreement with the previous techniques employed for obtaining the displacement field of a straight screw dislocation. An improvement has been made in the present case, obtaining a simple analytic expression for the atomic displacements around the defect without any exceptions. Such atomic displacements can be obtained by lattice dynamics computation, but these have the disadvantages of being difficult to use and being an entire numerical method [13].

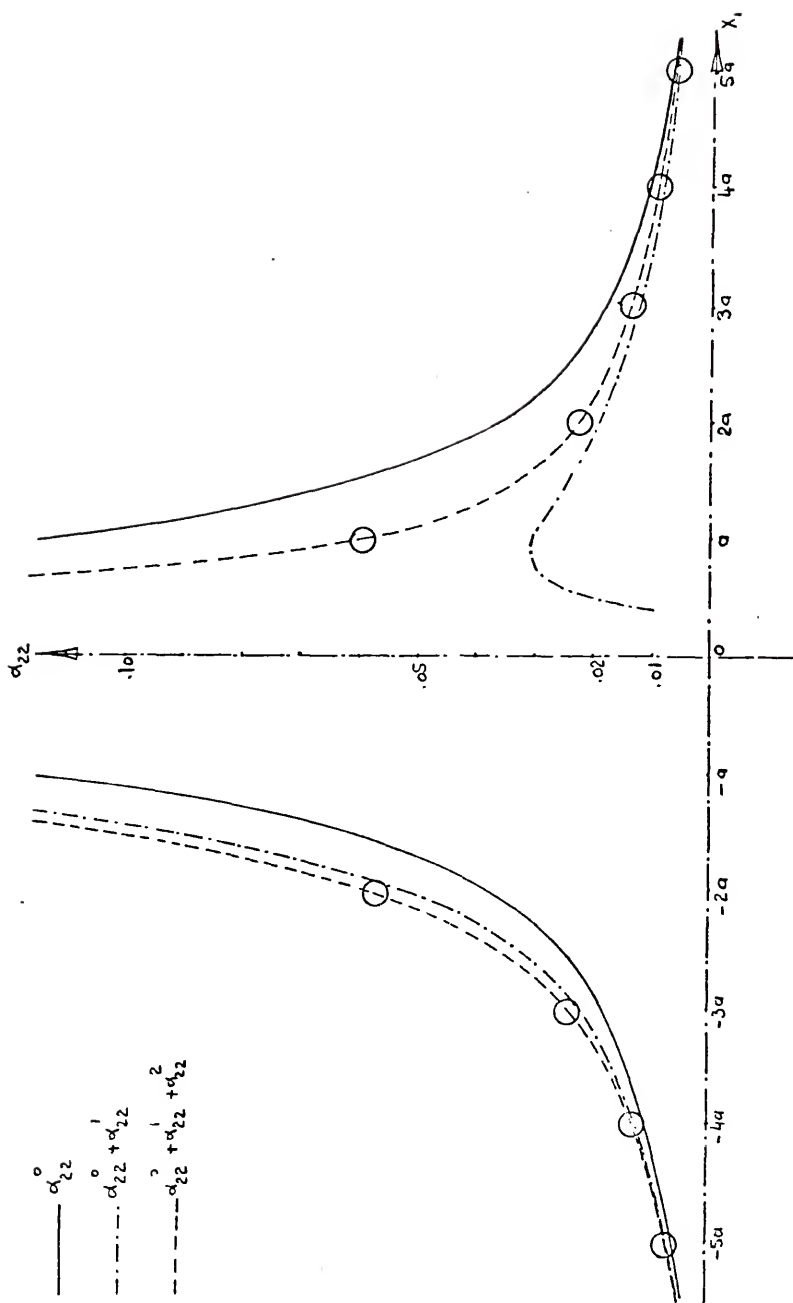


Figure 10. Distribution Function of a Screw Dislocation

Self-Energy of the Screw Dislocation

As it has been explained in the previous chapter, such an array of point forces can simulate a system composed of two infinitely long parallel screw dislocations of opposite signs if the length La is taken much larger than the separation distance, or width of the array, Ra . In this case, the energy of the system per unit length of screw dislocation becomes W/La when L is large.

$$\frac{W}{La} = \frac{R+1}{4\pi} \mu a^2 \left[4\pi \frac{\mu a}{C_2} + A \right] - \frac{\mu a^2}{2\pi} \ln \frac{R}{r'_0}, \quad (70)$$

where the constants A and r'_0 are defined by

$$A = \frac{2.8545 - 2.3676\nu}{1 - \nu} \quad (71)$$

and

$$\ln \frac{1}{r'_0} = 1.179. \quad (72)$$

Taking the special case of $\nu = 1/3$ leads to

$$\frac{W}{La} = \frac{R+1}{4\pi} \mu a^2 \left[4\pi \frac{\mu a}{C_2} + 3.0979 \right] - \frac{\mu a^2}{2\pi} \ln \frac{R}{.3076}. \quad (73)$$

As already mentioned, this energy is higher than the energy of the system composed of two parallel screw dislocations of opposite sign, because of the nonrealistic strain energy stored in the region between the planes of forces. The region of the continuum where the strain is larger than $1/2$ is shown in Figure 11 and has the following boundaries:

$$\begin{cases} -\frac{a}{2} \leq x_3 \leq \frac{a}{2} \\ -.35a \leq x_1 \leq Ra + .35a \end{cases} \quad (74)$$

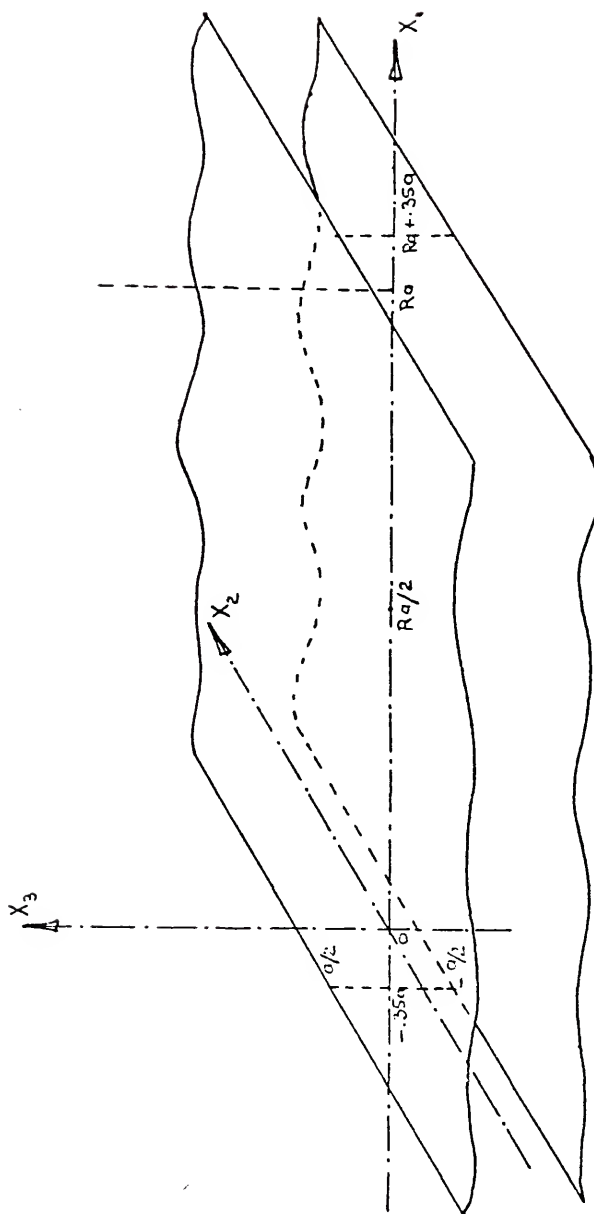


Figure 11. Region Where the Correction Energy Applies for a Screw Dislocation

The points $x_1 = -.35a$ and $x_1 = Ra + .35a$ are those where $\Delta u_2(x_1) = a/2$. Outside these limits, $\Delta u_2(x_1)$ is smaller than $a/2$. The correction energy which has to be subtracted from W/La is composed of the strain energy per unit length of screw dislocation due to the displacement field $\vec{u}(x_1, x_3)$, minus the strain energy per unit length of screw dislocation due to the displacement field measured relative to the final atomic positions inside the slab, $\vec{v}(x_1, x_3)$ described as follows:

$$\begin{cases} v_1(x_1, x_3) = 0 \\ v_2(x_1, x_3) = u_2(x_1, x_3) - x_3 \\ v_3(x_1, x_3) = 0 \end{cases} \quad (75)$$

The stress fields associated with these two displacement fields are

$$\underline{\sigma} = \begin{cases} \sigma_{12} = \mu \frac{\partial u_2}{\partial x_1} \\ \sigma_{23} = \mu \frac{\partial u_2}{\partial x_3} \end{cases} \quad (76)$$

and

$$\underline{\tau} = \begin{cases} \tau_{12} = \mu \frac{\partial v_2}{\partial x_1} = \mu \frac{\partial u_2}{\partial x_1} \\ \tau_{23} = \mu \frac{\partial v_2}{\partial x_3} = \mu \left(\frac{\partial u_2}{\partial x_3} - 1 \right) \end{cases} \quad (77)$$

The correction energy is the following integral computed over the volume mentioned above.

$$E_c = \frac{1}{2} \int_V \left(\sigma_{ij} \epsilon_{ij}^u - \tau_{ij} \epsilon_{ij}^v \right) dV \quad (78)$$

Using Green's theorem, this volume integral can be transformed into a surface integral,

$$E_c = \frac{1}{2} \int_S (\sigma_{ij} u_i - \tau_{ij} v_i) n_j dS, \quad (79)$$

where \vec{n} is the normal to the surface S . Using Equations (75) and (76) leads to

$$E_c = \frac{\mu}{2} \int_S \left[\left(u_2 \frac{\partial u_2}{\partial x_1} - v_2 \frac{\partial v_2}{\partial x_1} \right) n_1 + \left(u_2 \frac{\partial u_2}{\partial x_3} - v_2 \frac{\partial v_2}{\partial x_3} \right) n_3 \right] dS \quad (80)$$

or

$$E_c = \frac{\mu}{2} \int_S \left[x_3 \frac{\partial u_2}{\partial x_1} n_1 + \left(x_3 \frac{\partial u_2}{\partial x_3} - x_3 + u_2 \right) n_3 \right] dS, \quad (81)$$

where the surface, S , is composed of the areas

$$S_1: x_3 = \pm \frac{a}{2}, \quad -35a \leq x_1 \leq Ra + .35a;$$

$$S_2: x_1 = -.35a, \quad -\frac{a}{2} \leq x_3 \leq \frac{a}{2};$$

$$S_3: x_1 = Ra + .35a, \quad -\frac{a}{2} \leq x_3 \leq \frac{a}{2}.$$

Taking the symmetry with respect to $x_1 = Ra/2$ into account, and the fact that the integrand is not dependent on x_2 , lead us to the final formal expression for E_c/La :

$$\begin{aligned} \frac{E_c}{La} = & -\mu \int_{-a/2}^{a/2} x_3 \frac{\partial u_2}{\partial x_1} (-.35a, x_3) dx_3 \\ & + 2\mu \int_{-.35a}^{Ra/2} \left[\frac{a}{2} \frac{\partial u_2}{\partial x_3} \left(x_1, \frac{a}{2} \right) - \frac{a}{2} + u_2 \left(x_1, \frac{a}{2} \right) \right] dx_1. \end{aligned} \quad (82)$$

The analytical expressions for u_2 , $\partial u_2 / \partial x_1$, $\partial u_2 / \partial x_3$ are obtained from Equation (31) and its derivatives:

$$u_2(x_1, x_3) = \frac{a}{4\pi} \sum_{p=0}^R \varrho_n \frac{(x_1 - pa)^2 + (x_3 + \frac{a}{2})^2}{(x_1 - pa)^2 + (x_3 - \frac{a}{2})^2}, \quad (83)$$

$$x_3 \frac{\partial u_2}{\partial x_1}(x_1, x_3) = \frac{a}{2\pi} \sum_{p=0}^R x_3 \left[\frac{x_1 - pa}{(x_1 - pa)^2 + (x_3 + \frac{a}{2})^2} - \frac{x_1 - pa}{(x_1 - pa)^2 + (x_3 - \frac{a}{2})^2} \right] \quad (84)$$

and

$$\frac{\partial u_2}{\partial x_3}(x_1, x_3) = \frac{a}{2\pi} \sum_{p=0}^R \left[\frac{x_3 + \frac{a}{2}}{(x_1 - pa)^2 + (x_3 + \frac{a}{2})^2} - \frac{x_3 - \frac{a}{2}}{(x_1 - pa)^2 + (x_3 - \frac{a}{2})^2} \right]. \quad (85)$$

The mathematical problem of integrating a function over a region where the integrand has singular points for certain values of x_1 is removed by the same argument as the one used in the previous section.

After integration, Equation (82) becomes

$$\begin{aligned} \frac{E_c}{La} &= \frac{\mu a^2}{\pi} \sum_{p=0}^R \left[(p + .35) \varrho_n \frac{(p + .35)^2 + 1}{(p + .35)^2} + 2 \tan^{-1}(p + .35) \right] \\ &- \mu a^2 \left(.35 + \frac{R}{2} \right). \end{aligned} \quad (86)$$

The summation over p is computed in the same way as before using Equation (26), which gives finally for the correction energy

$$\frac{E_c}{La} = \frac{\mu a^2}{2} R - \frac{\mu a^2}{\pi} \varrho_n \frac{R}{r_0} \quad (87)$$

and

$$\varrho_n r_0'' = .3129. \quad (88)$$

The total energy of the system composed of two antiparallel screw dislocations is

$$\frac{E_T}{La} = \frac{W}{La} - \frac{E_c}{La} \quad (89)$$

or

$$\frac{E_T}{La} = \frac{R+1}{4\pi} \mu a^2 \left[4\pi \frac{\mu a}{C_2} + A - 2\pi \right] + \frac{\mu a^2}{2\pi} \ln \frac{R \cdot r_0'}{(r_0'')^2} + \frac{\mu a^2}{2} \quad (90)$$

From the usual continuum theory of dislocations, this energy has to be equal to the sum of the self-energies of both screw dislocations, minus their interaction energy

$$\frac{E_T}{La} = 2 \frac{\mu a^2}{4\pi} \ln \frac{r}{r_0} - \frac{\mu a^2}{2\pi} \ln \frac{r}{R} \quad (91)$$

The requirement that our expression (90) has to be identical in form to Equation (91), will force us to choose the still unknown parameter C_2 such that the term divergent with R vanishes. Thus,

$$\frac{E_T}{La} = \frac{\mu a^2}{2\pi} \ln \frac{R}{r_0} \quad (92)$$

with

$$\ln \frac{1}{r_0} = 1.3367, \quad (93)$$

if

$$\frac{\mu a}{C_2} = \frac{1}{2} - \frac{2.8545 - 2.3676\nu}{4\pi(1-\nu)} \quad (94)$$

For $\nu = 1/3$

$$\frac{E_T}{La} = \frac{\mu a^2}{2\pi} \ln \frac{Ra}{.2631a} \quad (95)$$

if

$$C_2 = 3.945\mu a \quad (96)$$

From Equation (91), the self-energy of a pure single screw dislocation can be written

$$\frac{E_S}{La} = \frac{\mu a^2}{4\pi} \ln \frac{r}{.263a} . \quad (97)$$

Two important remarks can be made here. First, the value found for C_2 is very close to those found from the displacement field computations. This proves the consistency of the correction energy with the displacement field included from the array of forces. Secondly, it is found that the core parameter in Equation (97) is independent of ν , Poisson's ratio. This is in complete agreement with Peierls' result, which gives a value of r_0 equal to a/e , that is, equal to $.37a$, where e is the naperian base of logarithms.

So both models give nearly identical results, but with a slightly different r_0 .

For a direct comparison with Volterra's dislocation model, the core radius r_0 in Volterra's model has to be reinterpreted and cannot be considered anymore as a cut-off core radius where Hooke's law does not apply. It is rather a constant containing all the constant terms arising in the computation of the core energy. The Volterra cut-off radius could be evaluated in a better way by defining the region where Hooke's law does not apply, e.g., where the strain is larger than .10. From Figure 8, such a cut-off radius can be approximated as being about $r_0 = 1.5a$.

So, the technique of simulating dislocations by a point force array seems to be very successful in describing the principal features of the defect, even though a complete accuracy in the computation of the

atomic displacements cannot be reached because of the elastic and isotropic approximation.

Single and Double Kinks in a Screw Dislocation

A single or a double kink can be simulated by simply adding to the array of forces an extra row of shear loops, parallel to the screw dislocation line, and a semi-infinite or finite extent, respectively. A representation of the modified array is sketched in Figures 12 and 13. The displacement field and the energy of these defects are handled in the same way as for the straight screw dislocation.

A. Displacement field

The displacement field of these defects is obtained by adding to the displacement field of the pure screw dislocation, the displacement field resulting from the extra row of forces. The latter, \vec{u}' , has the following expressions for, respectively, a single kink and a double kink of length $2Na$.

$$\begin{aligned}
 u'_{1(SK)}(x_1, x_2, x_3) = & \mu a^2 \sum_{q=0}^{\infty} \left[G_{2i}(x_1+a, x_2-qa, x_3-\frac{a}{2}) \right. \\
 & - G_{2i}(x_1+a, x_2-qa, x_3+\frac{a}{2}) \Big] - \frac{\mu a^2}{2} \left[G_{2i}(x_1+a, x_2, x_3-\frac{a}{2}) \right. \\
 & - G_{2i}(x_2+a, x_2, x_3+\frac{a}{2}) \Big] - \frac{\mu a^2}{2} \left[G_{3i}(x_1+a, x_2, x_3-\frac{a}{2}) \right. \\
 & \left. + G_{3i}(x_1+a, x_2, x_3+\frac{a}{2}) \right] .
 \end{aligned} \tag{98}$$

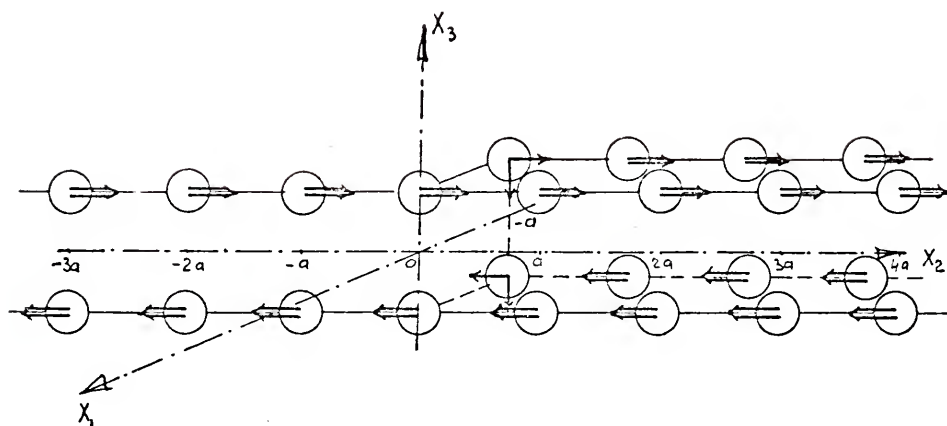


Figure 12. Array of Forces for a Single Kink in a Screw Dislocation

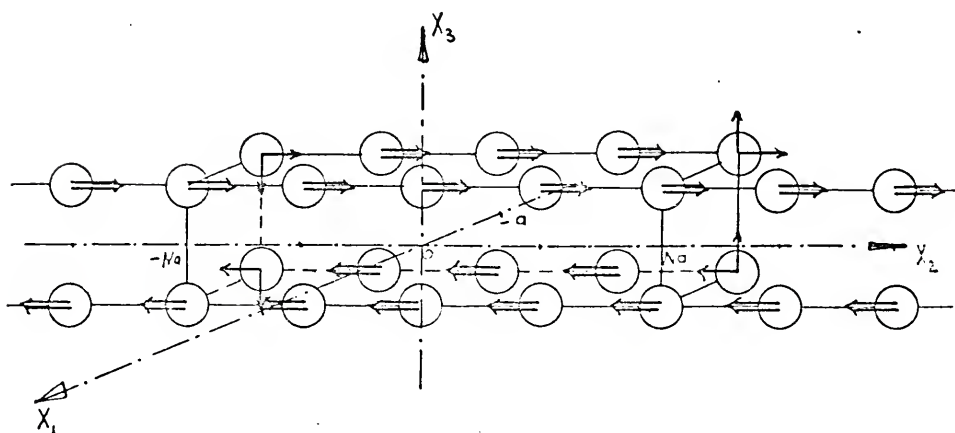


Figure 13. Array of Forces for a Double Kink in a Screw Dislocation

$$\begin{aligned}
u'_{1(DK)}(x_1, x_2, x_3) = & \mu a^2 \sum_{q=-N}^N \left[G_{2i}(x_1+a, x_2-qa, x_3-\frac{a}{2}) \right. \\
& - G_{2i}(x_1+a, x_2-qa, x_3+\frac{a}{2}) \Big] - \frac{\mu a^2}{2} \left[G_{2i}(x_1+a, x_2+na, x_3-\frac{a}{2}) \right. \\
& - G_{2i}(x_1+a, x_2+Na, x_3+\frac{a}{2}) + G_{2i}(x_1+a, x_2-Na, x_3-\frac{a}{2}) \\
& - G_{2i}(x_1+a, x_2-Na, x_3+\frac{a}{2}) \Big] + \frac{\mu a^2}{2} \left[G_{3i}(x_1+a, x_2-Na, x_3-\frac{a}{2}) \right. \\
& + G_{3i}(x_1+a, x_2-Na, x_3+\frac{a}{2}) - G_{3i}(x_1+a, x_2+Na, x_3-\frac{a}{2}) \\
& \left. - G_{3i}(x_1+a, x_2+Na, x_3+\frac{a}{2}) \right]. \tag{99}
\end{aligned}$$

Computations of u'_1 and u'_3 for both kinds show that these displacements are very small, even of the region of high distortion in the \vec{x}_2 direction. They reach a magnitude of a few thousandths of an atomic distance. Therefore, we shall concentrate our attention on the u'_2 component of \vec{u}' , and, more specifically, on the atomic displacements in the planes just above and below the slip plane ($x_3 = \pm a/2$), since this is the region of highest distortion.

Because of the existence of singular points at the points of application of the point forces, several special cases will be considered. As a first step, we shall restrict our range of interest by noticing the various symmetries in the expression of u'_2 . It shows an odd symmetry with respect to $x_3 = 0$, and an even symmetry with respect to $x_1 = -a$ for both cases, single and double kinks. It shows an even symmetry with respect to $x_2 = 0$ in the special case of the double kink.

(1) Displacement field of the single kink

The single kink will be the first case considered. For most of the values taken by x_1 and x_2 , $u'_{2(SK)}$ has the following expression:

$$u'_{2(SK)}(x_1, x_2, \frac{a}{2}) = \frac{a}{8\pi} \left[\sum_{q=0}^{\infty} f(x_2 - qa) - \frac{1}{2} f(x_2) \right] - \frac{a}{32\pi} \frac{1}{1-\nu} \frac{a^2 x_2^2}{[(x_1+a)^2 + x_2^2 + a^2]^{3/2}} \quad (100)$$

with

$$f(x_2 - qa) = \frac{3-4\nu}{2(1-\nu)} \left[\frac{1}{\sqrt{(x_1+a)^2 + (x_2-qa)^2}} - \frac{1}{\sqrt{(x_1+a)^2 + (x_2-qa)^2 + a^2}} \right] + \frac{1}{2(1-\nu)} \left[\frac{(x_2-qa)^2}{[(x_1+a)^2 + (x_2-qa)^2]^{3/2}} - \frac{(x_2-qa)^2}{[(x_1+a)^2 + (x_2-qa)^2 + a^2]^{3/2}} \right] \quad (101)$$

On atomic positions, different expressions apply because of the singular points situated on $x_1 = -a$:

$$(a) \quad x_2 = na \quad \text{and} \quad x_1 \neq -a$$

$$u'_{2(SK)}(x_1, na, \frac{a}{2}) = \frac{a}{8\pi} \left[\left(\sum_{q=1}^{\infty} + \sum_{q=0}^n \right) f(qa) - \frac{1}{2} f(na) \right] - \frac{a}{32\pi(1-\nu)} \frac{na^3}{[(x_1+a)^2 + n^2 a^2 + a^2]^{3/2}} \quad (102)$$

$$(b) \quad x_2 = -na \quad \text{for any } x_1$$

$$u'_{2(SK)}(x_1, -na, \frac{a}{2}) = \frac{a}{8\pi} \left[\left(\sum_{q=1}^{\infty} - \sum_{q=1}^n \right) f(qa) + \frac{1}{2} f(na) \right] + \frac{a}{32\pi(1-\nu)} \frac{na^3}{[(x_1+a)^2 + n^2 a^2 + a^2]^{3/2}} \quad (103)$$

(c) $x_2 = na$ with $n > 0$, and $x_1 = -a$

$$u'_{2(SK)}(-a, na, \frac{a}{2}) = \frac{a}{8\pi} \left\{ \left(\sum_{q=1}^{\infty} + \sum_{q=1}^n \right) \left[2 \left(\frac{1}{q} - \frac{1}{\sqrt{\frac{2}{q}+1}} \right) + \frac{1}{2(1-\nu)} \frac{1}{(q^2+1)^{3/2}} \right] \right. \\ \left. - \frac{1}{2} \left[2 \frac{1}{n} - \frac{1}{\sqrt{n^2+1}} + \frac{1}{2(1-\nu)} \frac{n+1}{(n^2+1)^{3/2}} \right] \right\} + \frac{\mu a^2}{C_2} - \frac{a}{16\pi} \frac{3-4\nu}{1-\nu} \quad (104)$$

(d) $x_2 = 0$ and $x_1 = -a$

$$u'_{2(SK)}(-a, 0, \frac{a}{2}) = \frac{a}{8\pi} \sum_{q=1}^{\infty} \left[2 \left(\frac{1}{q} - \frac{1}{\sqrt{\frac{2}{q}+1}} \right) + \frac{1}{2(1-\nu)} \frac{1}{(q^2+1)^{3/2}} \right] \\ + \frac{\mu a^2}{2C_2} - \frac{a}{32\pi} \frac{(3-4\nu)}{(1-\nu)} \quad (105)$$

In all these cases, f has the same form as in Equation (101).

C_2 has the same meaning as before. Since it has been noticed that the force constant is very nearly constant for all rows of point forces, we shall give it the value found from Equation (57). The atomic displacements are tabulated in Table 3 for the following values of x_1 and x_2 :

$$x_1 = -2a, -a, 0, a$$

$$x_2 = -5a, -4a, \dots, 0, \dots, 4a, 5a.$$

To these values have to be added the corresponding atomic displacements due to the straight screw dislocations. A mapping of the atomic configuration above and below the slip plane is shown in Figure 14. This sketch shows a very high distortion around the point ($x_1 = -a, x_2 = 0$), but after a few atomic distances from this point,

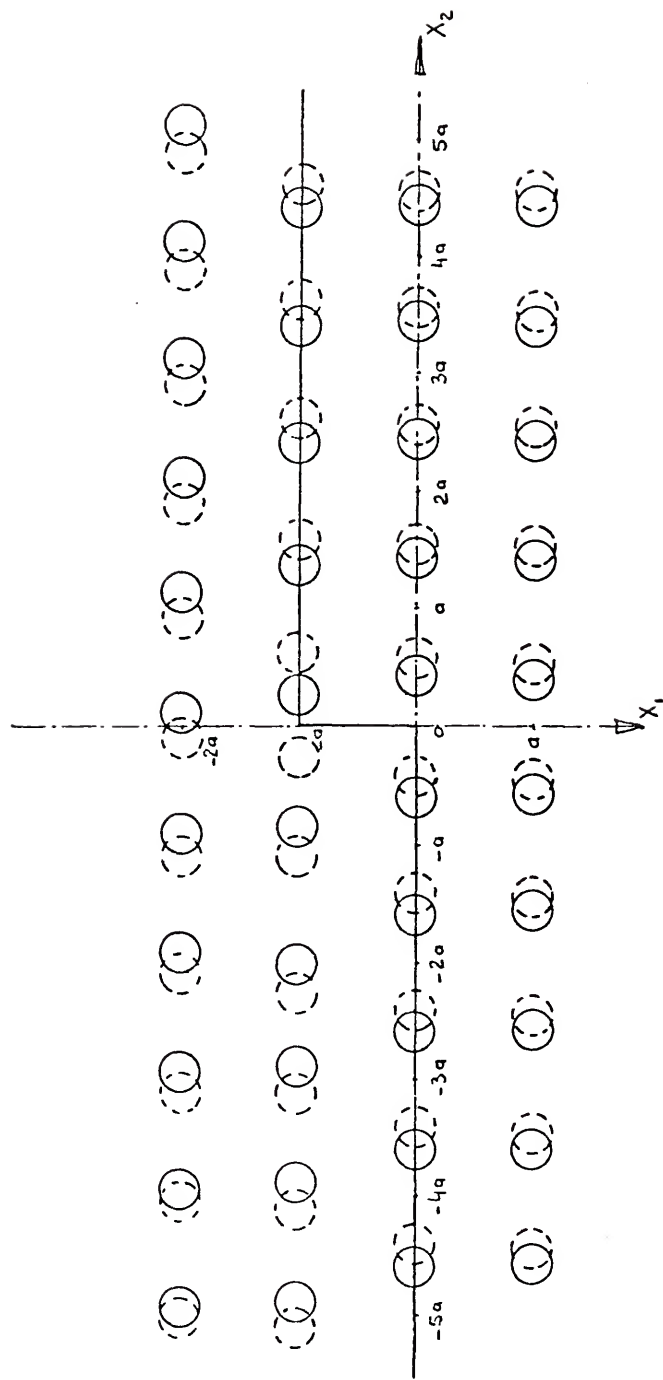


Figure 14. Atomic Arrangement Around a Single Kink in a Screw Dislocation

the atomic configuration shows very little difference from the configuration of the pure screw dislocation. Even if the actual width of the kink cannot be expressed analytically, one can conclude that the defect is very localized.

TABLE 3. Atomic Displacements for a Single Kink in a Screw Dislocation

x_2/a	$u'_{2(SK)}/a$			
	$x_1 = -2a$	$x_1 = -a$	$x_1 = 0$	$x_1 = a$
-5	.0019	.0020	.0019	.0016
-4	.0028	.0030	.0028	.0023
-3	.0046	.0052	.0046	.0034
-2	.0086	.0111	.0086	.0052
-1	.0173	.0341	.0173	.0073
0	.0347	.1473	.0347	.0102
1	.0374	.2605	.0374	.0105
2	.0461	.2834	.0461	.0126
3	.0501	.2893	.0501	.0163
4	.0519	.2915	.0519	.0154
5	.0529	.2926	.0529	.0161

(2) Displacement field of the double kink

We shall consider here a double kink of length $2Na$. The computations have the same form for a kink of length $(2N+1)a$. The displacement field at a general point in the plane $x_3 = a/2$ has the following expression:

$$\begin{aligned}
 u'_{2(DK)}(x_1, x_2, \frac{a}{2}) &= \frac{a^2}{8\pi} \left[\sum_{q=-N}^N f(x_2 - qa) - \frac{1}{2} f(x_2 - Na) - \frac{1}{2} f(x_2 + Na) \right] \\
 &+ \frac{a^3}{32\pi(1-\nu)} \left[\frac{x_2 - Na}{[(x_1 + a)^2 + (x_2 - Na)^2 + a^2]^{3/2}} - \frac{x_2 + Na}{[(x_1 + a)^2 + (x_2 + Na)^2 + a^2]^{3/2}} \right]
 \end{aligned}
 \tag{106}$$

with

$$f(x_2 - qa) = \frac{3-4\nu}{2(1-\nu)} \left[\frac{1}{\sqrt{(x_1+a)^2 + (x_2-qa)^2}} - \frac{1}{\sqrt{(x_1+a)^2 + (x_2-qa)^2 + a^2}} \right] + \frac{1}{2(1-\nu)} \left[\frac{(x_2-qa)^2}{\left[(x_1+a)^2 + (x_2-qa)^2 \right]^{3/2}} - \frac{(x_2-qa)^2}{\left[(x_1+a)^2 + (x_2-qa)^2 + a^2 \right]^{3/2}} \right]. \quad (107)$$

The points where this expression do not apply are the points of application of the point forces on the row $x_1 = -a$. Two separate cases are considered.

(a) $x_1 = -a$ and $x_2 = \pm na$ for $n < N$

$$u'_{2(DK)}(-a, \pm na, \frac{a}{2}) = \frac{a}{8\pi} \left[\left(\sum_{q=1}^{N+n} + \sum_{q=1}^{N-n} \right) f(q) - \frac{1}{2} f(N+n) - \frac{1}{2} f(N-n) \right] + \frac{a}{32\pi(1-\nu)} \left[\frac{N-n}{\left[(N-n)^2 + 1 \right]^{3/2}} - \frac{N+n}{\left[(N+n)^2 + 1 \right]^{3/2}} \right] + \frac{\mu a^2}{C_2} - \frac{a}{16\pi} \left(\frac{3-4\nu}{1-\nu} \right). \quad (108)$$

(b) $x_1 = -a$ and $x_2 = \pm Na$

$$u'_{2(DK)}(-a, \pm Na, \frac{a}{2}) = \frac{a}{8\pi} \left[\sum_{q=1}^{2N} f(q) - \frac{1}{2} f(2N) \right] - \frac{a}{16\pi(1-\nu)} \frac{N}{(4N^2+1)^{3/2}} + \frac{\mu a^2}{2C_2} - \frac{a}{32\pi} \left(\frac{3-4\nu}{1-\nu} \right). \quad (109)$$

with, in both cases,

$$f(q) = 2 \left(\frac{1}{q} - \frac{1}{\sqrt{q^2+1}} \right) + \frac{1}{2(1-\nu)} \frac{1}{(q^2+1)^{3/2}}. \quad (110)$$

The sizes of double kinks have been considered, corresponding to the values of N equal to 1, 2, and 3. Due to the symmetry already mentioned, only the values of $u'_{2(DK)}$ for the following values of x_1 and x_2 have been computed:

$$x_1 = -a, 0, a, 2a$$

$$x_2 = 0, a, 2a, 3a, 4a, 5a.$$

These values of $u'_{2(DK)}$ are tabulated in Tables 4, 5, and 6, corresponding, respectively, to $N = 1, 2$, and 3.

TABLE 4. Atomic Displacements for a Double Kink of Length $2a$ in a Screw Dislocation

x_2/a	$u'_{2(DK)}/a$				
	$x_1 = -2a$	$x_1 = -a$	$x_1 = 0$	$x_1 = a$	$x_1 = 2a$
0	.0201	.2374	.0201	.0031	.0009
1	.0188	.1363	.188	.0037	.0011
2	.0127	.0288	.0127	.0038	.0014
3	.0058	.0081	.0058	.0028	.0013
4	.0028	.0033	.0028	.0018	.0011
5	.0015	.0012	.0015	.0011	.0008

TABLE 5. Atomic Displacements for a Double Kink of Length $4a$ in a Screw Dislocation

x_2/a	$u'_{2(DK)}/a$				
	$x_1 = -2a$	$x_1 = -a$	$x_1 = 0$	$x_1 = a$	$x_1 = 2a$
0	.0375	.2781	.0375	.0074	.0022
1	.0328	.2661	.0328	.0080	.0023
2	.0246	.1444	.0246	.0066	.0024
3	.0155	.0321	.0155	.0057	.0024
4	.0073	.0097	.0073	.0040	.0020
5	.0037	.0042	.0037	.0005	.0006

TABLE 6. Atomic Displacements for a Double Kink of Length $6a$ in a Screw Dislocation

x_2/a	$u'_{2(DK)}/a$				
	$x_1 = -2a$	$x_1 = -a$	$x_1 = 0$	$x_1 = a$	$x_1 = 2a$
0	.0455	.2872	.0455	.0109	.0036
1	.0429	.2861	.0433	.0103	.0035
2	.0356	.2694	.0356	.0088	.0033
3	.0261	.1461	.0261	.0077	.0031
4	.0164	.0330	.0164	.0064	.0029
5	.0089	.0103	.0089	.0044	.0024

A mapping of the atomic arrangement is attempted in Figures 15, 16, and 17, corresponding to the cases $N = 1, 2$, and 3 , respectively. The same remarks can be made about the double kink configuration as has been made for the single kink. Once again, the kink seems to be a very localized defect for a structure like a simple cubic crystal. In the case of $N = 3$, that is, where the length of the double kink is $6a$, each single kink part of the whole kink seems to behave like a pure single kink, which is to be expected when the double kink grows in size. This argument will be used to extrapolate the energy of a single kink from the energy of a very long double kink.

B. Energy of a double and a single kink

The energy of a double kink is defined as being the difference between the energy of the modified array of forces and the energy of the rectangular dislocation loop. As has been developed for the screw dislocation, a correction energy term will be introduced to take into account the actual strain field across the slip plane.

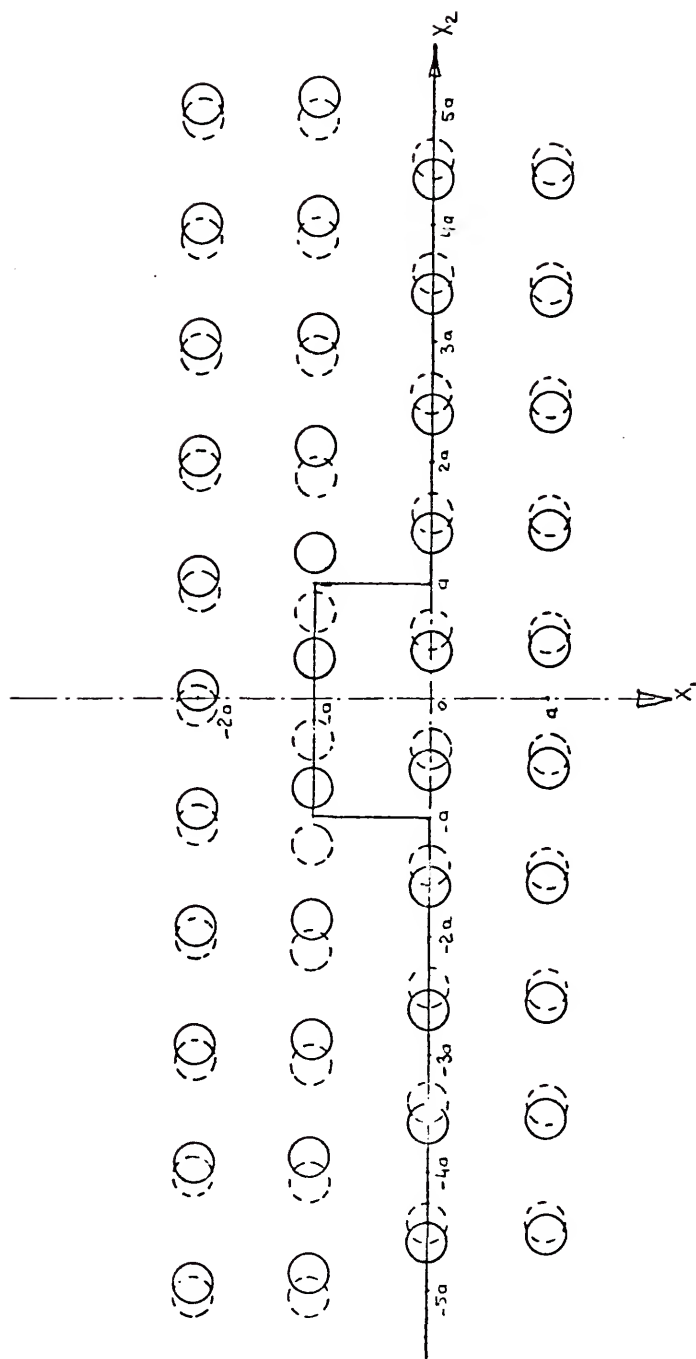


Figure 15. Atomic Arrangement Around a Double Kink of Length $2a$ in a Screw Dislocation

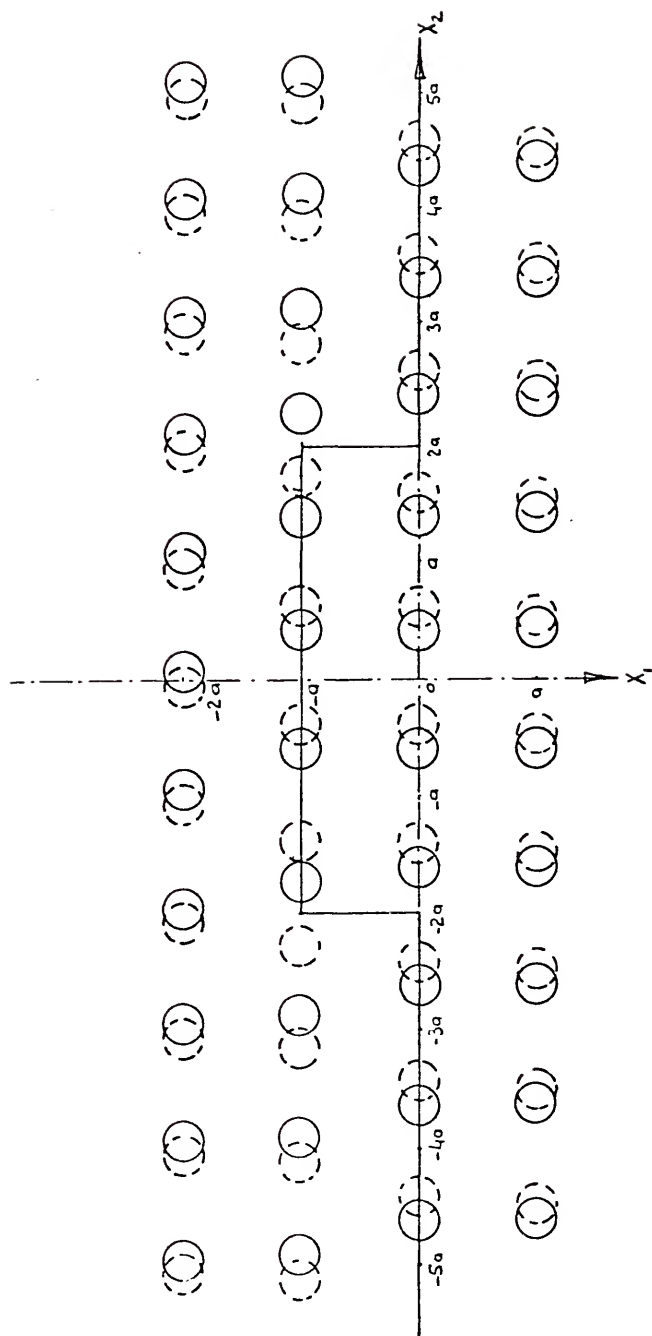


Figure 16. Atomic Arrangement Around a Double Kink of Length $4a$ in a Screw Dislocation

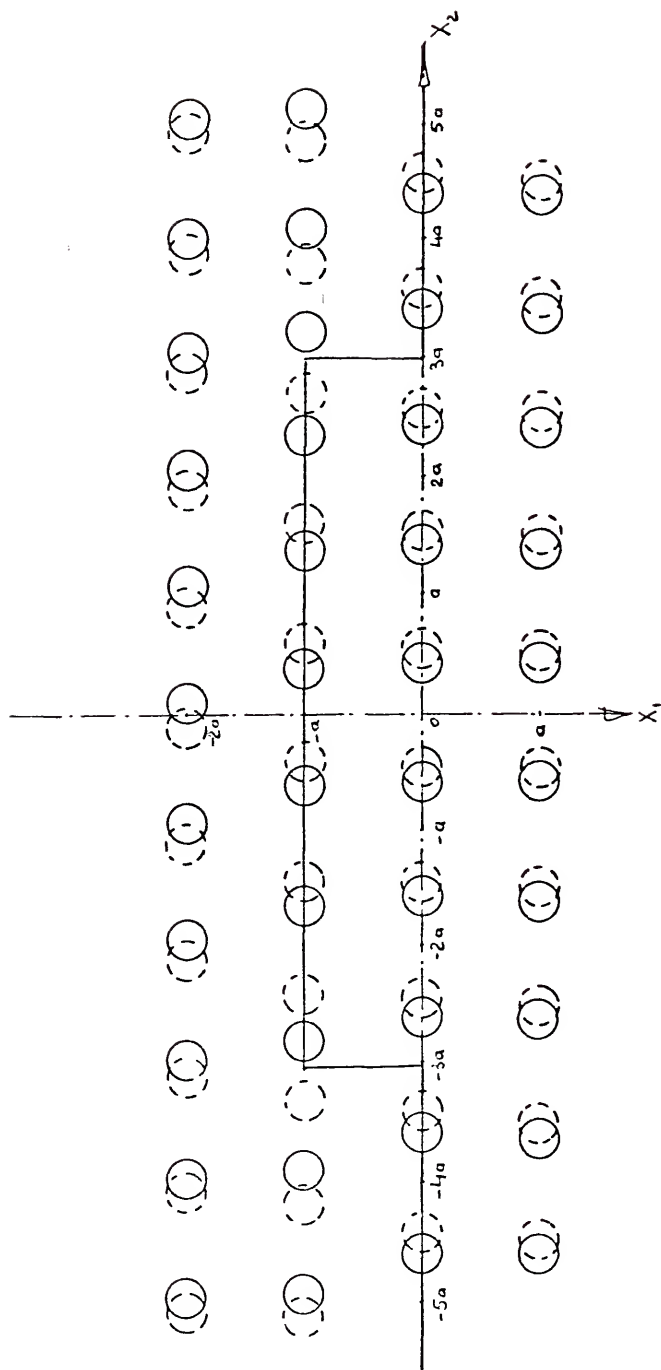


Figure 17. Atomic Arrangement Around a Double Kink of Length $6a$ in a Screw Dislocation

In a first step, the difference between the energies of the systems of forces has to be computed. It is simply the self-energy of the extra double row of forces of length $2Na$, and the interaction energy between this double row of forces and the dislocation loop array.

$$\begin{aligned}
 W = & \frac{\mu^2 a^4}{2} (4N-1) \left[\frac{1}{C_2} - G_{22}(0,0,a) \right] + \frac{\mu^2 a^4}{2} \left[\frac{1}{C_3} + G_{33}(0,0,a) \right] \\
 & + \frac{\mu^2 a^4}{2} \left[G_{22}(0,2Na,0) - G_{22}(0,2Na,a) - G_{33}(0,2Na,0) - G_{33}(0,2Na,a) \right] \\
 & - \mu^2 a^4 G_{23}(0,2Na,a) + 2\mu^2 a^4 \sum_{q=1}^{2N-1} (2N-q) \left[G_{22}(0,qa,0) - G_{22}(0,qa,a) \right] \\
 & - 2\mu^2 a^4 \sum_{q=1}^{2N-1} G_{23}(0,qa,a) + \mu^2 a^4 \sum_{p=1}^{R+1} \left\{ G_{22}\left(pa, \frac{La}{2} - Na, 0\right) \right. \\
 & - G_{22}\left(pa, \frac{La}{2} - Na, a\right) + G_{22}\left(pa, \frac{La}{2} + Na, 0\right) - G_{22}\left(pa, \frac{La}{2} + Na, a\right) \\
 & + G_{33}\left(pa, \frac{La}{2} - Na, 0\right) + G_{33}\left(pa, \frac{La}{2} - Na, a\right) - G_{33}\left(pa, \frac{La}{2} + Na, 0\right) \\
 & - G_{33}\left(pa, \frac{La}{2} + Na, a\right) - 2G_{23}\left(pa, \frac{La}{2} + Na, a\right) - \sum_{q=-\frac{L}{2}+N+1}^{\frac{L}{2}+N-1} G_{23}(pa, qa, a) \\
 & + 4N \left[G_{22}(pa, 0, 0) - G_{22}(pa, 0, a) \right] \\
 & + \left[\sum_{q=1}^{\frac{L}{2}-N-1} 8N + 2 \sum_{q=\frac{L}{2}-N}^{\frac{L}{2}+N-1} (L+2N-1-2q) \right] \left[G_{22}(pa, qa, 0) - G_{22}(pa, qa, a) \right] \}.
 \end{aligned} \tag{111}$$

We shall consider cases for which the length of the double kink is much smaller than the length of the dislocation line. Under this condition, the expression of W is greatly simplified.

$$\begin{aligned}
\frac{W}{\mu a^3} = & 2N \left\{ \frac{\mu a}{C_2} - \frac{1}{8\pi} \frac{3-4\nu}{2(1-\nu)} + \frac{1}{4\pi} \sum_{q=1}^{2N-1} \left[2 \left(\frac{1}{q} - \frac{1}{\sqrt{\frac{q^2}{2}+1}} \right) + \frac{1}{2(1-\nu)} \frac{1}{(q+1)^{3/2}} \right] \right. \\
& + \left. \frac{1}{8\pi} \sum_{q=1}^{\infty} \left[\frac{3-4\nu}{1-\nu} \ln \frac{q^2+1}{q^2} + \frac{1}{1-\nu} \left(\frac{2}{q+1} - \frac{1}{q} + \frac{1}{\sqrt{\frac{q^2}{2}+1}} - \frac{1}{(q+1)^{3/2}} \right) \right] \right\} \\
& - \frac{\mu a}{2C_2} + \frac{\mu a}{2C_3} + \frac{1}{32\pi} \frac{1}{1-\nu} - \frac{1}{32\pi} \left[\frac{7-8\nu}{1-\nu} \frac{1}{\sqrt{4N+1}} + \frac{1}{1-\nu} \frac{4N}{(4N+1)^{3/2}} \right] \\
& - \frac{1}{2\pi} \sum_{q=1}^{2N-1} \left[\left(1 - \frac{q}{\sqrt{\frac{q^2}{2}+1}} \right) + \frac{1}{2(1-\nu)} \frac{q}{(q+1)^{3/2}} \right]. \quad (112)
\end{aligned}$$

The force constant C_2 has been determined from previous computations for the screw dislocation. Assuming that the slight modification of the array does not have any influence on the value of C_2 , it is determined such that

$$\frac{\mu a}{C_2} + \frac{A}{4\pi} = \frac{1}{2}, \quad (113)$$

with

$$\begin{aligned}
A = & - \frac{1}{16\pi} \frac{3-4\nu}{1-\nu} + \frac{1}{8\pi} \frac{3-4\nu}{1-\nu} \sum_{q=1}^{\infty} \left(\frac{1}{q} - \frac{1}{\sqrt{\frac{q^2}{2}+1}} \right) + \frac{1}{8\pi} \frac{3-4\nu}{1-\nu} \sum_{q=1}^{\infty} \ln \frac{q^2+1}{q^2} \\
& + \frac{1}{4\pi} \frac{1}{1-\nu} \sum_{q=1}^{\infty} \frac{1}{q+1}. \quad (114)
\end{aligned}$$

So, $W/\mu a^3$ becomes, after transformation,

$$\frac{W}{\mu a^3} = 2N \left\{ \frac{1}{2} - \frac{1}{4\pi} \sum_{q=1}^{\infty} \left[2 \left(\frac{1}{q} - \frac{1}{\sqrt{\frac{q^2}{2}+1}} \right) + \frac{1}{2(1-\nu)} \frac{1}{(q+1)^{3/2}} \right] \right\} -$$

$$\begin{aligned}
& -\frac{\mu a}{2C_2} + \frac{\mu a}{2C_3} + \frac{1}{32\pi} \frac{1}{1-\nu} - \frac{1}{32\pi} \left[\frac{7-8\nu}{1-\nu} \frac{1}{\sqrt{4N^2+1}} + \frac{1}{1-\nu} \frac{4N}{(4N^2+1)^{3/2}} \right] \\
& - \frac{1}{2\pi} \sum_{q=1}^{2N-1} \left[\left(1 - \frac{q}{\sqrt{q^2+1}} \right) + \frac{1}{2(1-\nu)} \frac{q}{(q^2+1)^{3/2}} \right] \quad (115)
\end{aligned}$$

If Na is sufficiently large, but still smaller than the length of the dislocation line, the corresponding double kink will behave like two separate single kinks. Each will have an energy equal to half the energy of the whole kink, that is,

$$\begin{aligned}
\frac{W}{\mu a^2} = N - \frac{\mu a}{2C_2} + \frac{\mu a}{2C_3} + \frac{1}{32\pi} \frac{1}{1-\nu} - \frac{1}{2\pi} \sum_{q=1}^{\infty} \left[\left(1 - \frac{q}{\sqrt{q^2+1}} \right) \right. \\
\left. + \frac{1}{2(1-\nu)} \frac{q}{(q^2+1)^{3/2}} \right]. \quad (116)
\end{aligned}$$

The difference between twice the energy of a single kink and the energy of a double kink represents the interaction energy between the kinks. Two remarks are necessary here. First, a term proportional to the length of the kink is included in the final expression, and is expected to cancel out with a similar term in the correction energy. Secondly, the force constant C_3 appears. This has to be considered an unknown parameter, since there is no physical condition which can be applied to evaluate it. An approximation could be made by setting C_3 equal to C_2 , but there seems to be no particular justification for such an assumption.

The second step needed to obtain the final expression for the energy of a double kink is the computation of the difference between the correction energy for the pure screw dislocation and the correction

energy for the kinked screw dislocation. Since the former has already been computed, we shall focus our attention mainly on the latter.

The region that suffers a strain larger than one-half is bounded by the planes $x_3 = \pm a/2$, the surface parallel to \vec{x}_3 where the relative displacement is equal to $a/2$ and the plane $x_1 = Ra/2$ (see Figure 18). The region situated between $x_1 = Ra/2$ and $x_1 = Ra$ will not be considered, since its deformation is the same as for the straight screw dislocation.

We have already seen that the displacement field caused by the array of forces is

$$\begin{cases} u'_1(x_1, x_2, x_3) \\ u_2(x_1, x_3) + u'_2(x_1, x_2, x_3) \\ u'_3(x_1, x_2, x_3) \end{cases} \quad (117)$$

By taking into account the fact that after relaxation, the atomic positions need to be referred to their closest neighbors (see Figure 19), we are led to choose as actual displacement field across the slip plane the following expressions:

$$\begin{cases} v_1(x_1, y_2, x_3) = u'_1(x_1, x_2, x_3) \\ v_2(x_1, y_2, x_3) = u_2(x_1, x_3) + u'_2(x_1, x_2, x_3) - x_3 \\ v_3(x_1, y_2, x_3) = u'_3(x_1, x_2, x_3) \end{cases} \quad (118)$$

where y_2 is related to x_2 such that

$$\begin{aligned} x_3 > 0 & \quad y_2 = x_2 + \frac{a}{2} \\ x_3 < 0 & \quad y_2 = x_2 - \frac{a}{2} \end{aligned}$$

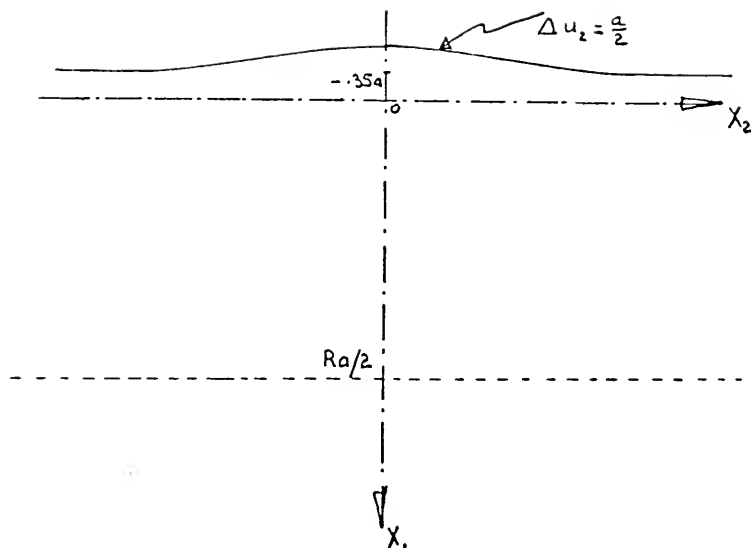


Figure 18. Region of High Strain for a Double Kink in a Screw Dislocation

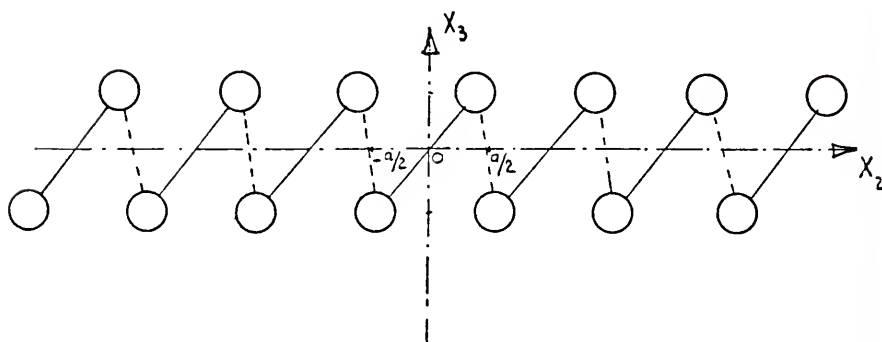


Figure 19. Atomic Relaxation for a Double Kink in a Screw Dislocation

The stress fields corresponding to \vec{u} and \vec{v} have the following components σ_{ij} and τ_{ij} , respectively,

$$\left\{ \begin{array}{l} \sigma_{11}(x_1, x_2, x_3) = (\lambda + 2\mu) \frac{\partial u'_1}{\partial x_1} + \lambda \left(\frac{\partial u'_2}{\partial x_2} + \frac{\partial u'_3}{\partial x_3} \right) \\ \sigma_{22}(x_1, x_2, x_3) = (\lambda + 2\mu) \frac{\partial u'_2}{\partial x_2} + \lambda \left(\frac{\partial u'_1}{\partial x_1} + \frac{\partial u'_3}{\partial x_3} \right) \\ \sigma_{33}(x_1, x_2, x_3) = (\lambda + 2\mu) \frac{\partial u'_3}{\partial x_3} + \lambda \left(\frac{\partial u'_1}{\partial x_1} + \frac{\partial u'_2}{\partial x_2} \right) \\ \sigma_{12}(x_1, x_2, x_3) = \mu \left(\frac{\partial u_2}{\partial x_1} + \frac{\partial u'_2}{\partial x_1} + \frac{\partial u'_1}{\partial x_2} \right) \\ \sigma_{13}(x_1, x_2, x_3) = \mu \left(\frac{\partial u'_1}{\partial x_3} + \frac{\partial u'_3}{\partial x_1} \right) \\ \sigma_{23}(x_1, x_2, x_3) = \mu \left(\frac{\partial u_2}{\partial x_3} + \frac{\partial u'_2}{\partial x_3} + \frac{\partial u'_3}{\partial x_2} \right) \end{array} \right. \quad (119)$$

and

$$\left\{ \begin{array}{l} \tau_{11}(x_1, y_2, x_3) = \sigma_{11}(x_1, x_2, x_3) \\ \tau_{22}(x_1, y_2, x_3) = \sigma_{22}(x_1, x_2, x_3) \\ \tau_{33}(x_1, y_2, x_3) = \sigma_{33}(x_1, x_2, x_3) \\ \tau_{12}(x_1, y_2, x_3) = \sigma_{12}(x_1, x_2, x_3) \\ \tau_{13}(x_1, y_2, x_3) = \sigma_{13}(x_1, x_2, x_3) \\ \tau_{23}(x_1, y_2, x_3) = \sigma_{23}(x_1, x_2, x_3) - \mu \end{array} \right. \quad (120)$$

Recalling Equation (79), the general form for the correction energy is the difference between the strain energies in the region of interest,

$$E_c = \frac{1}{2} \int_S \sigma_{ij} u_i n_j dS - \frac{1}{2} \int_{S'} \tau_{ij} v_i n_j dS' . \quad (121)$$

The surfaces S and S' differ only by the range of integration over x_2 and y_2 , respectively. When x_3 is positive, y_2 is defined between $-La/2 + a/2$ and $La/2 + a/2$, and when x_3 is negative, y_2 is defined between $-La/2 - a/2$ and $La/2 - a/2$. Under these conditions, the integrals involved with functions of y_2 can be considered as integrals of functions of x_2 with different limits. The various identities follow:

$$\int_{-La/2+a/2}^{La/2+a/2} f(y_2) dy_2 = \int_{-La/2}^{La/2} f(x_2) dx_2 \quad \text{for } x_3 > 0, \quad (122)$$

$$\int_{-La/2-a/2}^{La/2-a/2} f(y_2) dy_2 = \int_{-La/2}^{La/2} f(x_2) dx_2 \quad \text{for } x_3 < 0. \quad (123)$$

So E_c can be written as a surface integral over a function, depending on a unique variable x_2 .

$$E_c = \frac{1}{2} \int_S (\sigma_{ij} u_i - \tau_{ij} v_i) n_j dS . \quad (124)$$

Replacing τ_{ij} and v_i by their expressions as functions of σ_{ij} and u_i , respectively, leads to

$$E_c = \frac{1}{2} \int_S \left\{ x_3 \sigma_{21} n_1 + (x_3 \sigma_{22} + \mu u_3) n_2 + [\mu(u_2 - x_3) + x_3 \sigma_{23}] n_3 \right\} dS, \quad (125)$$

or

$$E_c = \frac{1}{2} \int_{-a/2}^{a/2} dx_3 \int_C \left[x_3 \sigma_{21} n_1 + (x_3 \sigma_{22} + \mu u_3) n_2 \right] ds \\ - \int_{-a/2}^{a/2} dx_3 \int_{-La/2}^{La/2} x_3 \sigma_{21} \left(\frac{Ra}{2}, x_2, x_3 \right) dx_2 dx_3 +$$

$$+ \int_{-La/2}^{La/2} dx_2 \int_{X_1(x_2)}^{Ra/2} \left[\mu u_2(x_1, x_2, \frac{a}{2}) - \mu \frac{a}{2} + \frac{a}{2} \sigma_{23}(x_1, x_2, \frac{a}{2}) \right] dx_1. \quad (126)$$

In these integrals, C is the curve defined by

$$u_2(x_1, \frac{a}{2}) + u_2'(x_1, x_2, \frac{a}{2}) = \frac{a}{4}, \quad (127)$$

that is, the "line of the kink," and $X_1(x_2)$ corresponds to a point (x_1, x_2) on this curve.

The evaluation of these integrals is a complicated mathematical problem which has to be solved numerically. Unfortunately, such numerical computations have not been possible to achieve yet, mainly because of the very complicated expressions for the displacement and strain fields. However, further research on this mathematical problem can be carried out and will lead to the correct answer for the energy of a double kink. The final expression for the energy would be obtained by subtracting the difference between the correction energies given by Equation (115). The linear term is expected to cancel, so that the energy is a finite number. The limit of this number when N becomes large would be twice the energy of the single kink.

CHAPTER 5

EDGE DISLOCATION IN SIMPLE CUBIC CRYSTAL CONSTRUCTED FROM AN ARRAY OF SHEAR LOOPS

The same procedure as followed in the case of the screw dislocation will be used in the case of the edge dislocation.

Displacement Field

As seen previously in the chapter concerning the whole rectangular array of point forces, the regions where the dislocation loop has a pure edge character are delimited by

$$\left\{ \begin{array}{l} x_1 = \epsilon_1 \\ x_2 = -\frac{La}{2} + \epsilon_2 \end{array} \right. \quad \text{and} \quad \left\{ \begin{array}{l} x_1 = \epsilon_1 \\ x_2 = \frac{La}{2} - \epsilon_2 \end{array} \right.$$

where ϵ_1 and ϵ_2 are small compared to Ra and La , respectively. Since both regions simulate two identical parallel dislocations of opposite sense, we shall only consider the first one. A translation of the \vec{x}_2 axis to the first row of forces $x_2 = -La/2$ will simplify the expressions. The same symbols x_1 and x_2 will be kept, having now the meaning of ϵ_1 and ϵ_2 , respectively. This part of the array of forces is represented in Figure 20. The only difference with Equation (21) is now the summation of q will be $\sum_{q=0}^L$ and $\sum_{q=1}^{L-1}$. So, $u_m(\vec{r})$ becomes:

$$u_m(\vec{r}) = \frac{\mu a^2}{2} \sum_{p=-R/2}^{R/2} \left\{ \left(\sum_{q=0}^L + \sum_{q=1}^{L-1} \right) \left[G_{2m}(x_1 - pa, x_2 - qa, x_3 - \frac{a}{2}) - \right. \right.$$

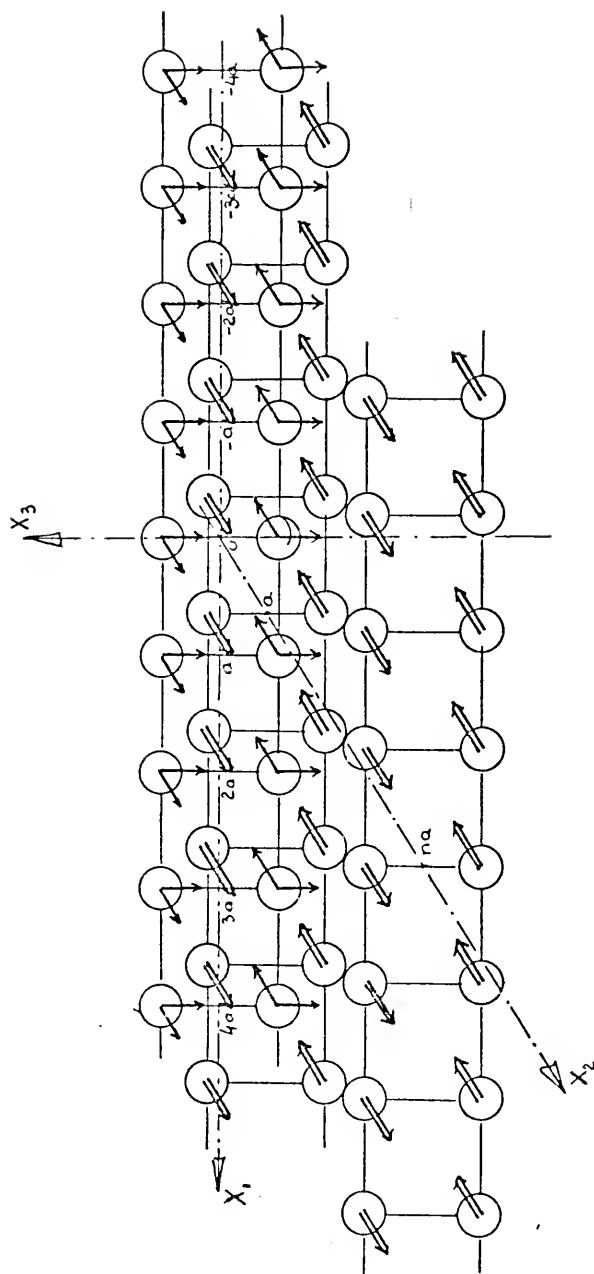


Figure 20. Array of Forces Simulating an Edge Dislocation

$$\begin{aligned}
& - G_{2m}(x_1 - pa, x_2 - qa, x_3 + \frac{a}{2}) - \left[G_{3m}(x_1 - pa, x_2, x_3 - \frac{a}{2}) \right. \\
& + G_{3m}(x_1 - pa, x_2, x_3 + \frac{a}{2}) + \left. G_{3m}(x_1 - pa, x_2 - La, x_3 - \frac{a}{2}) \right. \\
& \left. + G_{3m}(x_1 - pa, x_2 - La, x_3 + \frac{a}{2}) \right] \Bigg\}. \quad (128)
\end{aligned}$$

The summations on p and q will be accomplished as before, with the help of Euler's formula (Equation (29)). The first summation carried out will be on p , since the displacement field of the edge dislocation ought to be independent of x_1 . Euler's formula becomes simply,

$$\sum_{p=-R/2}^{R/2} f(p) = \int_{-\infty}^{+\infty} f(x) dx, \quad (129)$$

where f is a symbol for the whole expression to be summed. The displacement field takes the form:

$$u_1(x_1, x_2, x_3) = 0 \quad (130)$$

$$\begin{aligned}
u_2(x_1, x_2, x_3) = & \frac{a}{16\pi} \left(\sum_{q=0}^L + \sum_{q=1}^{L-1} \right) \left\{ \frac{3-4\nu}{2(1-\nu)} \ell\pi \frac{(x_2 - qa)^2 + (x_3 + \frac{a}{2})^2}{(x_2 - qa)^2 + (x_3 - \frac{a}{2})^2} \right. \\
& + \frac{1}{1-\nu} \left[\frac{(x_3 + \frac{a}{2})^2}{(x_2 - qa)^2 + (x_3 + \frac{a}{2})^2} - \frac{(x_3 - \frac{a}{2})^2}{(x_2 - qa)^2 + (x_3 - \frac{a}{2})^2} \right] \Bigg\} \\
& - \frac{a}{16\pi(1-\nu)} \left[\frac{x_2(x_3 - \frac{a}{2})}{x_2^2 + (x_3 - \frac{a}{2})^2} + \frac{x_2(x_3 + \frac{a}{2})}{x_2^2 + (x_3 + \frac{a}{2})^2} \right] \quad (131)
\end{aligned}$$

$$u_3(x_1, x_2, x_3) = \frac{a}{16\pi(1-\nu)} \left(\sum_{q=0}^L + \sum_{q=1}^{L-1} \right) \left[\frac{(x_2 - qa)(x_3 - \frac{a}{2})}{(x_2 - qa)^2 + (x_3 - \frac{a}{2})^2} - \right.$$

$$\begin{aligned}
& - \frac{(x_2 - qa)(x_3 + \frac{a}{2})}{(x_2 - qa)^2 + (x_3 + \frac{a}{2})^2} \Bigg] + \frac{a}{4\pi} \frac{1-2\nu}{1-\nu} \ell n \frac{R/2 + \sqrt{R^2/4 + L^2}}{R} \\
& - \frac{a}{8\pi} \frac{3-4\nu}{1-\nu} \ell n L + \frac{a}{32\pi} \frac{3-4\nu}{1-\nu} \left\{ \ell n \left[x_2^2 + (x_3 - \frac{a}{2})^2 \right] + \right. \\
& \left. + \ell n \left[x_2^2 + (x_3 + \frac{a}{2})^2 \right] \right\} - \frac{a}{16\pi} \frac{1}{1-\nu} \left\{ \frac{(x_3 - \frac{a}{2})^2}{x_2^2 + (x_3 - \frac{a}{2})^2} + \frac{(x_3 + \frac{a}{2})^2}{x_2^2 + (x_3 + \frac{a}{2})^2} \right\}.
\end{aligned} \tag{132}$$

Unfortunately, these expressions are much less simple than those found for the screw dislocation. But some of the essential features of the displacement field of the edge dislocation can be noticed already, that is, the lack of displacement in the \vec{x}_1 direction and the fact that u_2 and u_3 are independent of x_1 .

Euler's formula applied a second time will give us the final expression for the displacement field. The mathematical difficulty, arising because of the singular points in the integrand, is overcome in the same way as for the screw dislocation. The same symbols, u_2^i and u_3^j , will be used for the successive terms added to approximate u_2 and u_3 , respectively. For $u_2^i(x_1, x_2, x_3)$ we find

$$\begin{aligned}
u_2^0(x_1, x_2, x_3) &= \frac{1}{4\pi} \left\{ \begin{aligned} & \int_{-\pi a}^{\pi a} \left[2\pi x_3 + (x_3 + \frac{a}{2}) \left[\tan^{-1} \frac{x_2}{x_3 + \frac{a}{2}} + \tan^{-1} \frac{x_2 - a}{x_3 + \frac{a}{2}} \right] \right. \\ & \left. - (x_3 - \frac{a}{2}) \left[\tan^{-1} \frac{x_2}{x_3 - \frac{a}{2}} + \tan^{-1} \frac{x_2 - a}{x_3 - \frac{a}{2}} \right] \right] \end{aligned} \right\} \\
&+ \frac{1}{32\pi} \frac{3-4\nu}{1-\nu} \left[x_2 \ell n \frac{x_2^2 + (x_3 + \frac{a}{2})^2}{x_2^2 + (x_3 - \frac{a}{2})^2} + (x_2 - a) \ell n \frac{(x_2 - a)^2 + (x_3 + \frac{a}{2})^2}{(x_2 - a)^2 + (x_3 - \frac{a}{2})^2} \right] -
\end{aligned}$$

$$- \frac{a}{16\pi} \frac{1}{1-\nu} \left[\frac{x_2(x_3 - \frac{a}{2})}{x_2^2 + (x_3 - \frac{a}{2})^2} + \frac{x_2(x_3 + \frac{a}{2})}{x_2^2 + (x_3 + \frac{a}{2})^2} \right], \quad (133)$$

$$\begin{aligned} u_2^1(x_1, x_2, x_3) = & \frac{a}{16\pi} \frac{3-4\nu}{1-\nu} \left[\ell\pi \frac{x_2^2 + (x_3 + \frac{a}{2})^2}{x_2^2 + (x_3 - \frac{a}{2})^2} + \ell\pi \frac{(x_2 - a)^2 + (x_3 + \frac{a}{2})^2}{(x_2 - a)^2 + (x_3 - \frac{a}{2})^2} \right] \\ & + \frac{a}{32\pi} \frac{1}{1-\nu} \left[\frac{(x_3 - \frac{a}{2})^2}{x_2^2 + (x_3 - \frac{a}{2})^2} + \frac{(x_3 - \frac{a}{2})^2}{(x_2 - a)^2 + (x_3 - \frac{a}{2})^2} - \frac{(x_3 + \frac{a}{2})^2}{x_2^2 + (x_3 + \frac{a}{2})^2} \right. \\ & \left. - \frac{(x_3 + \frac{a}{2})^2}{(x_2 - a)^2 + (x_3 + \frac{a}{2})^2} \right], \quad (134) \end{aligned}$$

$$\begin{aligned} u_2^2(x_1, x_2, x_3) = & - \frac{a^2}{192\pi} \frac{3-4\nu}{1-\nu} \left[\frac{x_2}{x_2^2 + (x_3 - \frac{a}{2})^2} + \frac{x_2 - a}{(x_2 - a)^2 + (x_3 - \frac{a}{2})^2} \right. \\ & \left. - \frac{x_2}{x_2^2 + (x_3 + \frac{a}{2})^2} - \frac{x_2 - a}{(x_2 - a)^2 + (x_3 + \frac{a}{2})^2} \right] + \frac{a^2}{96\pi} \frac{1}{1-\nu} \left[\frac{x_2(x_3 - \frac{a}{2})^2}{[x_2^2 + (x_3 - \frac{a}{2})^2]^2} \right. \\ & \left. + \frac{(x_2 - a)(x_3 - \frac{a}{2})^2}{[(x_2 - a)^2 + (x_3 - \frac{a}{2})^2]^2} - \frac{x_2(x_3 + \frac{a}{2})^2}{[x_2^2 + (x_3 + \frac{a}{2})^2]^2} - \frac{(x_2 - a)(x_3 + \frac{a}{2})^2}{[(x_2 - a)^2 + (x_3 + \frac{a}{2})^2]^2} \right], \quad (135) \end{aligned}$$

$$\begin{aligned} u_2^3(x_1, x_2, x_3) = & \frac{a^5}{5760\pi} \frac{3-4\nu}{1-\nu} \left\{ \frac{x_2 [x_2^2 - 3(x_3 - \frac{a}{2})^2]}{[x_2^2 + (x_3 - \frac{a}{2})^2]^3} + \right. \\ & + \frac{(x_2 - a) [(x_2 - a)^2 - 3(x_3 - \frac{a}{2})^2]}{[(x_2 - a)^2 + (x_3 - \frac{a}{2})^2]^3} - \frac{x_2 [x_2^2 - 3(x_3 + \frac{a}{2})^2]}{[x_2^2 + (x_3 + \frac{a}{2})^2]^3} \\ & \left. - \frac{(x_2 - a) [(x_2 - a)^2 - 3(x_3 + \frac{a}{2})^2]}{[(x_2 - a)^2 + (x_3 + \frac{a}{2})^2]^3} \right\} - \frac{a^4}{480\pi} \frac{1}{1-\nu} x \end{aligned}$$

$$\begin{aligned}
& \left\{ \left(x_3 - \frac{a}{2}\right)^2 \frac{x_2 \left[x_1^2 - \left(x_3 - \frac{a}{2}\right)^2\right]}{\left[x_2^2 + \left(x_3 - \frac{a}{2}\right)^2\right]^4} - \left(x_3 + \frac{a}{2}\right)^2 \frac{x_2 \left[x_2^2 - \left(x_3 + \frac{a}{2}\right)^2\right]}{\left[x_2^2 + \left(x_3 + \frac{a}{2}\right)^2\right]^4} \right. \\
& + \left(x_3 - \frac{a}{2}\right)^2 \frac{(x_2 - a) \left[(x_2 - a)^2 - \left(x_3 - \frac{a}{2}\right)^2\right]}{\left[(x_2 - a)^2 + \left(x_3 - \frac{a}{2}\right)^2\right]^4} \\
& \left. - \left(x_3 + \frac{a}{2}\right)^2 \frac{(x_2 - a) \left[(x_2 - a)^2 - \left(x_3 + \frac{a}{2}\right)^2\right]}{\left[(x_2 - a)^2 + \left(x_3 + \frac{a}{2}\right)^2\right]^4} \right\} \quad (136)
\end{aligned}$$

with

$$u_2 = u_2^0 + u_2^1 + u_2^2 + u_2^3 + \dots \quad (137)$$

For $u_3^j(x_1, x_2, x_3)$ we find

$$\begin{aligned}
u_3^0 &= \frac{(1-2\nu)a}{4\pi(1-\nu)} \ell n \frac{R/2 + \sqrt{R^2/4 + L^2}}{RLa} + \frac{1}{32\pi(1-\nu)} \left\{ \left(x_3 - \frac{a}{2}\right) \right. \\
& \left[\ell n \left[\left(x_3 - \frac{a}{2}\right)^2 + x_2^2 \right] + \ell n \left[\left(x_3 - \frac{a}{2}\right)^2 + (x_2 - a)^2 \right] \right] - \left(x_3 + \frac{a}{2}\right) \\
& \left[\ell n \left[\left(x_3 + \frac{a}{2}\right)^2 + x_2^2 \right] + \ell n \left[\left(x_3 + \frac{a}{2}\right)^2 + (x_2 - a)^2 \right] \right] \Big\} \\
& + \frac{a(3-4\nu)}{32\pi(1-\nu)} \left\{ \ell n \left[x_2^2 + \left(x_3 - \frac{a}{2}\right)^2 \right] + \ell n \left[x_2^2 + \left(x_3 + \frac{a}{2}\right)^2 \right] \right\} \\
& - \frac{a}{16\pi(1-\nu)} \left[\frac{\left(x_3 - \frac{a}{2}\right)^2}{x_2^2 + \left(x_3 - \frac{a}{2}\right)^2} + \frac{\left(x_3 + \frac{a}{2}\right)^2}{x_2^2 + \left(x_3 + \frac{a}{2}\right)^2} \right] , \quad (138)
\end{aligned}$$

$$u_3^1(x_1, x_2, x_3) = \frac{a}{32\pi(1-\nu)} \left[\frac{x_2 \left(x_3 - \frac{a}{2}\right)}{x_2^2 + \left(x_3 - \frac{a}{2}\right)^2} - \frac{x_2 \left(x_3 + \frac{a}{2}\right)}{x_2^2 + \left(x_3 + \frac{a}{2}\right)^2} + \right.$$

$$+ \frac{(x_2 - a)(x_3 - \frac{a}{2})}{(x_2 - a)^2 + (x_3 - \frac{a}{2})^2} - \frac{(x_2 - a)(x_3 + \frac{a}{2})}{(x_2 - a)^2 + (x_3 + \frac{a}{2})^2} \Bigg], \quad (139)$$

$$u_3^2(x_1, x_2, x_3) = -\frac{a^2}{1920\pi(1-\nu)} \left\{ (x_3 - \frac{a}{2}) \left[\frac{x_2^2 - (x_3 - \frac{a}{2})^2}{[(x_2^2 + (x_3 - \frac{a}{2})^2]^2} \right. \right. \\ + \frac{(x_2 - a)^2 - (x_3 - \frac{a}{2})^2}{[(x_2 - a)^2 + (x_3 - \frac{a}{2})^2]^2} \Bigg] + (x_3 + \frac{a}{2}) \left[\frac{x_2^2 - (x_3 + \frac{a}{2})^2}{[x_2^2 + (x_3 + \frac{a}{2})^2]^2} \right. \\ + \left. \left. \frac{(x_2 - a)^2 - (x_3 + \frac{a}{2})^2}{[(x_2 - a)^2 + (x_3 + \frac{a}{2})^2]^2} \right] \right\}, \quad (140)$$

$$u_3^3(x_1, x_2, x_3) = \frac{a^4}{1920\pi(1-\nu)} \left\{ (x_3 - \frac{a}{2}) \left[\frac{x_2^4 - 6(x_3 - \frac{a}{2})^2 x_2^2 + (x_3 - \frac{a}{2})^4}{[x_2^2 + (x_3 - \frac{a}{2})^2]^4} \right. \right. \\ + \frac{(x_2 - a)^4 - 6(x_3 - \frac{a}{2})^2 (x_2 - a)^2 + (x_3 - \frac{a}{2})^4}{[(x_2 - a)^2 + (x_3 - \frac{a}{2})^2]^4} \Bigg] \\ - (x_3 + \frac{a}{2}) \left[\frac{x_2^4 - 6(x_3 + \frac{a}{2})^2 x_2^2 + (x_3 + \frac{a}{2})^4}{[x_2^2 + (x_3 + \frac{a}{2})^2]^4} \right. \\ + \left. \left. \frac{(x_2 - a)^4 - 6(x_3 + \frac{a}{2})^2 (x_2 - a)^2 + (x_3 - \frac{a}{2})^4}{[(x_2 - a)^2 + (x_3 + \frac{a}{2})^2]^4} \right] \right\} \quad (141)$$

with

$$u_3 = u_3^0 + u_3^1 + u_3^2 + u_3^3 + \dots \quad (142)$$

The constant in the expression of u_3 means only that the point of non-bending of the lattice planes is set at $x_2 = La/2$. However, the relative positions of the atoms with respect to each other are independent of this constant, and the stress and strain fields will not depend on the constant terms.

The component $u_2(x_1, x_2, x_3)$ has four singular points ($x_2 = 0$, $x_2 = a$ with $x_3 = \pm a/2$) and $u_3(x_1, x_2, x_3)$ has two singular points ($x_2 = 0$ with $x_3 = \pm a/2$). This is not surprising, since the whole array of forces is a superposition of two arrays of forces having magnitude $\mu a^2/2$, one starting at $x_2 = 0$ and one starting at $x_2 = a$.

An asymptotic expression for u_2 and u_3 can be computed by considering x_2 and x_3 large with respect to the atomic distance.

The following expressions are found:

$$u_1(x_1, x_2, x_3) = 0, \quad (143)$$

$$u_2(x_1, x_2, x_3) = \frac{a}{2\pi} \left\{ \begin{array}{c} \pi/2 \\ -\pi/2 \end{array} + \tan^{-1} \frac{x_2}{x_3} - \frac{1}{2(1-\nu)} \frac{x_2 x_3}{x_2^2 + x_3^2} \right\}, \quad (144)$$

$$u_3(x_1, x_2, x_3) = \frac{a}{2\pi} \left\{ \frac{1-2\nu}{4(1-\nu)} \ln(x_2^2 + x_3^2) - \frac{1}{2(1-\nu)} \frac{x_3^2}{x_2^2 + x_3^2} \right\}. \quad (145)$$

These equations can be compared to those arising from the ordinary continuum model for an edge dislocation of the same sign [20]:

$$u_1(x_1, x_2, x_3) = 0, \quad (146)$$

$$u_2(x_1, x_2, x_3) = -\frac{a}{2\pi} \left[\tan^{-1} \frac{x_3}{x_2} + \frac{x_2 x_3}{2(1-\nu)(x_2^2 + x_3^2)} \right], \quad (147)$$

$$u_3(x_1, x_2, x_3) = \frac{a}{2\pi} \left[\frac{1-2\nu}{4(1-\nu)} \ln(x_2^2 + x_3^2) + \frac{x_2^2 - x_3^2}{4(1-\nu)(x_2^2 + x_3^2)} \right]. \quad (148)$$

Both sets of equations are identical when one is aware that u_3 is determined only up to a constant. Adding the expression $a/8\pi(1-\nu)$ to Equation (145) leads automatically to Equation (148); this physically means a change in the "cut plane." One can notice too that these asymptotic expressions for \vec{u} come only from the first approximation \vec{u}^0 . This means that for a point situated at a large distance from the dislocation line, the discrete array of point forces appears to be a continuous distribution of force on the two planes $x_3 = \pm a/2$.

A mapping of the atomic displacements, except for the singular points, is shown in Figure 21. Obviously, this model shows a strong dissymmetry with respect to the extra half plane ($x_2 = .75a$, with $x_3 < 0$) in the region of the core.

The relative displacement across the slip plane in the direction \vec{x}_2 is simply a particular case of the expression of $u_2(x_1, x_2, x_3)$, as obtained before for the screw dislocation:

$$\Delta u_2(x_2) = u_2(x_2, \frac{a}{2}) - u_2(x_2, -\frac{a}{2}) = 2u_2(x_2, \frac{a}{2}). \quad (149)$$

A suitable form for $\Delta u_2(x_2)$ can be obtained either from Equation (131) or the set of Equations (133) to (136):

$$\Delta u_2(x_2) = \frac{a}{8\pi} \left(\sum_{q=0}^L + \sum_{q=1}^{L-1} \right) \left\{ \frac{3-4\nu}{2(a-\nu)} \ln \frac{(x_2 - qa)^2 + a^2}{(x_2 - qa)^2} + \frac{1}{1-\nu} \frac{a^2}{(x_2 - qa)^2 + a^2} \right\} - \frac{a}{8\pi(1-\nu)} \frac{ax_2}{x_2^2 + a^2}, \quad (150)$$

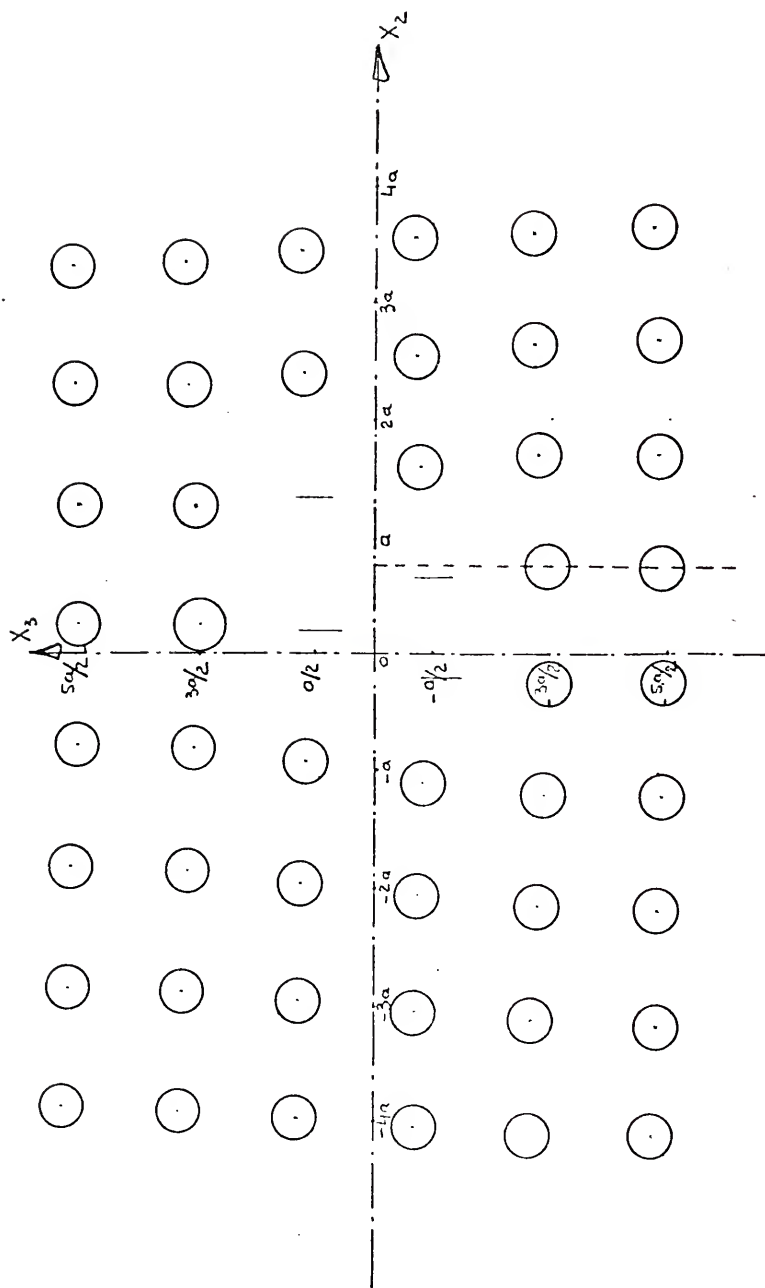


Figure 21. Atomic Arrangement in $x_1 = 0$ Plane for an Edge Dislocation

or

$$\Delta u_2(x_2) = \Delta u_2^0(x_2) + \Delta u_2^1(x_2) + \Delta u_2^2(x_2) + \Delta u_2^3(x_2) + \dots \quad (151)$$

with

$$\begin{aligned} \Delta u_2^0(x_2) = & \frac{a}{2\pi} \left\{ \pi + \tan^{-1} \frac{x_2}{a} + \tan^{-1} \frac{x_2 - a}{a} \right\} + \frac{a^2}{8\pi} \frac{1}{1-\nu} \frac{x_2}{x_2 + a^2} \\ & + \frac{1}{16\pi} \frac{3-4\nu}{1-\nu} \left\{ x_2 \ell n \frac{x_2^2 + a^2}{x_2^2} + (x_2 - a) \ell n \frac{(x_2 - a)^2 + a^2}{(x_2 - a)^2} \right\}, \end{aligned} \quad (152)$$

$$\begin{aligned} \Delta u_2^1(x_2) = & \frac{a}{32\pi} \frac{3-4\nu}{1-\nu} \left[\ell n \frac{x_2^2 + a^2}{x_2^2} + \ell n \frac{(x_2 - a)^2 + a^2}{(x_2 - a)^2} \right] \\ & - \frac{a^3}{16\pi} \frac{1}{1-\nu} \left[\frac{1}{x_2^2 + a^2} + \frac{1}{(x_2 - a)^2 + a^2} \right], \end{aligned} \quad (153)$$

$$\begin{aligned} \Delta u_2^2(x_2) = & - \frac{a^2}{96\pi} \frac{3-4\nu}{1-\nu} \left[\frac{1}{x_2} + \frac{1}{x_2 - a} - \frac{x_2}{x_2^2 + a^2} - \frac{x_2 - a}{(x_2 - a)^2 + a^2} \right] \\ & - \frac{a^4}{48\pi} \frac{1}{1-\nu} \left[\frac{x_2}{\left(\frac{x_2^2 + a^2}{x_2^2 + a^2} \right)^2} + \frac{x_2 - a}{\left[\frac{(x_2 - a)^2 + a^2}{(x_2 - a)^2 + a^2} \right]^2} \right], \end{aligned} \quad (154)$$

$$\begin{aligned} \Delta u_2^3(x_2) = & \frac{a^4}{2880\pi} \frac{3-4\nu}{1-\nu} \left\{ \left[\frac{1}{x_2^3} + \frac{1}{(x_2 - a)^3} - \frac{x_2(x_2^2 - 3a^2)}{(x_2^2 + a^2)^3} \right] \right. \\ & - \frac{(x_2 - a) \left[(x_2 - a)^2 - 3a^2 \right]}{\left[(x_2 - a)^2 + a^2 \right]^3} \left. \right\} + \frac{a^6}{240\pi} \frac{1}{1-\nu} \left\{ \frac{x_2(x_2^2 - a^2)}{\left(\frac{x_2^2 + a^2}{x_2^2 + a^2} \right)^4} \right. \\ & + \frac{(x_2 - a) \left[(x_2 - a)^2 - a^2 \right]}{\left[(x_2 - a)^2 + a^2 \right]^4} \left. \right\}. \end{aligned} \quad (155)$$

The curves representing Δu_2 are plotted in Figures 22 and 23, corresponding to the region close to the dislocation line and to a more extended region, respectively. Only a few terms Δu_2^i are needed to obtain relative precision equal to 10^{-3} in the region outside the points $x_2 = -a$ and $x_2 = 2a$. Unfortunately, the region in between is not known and $\Delta u_2(0)$ and $\Delta u_2(a)$ must be evaluated by an interpolation scheme. Values of Δu_2 are listed in Table 7.

TABLE 7. Relative Displacement Across the Slip Plane for an Edge Dislocation

x_2/a	$\Delta u_2/a$
- 5	.0512
- 4	.0626
- 3	.0805
- 2	.1123
- 1	.1817
0	\approx .4
1	\approx .68
2	.8280
3	.8921
4	.9221
5	.9391

The width of the dislocation can be reached by evaluating the region where the relative displacement has values between $a/4$ and $3a/4$. From Figure 22, this region can be easily measured and has the value $W = 1.93a$. This value is slightly higher than that obtained from Peierls' model ($W = 1.5a$ for $\nu = 1/3$). This would mean that our model shows a dislocation slightly more extended than Peierls' model. This result is opposite to what has been found for the screw dislocation.

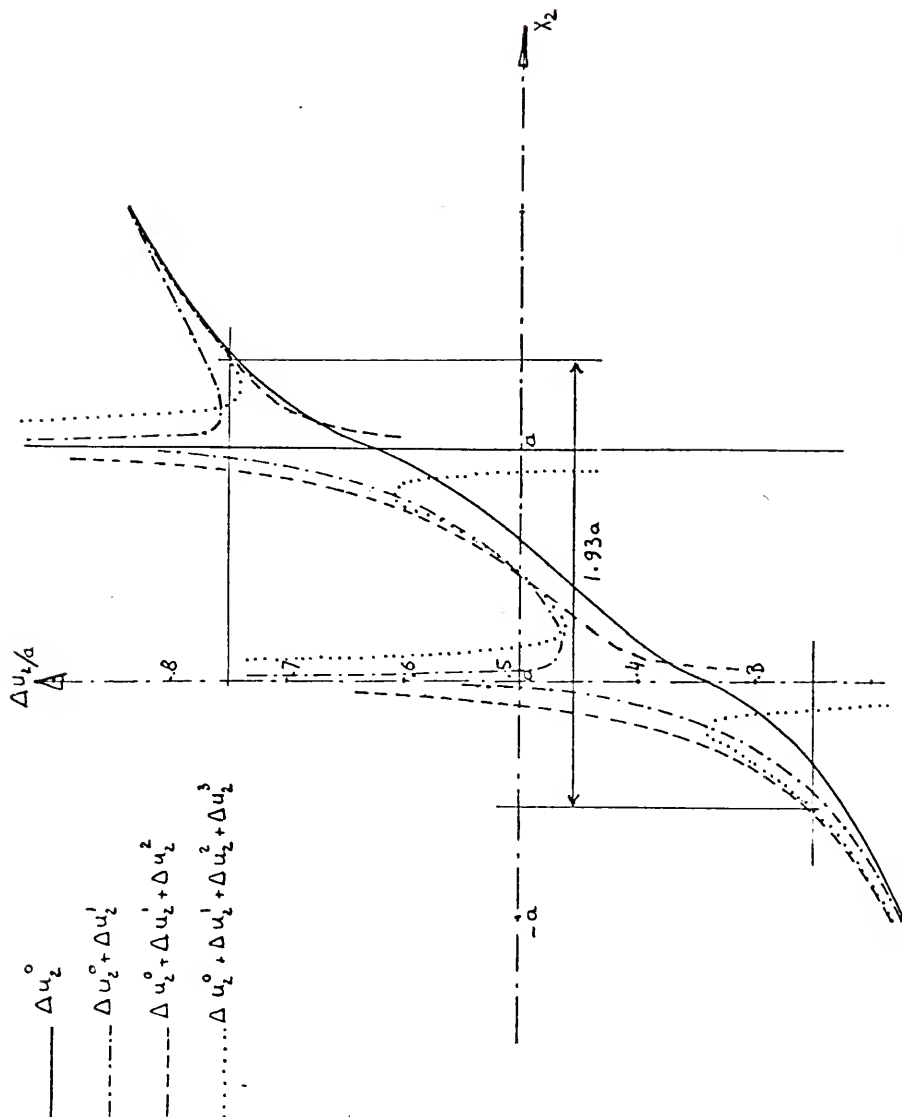


Figure 22. Relative Displacement Close to the Core of an Edge Dislocation

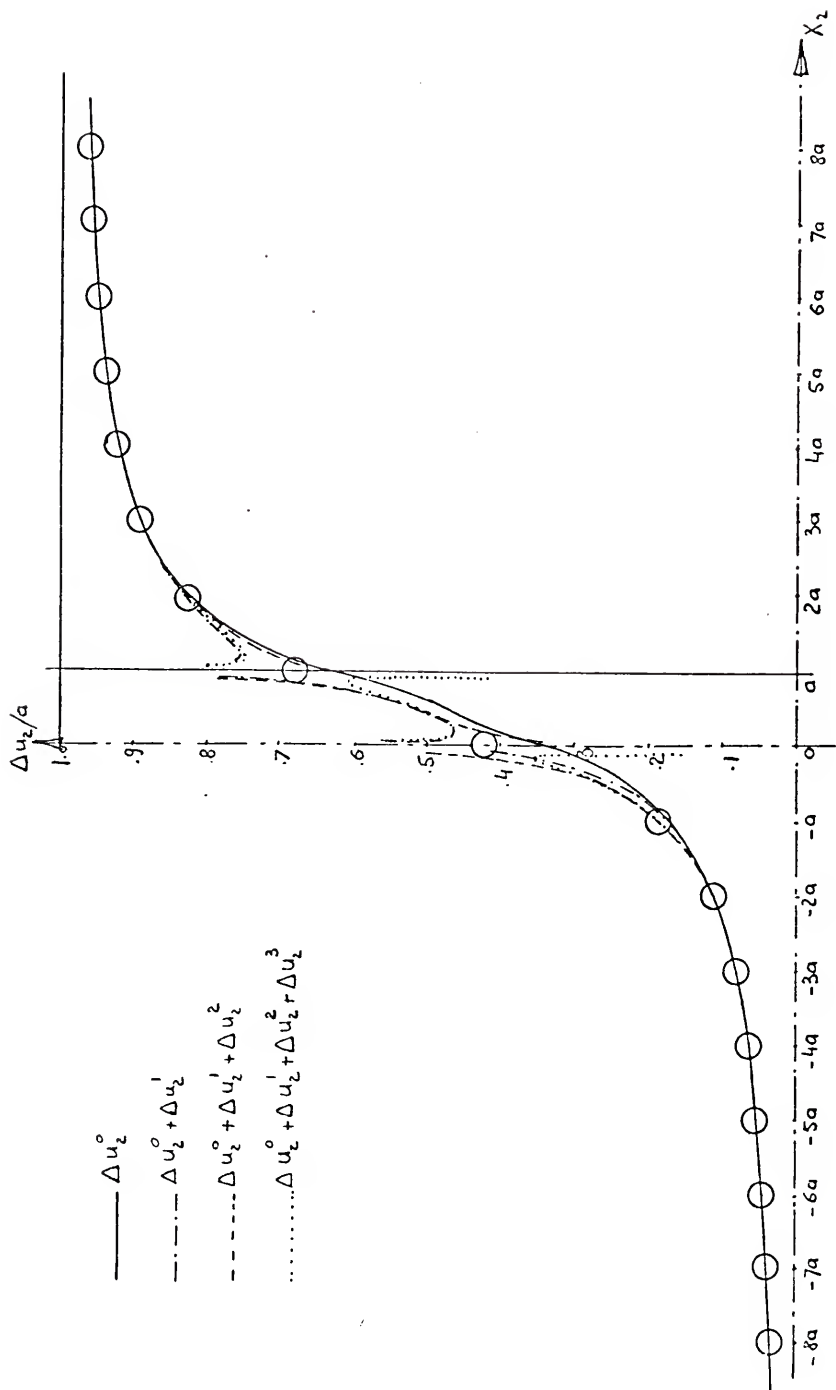


Figure 23. Relative Displacement for an Edge Dislocation

The relative displacement at atomic points can also be obtained directly from Equation (128):

$$\Delta u_2(na) = \mu a^2 \sum_{p=-\infty}^{+\infty} \left\{ \left(\sum_{q=0}^{\infty} + \sum_{q=1}^{\infty} \right) \left[G_{22}(pa, na-qa, 0) - G_{22}(pa, na-qa, a) \right] - \left[G_{23}(pa, na, 0) + G_{23}(pa, na, a) \right] \right\}. \quad (156)$$

Replacing the variable $(n-q)$ by u and making the singular point appear at $q=n$, leads to the three following equations for $\Delta u_2(na)$ corresponding to $n > 1$, $n = 1$ and $n = 0$, respectively.

$$\begin{aligned} \Delta u_2(na) = & \mu a^2 \sum_{p=-\infty}^{+\infty} \left(\sum_{u=1}^n + \sum_{u=1}^{n-1} + \sum_{u=1}^{\infty} \right) \left[G_{22}(pa, ua, 0) - G_{22}(pa, ua, a) \right] - \mu a^2 \sum_{p=-\infty}^{+\infty} G_{23}(pa, na, a) \\ & + 4\mu a^2 \sum_{p=1}^{\infty} \left[G_{22}(pa, 0, 0) - G_{22}(pa, 0, a) \right] + \frac{2\mu a^2}{C_2} - 2\mu a^2 G_{22}(0, 0, a), \end{aligned} \quad (157)$$

$$\begin{aligned} \Delta u_2(a) = & 2\mu a^2 \sum_{p=-\infty}^{+\infty} \sum_{u=1}^{\infty} \left[G_{22}(pa, ua, 0) - G_{22}(pa, ua, a) \right] \\ & + \mu a^2 \sum_{p=-\infty}^{+\infty} \left[G_{22}(pa, a, 0) - G_{22}(pa, a, a) - G_{23}(pa, a, a) \right] \\ & + 4\mu a^2 \sum_{p=1}^{\infty} \left[G_{22}(pa, 0, 0) - G_{22}(pa, 0, a) \right] + \frac{2\mu a^2}{C_2} - 2\mu a^2 G_{22}(0, 0, a), \end{aligned} \quad (158)$$

$$\begin{aligned} \Delta u_2(0) = & 2\mu a^2 \sum_{p=-\infty}^{+\infty} \sum_{u=1}^{\infty} \left[G_{22}(pa, ua, 0) - G_{22}(pa, ua, a) \right] \\ & + 2\mu a^2 \sum_{p=1}^{\infty} \left[G_{22}(pa, 0, 0) - G_{22}(pa, 0, a) \right] + \frac{\mu a^2}{C_2} - \mu a^2 G_{22}(0, 0, a). \end{aligned} \quad (159)$$

After computation of the discrete sums using Equation (26), these three equations become, in the same order:

$$\Delta u_2(na) = \frac{2\mu a^2}{C_2} + \frac{a}{8\pi} \frac{11.4392 - 9.4720\nu}{1-\nu} - \frac{a}{8\pi} \frac{1}{1-\nu} \frac{n}{n+1} - \frac{a}{16\pi} \left(\sum_{p=n}^{\infty} + \sum_{p=n+1}^{\infty} \right) \left[\frac{3-4\nu}{1-\nu} \ell n \frac{p^2+1}{p^2} + \frac{1}{1-\nu} \frac{2}{p+1} \right], \quad (160)$$

$$\Delta u_2(a) = \frac{2\mu a^2}{C_2} + \frac{a}{8\pi} \frac{6.4060 - 5.6512\nu}{1-\nu}, \quad (161)$$

$$\Delta u_2(0) = \frac{\mu a^2}{C_2} + \frac{a}{16\pi} \frac{11.4392 - 9.4720\nu}{1-\nu}. \quad (162)$$

For each value of n , a direct comparison can be made between Equations (160) to (162) on the one hand, and Equations (133) to (136) on the other hand. Since both ought to be identical, C_2 can be easily deduced by subtraction. Values of $\Delta u_2(na)$ computed in both ways and the corresponding $C_2(n)$ are listed in Table 8. These values have been computed for $\nu = 1/3$. The force constants C_2 seem to be much more sensitive to n in the case of the edge dislocation than in the case of the screw dislocation. Therefore the evaluation of the atomic displacements at $x_2 = 0$ and $x_2 = a$, using the technique employed for the screw dislocation is not possible due to the uncertainty of $C_2(0)$ and $C_2(1)$. If the variation of $C_2(n)$ is neglected after a few atomic distances from the dislocation line, and $C_2(n)$ set equal to $C_2(\infty)$ for every n , the relative displacement becomes

$$\Delta u_2(na) = a - \frac{a}{16\pi} \left(\sum_{p=n}^{\infty} + \sum_{p=n+1}^{\infty} \right) \left[\frac{3-4\nu}{1-\nu} \ell n \frac{p^2+1}{p^2} + \frac{1}{1-\nu} \frac{2}{p+1} \right] - \frac{a}{8\pi} \frac{1}{1-\nu} \frac{n}{n+1}. \quad (163)$$

Table 8. Relative Displacements and Force Constants C_2 at Singular Points for an Edge Dislocation

n	$\frac{1}{a} \left\{ \Delta u_2(n) - \frac{2\mu a^2}{C_2} \right\}$	$\Delta u_2(n)/a$	C_2
0	.253	$\approx .4$	≈ 6.80
1	.232	$\approx .68$	≈ 4.40
2	.3625	.8280	4.2792
3	.4027	.8921	4.0867
4	.4243	.9221	4.0176
5	.4376	.9391	3.9872
6	.4466	.9500	3.9729
7	.4531	.9576	3.9635
8	.4580	.9632	3.9588
9	.4619	.9675	3.9557
10	.4649	.9709	3.9526
\vdots	\vdots	\vdots	\vdots
∞	.4927	1.0000	3.9432

The relative displacement at atomic points corresponding to negative x_1 ($x_1 = -na$) can be deduced directly from Equation (150):

$$\Delta u_2(-na) = \frac{a}{16\pi} \left(\sum_{p=n}^{\infty} + \sum_{p=n+1}^{\infty} \right) \left[\frac{3-4\nu}{1-\nu} 2\pi \frac{p^2+1}{p^2} + \frac{1}{1-\nu} \frac{2}{p^2+1} \right] + \frac{a}{8\pi} \frac{1}{1-\nu} \frac{n}{n+1} \quad (164)$$

One can notice that adding Equations (163) and (164) leads simply to a. This means that making the approximation that $C_2(n)$ is constant and equal to $C_2^{(\infty)}$ for every n would imply that the relative displacement is symmetrical with respect to $x_1 = 0$. But this is in contradiction with the actual relative displacement computed from Equations (152) to (155) and listed in Table 8, where a symmetry with respect to $x_1 = a/2$ is

clearly apparent. So, contrary to the case of the screw dislocation, $C_2(n)$ cannot be replaced by $C_2^{(\infty)}$, and their difference is sufficient to shift the symmetry of the dislocation with respect to $x_1 = a/2$ to $x_1 = 0$. In fact, it seems logical that in both cases, for the screw dislocation as well as for the edge dislocation, the dislocation line lies between two rows of atoms.

As mentioned for the screw dislocation, a distribution function for infinitesimal dislocation loops can be introduced, following Equation (64). Its expression is the component α_{21} of the dislocation density tensor mentioned previously. So, by differentiating Equations (152) to (155), this distribution function $\alpha_{21}(x_2)$ has the form

$$\alpha_{21}(x_2) = \alpha_{21}^0(x_2) + \alpha_{21}^1(x_2) + \alpha_{21}^2(x_2) + \alpha_{21}^3(x_2) + \dots, \quad (165)$$

with

$$\begin{aligned} \alpha_{21}^0(x_2) = & \frac{1}{8\pi(1-\nu)} \left[\frac{a^2}{2+x_2^2} + \frac{a^2}{a^2+(x_2-a)^2} \right] + \frac{1}{16\pi} \frac{3-4\nu}{1-\nu} \left[\ell\pi \frac{x_2^2+a^2}{x_2^2} \right. \\ & \left. + \ell\pi \frac{(x_2-a)^2+a^2}{(x_2-a)^2} \right] - \frac{a^2}{8\pi} \frac{1}{1-\nu} \frac{a^2-x_2^2}{(x_2^2+a^2)^2}, \end{aligned} \quad (166)$$

$$\begin{aligned} \alpha_{21}^1(x_2) = & \frac{a}{16\pi} \frac{3-4\nu}{1-\nu} \left[\frac{x_2}{x_2^2+a^2} + \frac{x_2-a}{(x_2-a)^2+a^2} - \frac{1}{x_2} - \frac{1}{x_2-a} \right] \\ & + \frac{a^3}{8\pi} \frac{1}{1-\nu} \left[\frac{x_2}{(x_2^2+a^2)^2} + \frac{x_2-a}{(x_2-a)^2+a^2} \right], \end{aligned} \quad (167)$$

$$\alpha_{21}^2(x_2) = \frac{a^2}{96\pi} \frac{3-4\nu}{1-\nu} \left[\frac{1}{x_2} \frac{1}{(x_2-a)^2} + \frac{a^2-x_2^2}{(a^2+x_2^2)^2} + \frac{a^2-(x_2-a)^2}{[a^2+(x_2-a)^2]^2} \right] -$$

$$-\frac{a^4}{48\pi} \frac{1}{1-\nu} \left[\frac{a^2 - x_2^2}{(x_2^2 + a^2)^3} + \frac{a^2 - (x_2 - a)^2}{[(x_2 - a)^2 + a^2]^3} \right], \quad (168)$$

$$\begin{aligned} \alpha_{21}^3 = & -\frac{a^4}{960\pi} \frac{3-4\nu}{1-\nu} \left[\frac{1}{x_2^4} + \frac{1}{(x_2 - a)^4} + \frac{3a^2 x_2^2 - x_2^4 - a^4}{(x_2^2 + a^2)^4} \right. \\ & + \frac{3a^2 (x_2 - a)^4 - (x_2 - a)^4 - a^4}{[(x_2 - a)^2 + a^2]^4} \left. \right] + \frac{a^6}{240\pi} \frac{1}{1-\nu} \left[\frac{10x_2^2 a^2 - 5x_2^4 - a^4}{(x_2^2 + a^2)^3} \right. \\ & + \frac{10a^2 (x_2 - a)^2 - 5(x_2 - a)^4 - a^4}{[(x_2 - a)^2 + a^2]^3} \left. \right]. \quad (169) \end{aligned}$$

Successive approximations of $\alpha_{21}(x_2)$ are plotted in Figure 14.

A direct comparison with Peierls' model cannot be achieved successfully because of the lack of symmetry of the displacement field around the core in our model. Both models give the same result for points far from the dislocation line, but cannot be matched close to the core region. We shall see that a description of the edge dislocation from an array of prismatic loops is much more satisfactory and more close to the real atomic arrangement at the center of the defect.

Self-Energy of the Edge Dislocation

As seen previously, two steps are required to obtain the final energy of the edge dislocation. First the energy of the system of forces will be computed, and then a correction energy term will be introduced to subtract the excessive strain energy across the slip plane, due to the system of forces itself.

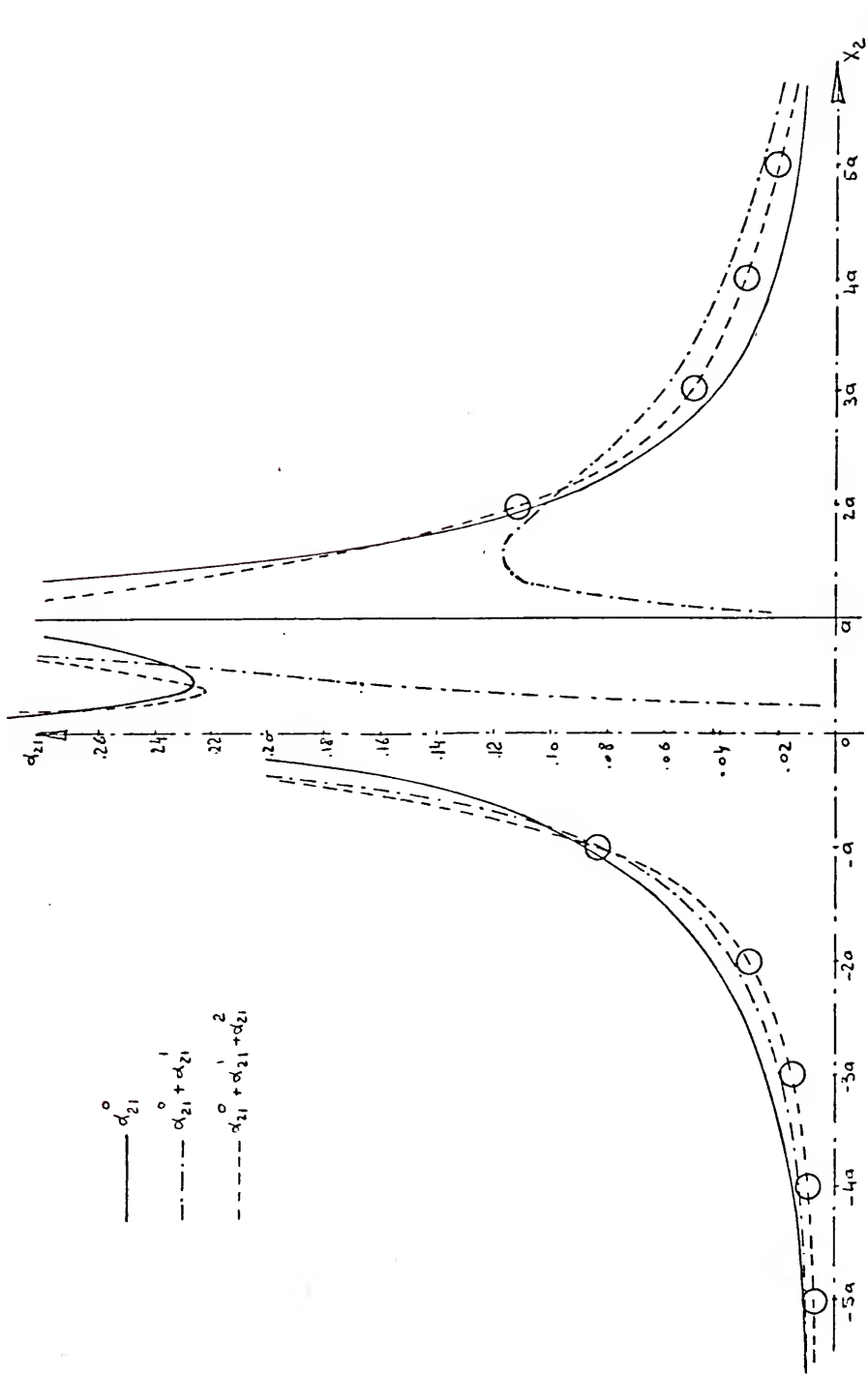


Figure 24. Distribution Function for an Edge Dislocation

When the rectangular array of forces is extended in the direction perpendicular to the Burgers vector, it simulates a system composed of two antiparallel straight edge dislocations separated by La . The energy per unit length of the array forces is the limit of W/Ra when R is much larger than L . From Equation (28), it takes the form,

$$\frac{W}{Ra} = L\mu a^2 \left[\frac{\mu a}{C_2} + \frac{A}{4\pi} \right] - \frac{\mu a^2}{2\pi(1-\nu)} \ln L + \mu a^2 \left[2\mu a \left(\frac{1}{C_2} - \frac{1}{C_3} \right) - \frac{7.6170 - 2.8588\nu}{4\pi(1-\nu)} \right], \quad (170)$$

with

$$A = \frac{2.860 - 2.368\nu}{1 - \nu}. \quad (171)$$

As previously seen for the energy of the kink in a screw dislocation, C_3 is an unknown parameter which cannot be obtained by a physical argument as in the case of C_2 .

The choice of a suitable displacement field describing the dislocation will be made as for the evaluation of the correction energy of the double kink in a screw dislocation. The region where the relative displacement across the slip plane is larger than $a/2$ is contained between the planes $x_2 = a/2$ and $x_2 = La - a/2$, as shown in Figure 25.

A displacement field chosen to approximate the actual relative displacements of atoms across the slip plane is:

$$v_1(x_1, y_2, x_3) = 0, \quad (172)$$

$$v_2(x_1, y_2, x_3) = u_2(x_1, x_2, x_3) - u_3, \quad (173)$$

$$v_3(x_1, y_2, x_3) = u_3(x_1, x_2, x_3), \quad (174)$$

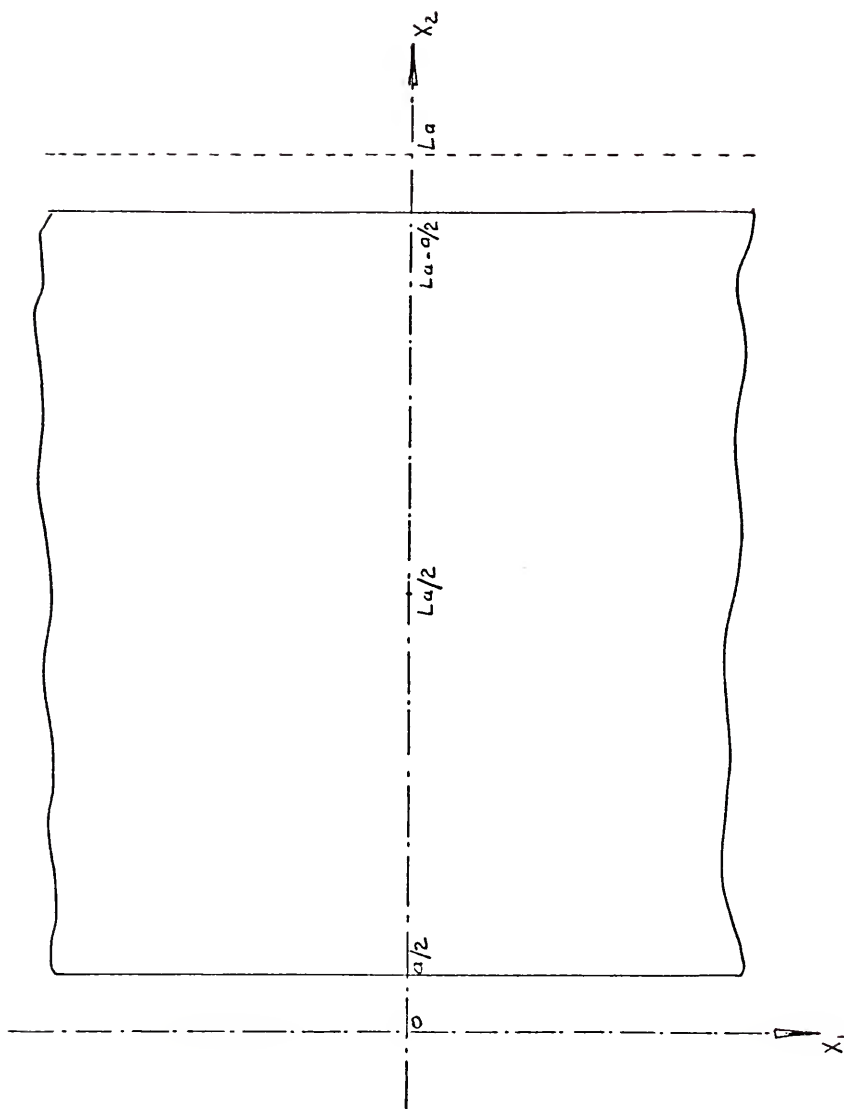


Figure 25. Region Where the Correction Energy is Computed for an Edge Dislocation

depending on whether x_3 is positive or negative, y_2 is taken as:

$$y_2 = x_2 + \frac{a}{2} \quad \text{for } x_3 > 0 \quad (175)$$

$$y_2 = x_2 - \frac{a}{2} \quad \text{for } x_3 < 0. \quad (176)$$

The principal difficulty with this choice of \vec{v} is that it is not symmetric with respect to $x_3 = 0$, since u_2 varies with x_2 . We have:

$$v_2(x_1, y_2, x_3) = u_2(x_1, x_2, x_3) - x_3 \quad (177)$$

and

$$v_2(x_1, y_2, -x_3) = -u_2(x_1, x_2 + a, x_3) + x_3, \quad (178)$$

where

$$|u_2(x_1, x_2, x_3)| \neq |u_2(x_1, x_2 + a, x_3)|. \quad (179)$$

Since this lack of symmetry will have an effect only on the constant terms which do not appear in the coefficients of R or ∇R , it will be considered a sufficient approximation for our study.

The tensors $\underline{\sigma}$ and $\underline{\tau}$ corresponding to the displacement fields \vec{u} and \vec{v} , respectively, have the following components:

$$\left\{ \begin{array}{l} \sigma_{11} = \lambda \left(\frac{\partial u_2}{\partial x_2} + \frac{\partial u_3}{\partial x_3} \right), \\ \sigma_{22} = (\lambda + 2\mu) \frac{\partial u_2}{\partial x_2} + \lambda \frac{\partial u_3}{\partial x_3}, \\ \sigma_{33} = (\lambda + 2\mu) \frac{\partial u_3}{\partial x_3} + \lambda \frac{\partial u_2}{\partial x_2}, \\ \sigma_{23} = \sigma_{32} = \mu \left(\frac{\partial u_2}{\partial x_3} + \frac{\partial u_3}{\partial x_2} \right), \end{array} \right. \quad (180)$$

$$\begin{cases} \tau_{11}(y_2, x_3) = \sigma_{11}(x_2, x_3) , \\ \tau_{22}(y_2, x_3) = \sigma_{22}(x_2, x_3) , \\ \tau_{33}(y_2, x_3) = \sigma_{33}(x_2, x_3) , \\ \tau_{23}(y_2, x_3) = \sigma_{23}(x_2, x_3) - \mu . \end{cases} \quad (181)$$

The correction energy is by definition the difference between the strain energies associated with the above stress fields contained within the volume of integration, i.e.,

$$E_c = \frac{1}{2} \int_V \sigma_{ij} \epsilon_{ij} dV - \frac{1}{2} \int_{V'} \tau_{ij} e_{ij} dV' . \quad (182)$$

By using Green's theorem, the volume integrals can be transformed into surface integrals on the surfaces bounding V and V' :

$$E_c = \frac{1}{2} \int_S \sigma_{ij} u_i n_j dS - \frac{1}{2} \int_{S'} \tau_{ij} v_i n_j dS' , \quad (183)$$

where \vec{n} is the normal to the surface of integration. The differences between S and S' are mainly due to a translation of the plane $x_3 = a/2$ of an amount $+a/2$, and a translation of the plane $x_3 = -a/2$ of an amount $-a/2$. Because of these differences between the limits of integration, all integrals over a function y_2 can be transformed into integrals over a function of x_2 :

$$x_3 > 0, \quad \int_a^{La} f(y_2) dy_2 = \int_{a/2}^{La-a/2} f(x_2) dx_2, \quad (184)$$

$$x_3 < 0, \quad \int_0^{La-a} f(y_2) dy_2 = \int_{a/2}^{La-a/2} f(x_2) dx_2 . \quad (185)$$

So the correction energy has the form

$$E_c = \frac{1}{2} \int_S (\sigma_{ij} u_i - \tau_{ij} v_i) n_j \, dS. \quad (186)$$

Replacing \vec{v} and $\underline{\tau}$ in function of \vec{u} and $\underline{\sigma}$, respectively, in Equation (186) leads to

$$\begin{aligned} \frac{E_c}{Ra} = & - \int_{-a/2}^{a/2} \left[x_3 \sigma_{22} \left(\frac{a}{2}, x_3 \right) + \mu u_3 \left(\frac{a}{2}, x_3 \right) \right] dx_3 \\ & + \int_{a/2}^{La-a/2} \left[\frac{a}{2} \sigma_{23} \left(x_2, \frac{a}{2} \right) + \mu u_2 \left(x_2, \frac{a}{2} \right) - \frac{\mu a}{2} \right] dx_2, \end{aligned} \quad (187)$$

or

$$\begin{aligned} \frac{E_c}{Ra} = & - 2 \int_0^{a/2} \left[(\lambda + 2\mu) x_3 \frac{\partial u_2}{\partial x_2} \left(\frac{a}{2}, x_3 \right) + (\mu - \lambda) u_3 \left(\frac{a}{2}, x_3 \right) \right] dx_3 \\ & - \lambda a u_3 \left(\frac{a}{2}, \frac{a}{2} \right) + \mu a \int_{a/2}^{La/2} \left[\frac{\partial u_2}{\partial x_3} \left(x_2, \frac{a}{2} \right) + 2 \frac{u_2 \left(x_2, \frac{a}{2} \right)}{a} - 1 \right] dx_2 \\ & + \mu a \left[u_3 \left(La/2, a/2 \right) - u_3 \left(a/2, a/2 \right) \right]. \end{aligned} \quad (188)$$

For computing these integrals, we shall use the expressions for u_i and its derivatives from Equations (131) and (132). The final summation with respect to q will be completed at the last step. Expressions used for $x_3(\partial u_2/\partial x_2)$ and $\partial u_2/\partial x_3$ are listed below.

$$\begin{aligned} x_3 \frac{\partial u_2}{\partial x_2} (x_2, x_3) = & \frac{ax_3}{16\pi} \left(\sum_{q=0}^L + \sum_{q=1}^{L-1} \right) \left\{ \frac{1-4\nu}{1-\nu} \left[\frac{x_2 - qa}{(x_3 - qa)^2 + (x_3 + \frac{a}{2})^2} \right. \right. \\ & - \frac{x_2 - qa}{(x_2 - qa)^2 + (x_3 - \frac{a}{2})^2} \left. \right] + \frac{2}{1-\nu} \left[\frac{(x_2 - qa)^3}{[(x_2 - qa)^2 + (x_3 + \frac{a}{2})^2]^2} \right. \\ & \left. \left. - \frac{(x_2 - qa)^3}{[(x_2 - qa)^2 + (x_3 - \frac{a}{2})^2]^2} \right] \right\} - \frac{ax_3}{16\pi(1-\nu)} \left\{ \left(x_3 - \frac{a}{2} \right) \frac{(x_3 - \frac{a}{2})^2 - x_2^2}{[x_2^2 + (x_3 - \frac{a}{2})^2]^2} + \right. \end{aligned}$$

$$+ (x_3 + \frac{a}{2}) \frac{(x_3 + \frac{a}{2})^2 - x_2^2}{[x_2^2 + (x_3 + \frac{a}{2})^2]^2} \Bigg\}, \quad (189)$$

$$\begin{aligned} \frac{\partial u_2}{\partial x_3}(x_2, x_3) = & \frac{a}{16\pi} \left(\sum_{q=0}^L + \sum_{q=1}^{L-1} \right) \left\{ \frac{5-4\nu}{1-\nu} \left[\frac{x_3 + \frac{a}{2}}{(x_2 - qa)^2 + (x_3 + \frac{a}{2})^2} - \right. \right. \\ & - \frac{x_3 - \frac{a}{2}}{(x_2 - qa)^2 + (x_3 - \frac{a}{2})^2} \Bigg] - \frac{2}{1-\nu} \left[\frac{(x_3 + \frac{a}{2})^3}{[(x_2 - qa)^2 + (x_3 + \frac{a}{2})^2]^2} - \right. \\ & \left. \left. - \frac{(x_3 - \frac{a}{2})^2}{[(x_2 - qa)^2 + (x_3 - \frac{a}{2})^2]^2} \right] \right\} - \frac{a}{16\pi(1-\nu)} \times \\ & \left\{ \frac{x_2 [x_2^2 - (x_3 - \frac{a}{2})^2]}{[x_2^2 + (x_3 - \frac{a}{2})^2]^2} + \frac{x_2 [x_2^2 - (x_3 + \frac{a}{2})^2]}{[x_2^2 + (x_3 + \frac{a}{2})^2]^2} \right\}. \quad (190) \end{aligned}$$

We will not reproduce here the details of integration, but only write the final results for each step of the computation. The correction energy becomes

$$\begin{aligned} \frac{E_c}{Ra} = & \frac{\mu a^2}{4\pi} \left(\sum_{q=0}^L + \sum_{q=1}^{L-1} \right) \left\{ \frac{1-2\nu}{1-\nu} \left(q - \frac{1}{2} \right) \ell n \frac{(q - \frac{1}{2})^2 + 1}{(q - \frac{1}{2})^2} + 4 \tan^{-1} \left(q - \frac{1}{2} \right) \right\} \\ & + \frac{\mu a^2}{2\pi} \frac{1-2\nu}{1-\nu} \ell n L - \frac{\mu a^2}{2} L + \frac{\mu a^2}{2\pi} \left\{ \frac{1}{1-2\nu} \left(\frac{1}{2} \ell n \frac{5}{4} + \frac{7}{40} \right) \right. \\ & \left. + \pi - \tan^{-1} 2 + \frac{1}{4} \frac{16\nu^2 - 18\nu + 5}{(1-\nu)(1-2\nu)} + \frac{\nu}{1-2\nu} \ell n 2 \right\}. \quad (191) \end{aligned}$$

Computing the single sums as mentioned in Equation (26) leads to the final expression for the correction energy of the system, per unit length of edge dislocation.

$$\frac{E_c}{Ra} = \frac{\mu a^2 L}{2} - \frac{\mu a^2}{\pi} \frac{1}{1-\nu} \ln L + \frac{\mu a^2}{2\pi} \left[\frac{.5198 + 2.3167\nu - .3182\nu^2}{(1-\nu)(1-2\nu)} \right]. \quad (192)$$

Recalling Equation (170), the total energy per unit length becomes

$$\frac{E_T}{Ra} = \frac{W}{Ra} - \frac{E_c}{Ra}, \quad (193)$$

that is,

$$\begin{aligned} \frac{E_T}{Ra} = L \mu a^2 & \left[\frac{\mu a}{C_2} + \frac{A}{4\pi} - \frac{1}{2} \right] + \frac{\mu a^2}{2\pi} \frac{1}{1-\nu} \ln L \\ & + \frac{\mu a^2}{2\pi} \left[4\pi \mu a \left(\frac{1}{C_2} - \frac{1}{C_3} \right) - \frac{4.3273 - 6.7297\nu + 2.5406\nu^2}{(1-\nu)(1-2\nu)} \right]. \end{aligned} \quad (194)$$

For E_T/Ra to represent the energy of the system, C_2 has to be chosen such that the term linear in L vanishes. Under this condition, C_2 takes the same value as for the screw dislocation. Unfortunately, C_3 remains unknown. It is clear here that it cannot be set equal to C_2 as it is a priori assumed for the energy of the kink in the screw dislocation. If it were, the core parameter would be unrealistically large if one expects the same order of magnitude as for the screw dislocation. We can even foresee that C_3 has to take a value much larger than C_2 ; this force constant C_2 , computed from the displacement field, was increasing greatly for atoms close to the dislocation line. Since C_3 corresponds to the closest atoms to the dislocation line, it can be expected to be of the order of magnitude of $C_2(0)$.

However, the total energy of the system composed of two parallel edge dislocations, and of opposite signs, has the form expected.

$$\frac{E_T}{Ra} = \frac{\mu a^2}{2\pi(1-\nu)} \ln \frac{La}{r_0}, \quad (195)$$

and the self-energy for a pure edge dislocation is simply

$$\frac{E_E}{Ra} = \frac{\mu a^2}{4\pi(1-\nu)} \ln \frac{l}{r_0} . \quad (196)$$

The fact that the essential features of the self-energy of the edge dislocation are reached with our model is very encouraging. The evaluation of the force constant C_3 remains the only uncertainty in the energy of the edge dislocation.

Single and Double Kinks in an Edge Dislocation

Similar to kinks in a screw dislocation, a single kink or a double kink in an edge dislocation can be simulated by adding only one shear loop at the end, $x_1 = 0$, of each row in the region $x_2 \leq 0$ for a single kink and in the region $-Na \leq x_2 \leq Na$ for a double kink. The array of forces takes the configuration shown in Figures 26 and 27, corresponding to single and double kinks, respectively.

A. Displacement field

The displacement field corresponding to these defects is given by the superposition of the displacement field of the edge dislocation and the displacement field of the extra forces introduced to simulate the defect. The latter, \vec{u}' , has the following expression, for a single kink or a double kink of length $2Na$, respectively.

$$u'_{i(SK)} = \frac{\mu a^2}{2} \sum_{p=0}^{-\infty} f(p) \quad (197)$$

and

$$u'_{i(DK)} = \frac{\mu a^2}{2} \sum_{p=-N}^N f(p) , \quad (198)$$

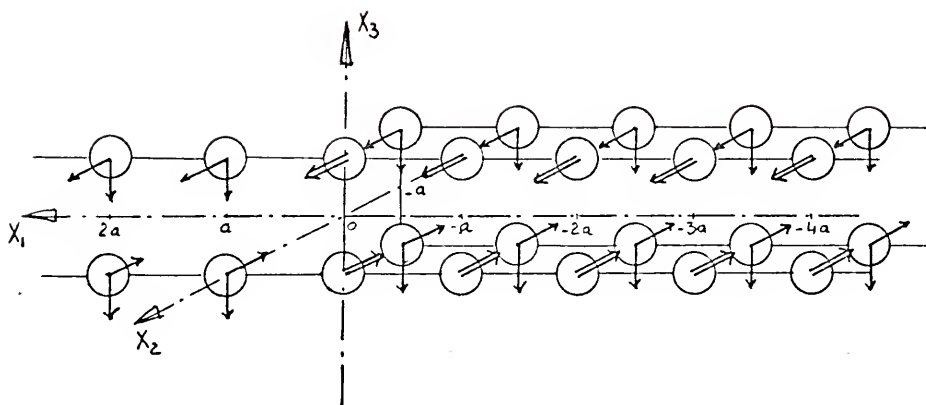


Figure 26. Array of Forces for Single Kink in an Edge Dislocation

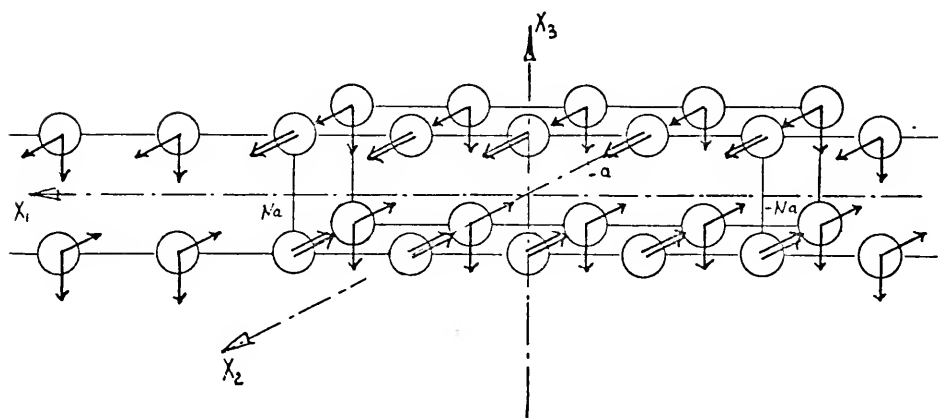


Figure 27. Array of Forces for Double Kink in an Edge Dislocation

where

$$\begin{aligned}
 f(p) = & G_{22}(x_1 - pa, x_2 + a, x_3 - \frac{a}{2}) - G_{22}(x_1 - pa, x_2 + a, x_3 + \frac{a}{2}) \\
 & + G_{22}(x_1 - pa, x_2, x_3 - \frac{a}{2}) - G_{22}(x_1 - pa, x_2, x_3 + \frac{a}{2}) \\
 & - G_{23}(x_1 - pa, x_2 + a, x_3 - \frac{a}{2}) - G_{23}(x_1 - pa, x_2 + a, x_3 + \frac{a}{2}) \\
 & + G_{23}(x_1 - pa, x_2, x_3 - \frac{a}{2}) + G_{23}(x_1 - pa, x_2, x_3 + \frac{a}{2}) .
 \end{aligned} \quad (199)$$

We shall only consider the displacements in the x_2 direction, since we are mainly interested in the change of the atomic configuration in a plane parallel to the slip plane. Due to the symmetry of the extra rows of forces with respect to $x_2 = -a/2$, we shall only take account of points corresponding to $x_2 > -a/2$, for example. The expressions for the displacement of points of application of point forces will be different from those for other atomic point, since the former are singular points. The following equations obtain in the plane $x_3 = a/2$ for single and double kinks, respectively.

(a) All x_2 except $x_2 = 0$ and $x_1 \leq 0$

$$\begin{aligned}
 u'_{2(SK)} = & \frac{a}{32\pi} \sum_{u=n}^{\infty} \left\{ \frac{3-4\nu}{1-\nu} \left[\frac{1}{\sqrt{u^2 a^2 + (x_2 + a)^2}} - \frac{1}{\sqrt{u^2 a^2 (x_2 + a)^2 + a^2}} \right. \right. \\
 & + \left. \frac{1}{\sqrt{u^2 a^2 + x_2^2}} - \frac{1}{\sqrt{u^2 a^2 + x_2^2 + a^2}} \right] + \frac{1}{1-\nu} \left[\frac{(x_2 + a)^2}{[u^2 a^2 + (x_2 + a)^2]^{3/2}} \right. \\
 & + \left. \frac{x_2^2}{[u^2 a^2 + x_2^2]^{3/2}} - \frac{(x_2 + a)(x_2 + 2a)}{[u^2 a^2 + (x_2 + a)^2 + a^2]^{3/2}} - \frac{x_2(x_2 - a)}{[u^2 a^2 + x_2^2 + a^2]^{3/2}} \right] \Bigg\} ;
 \end{aligned} \quad (200)$$

(b) $x_2 = 0$ and $x_1 \leq 0$

$$u'_{2(SK)}(-na, 0, \frac{a}{2}) = \frac{a}{32\pi} \sum_{u=-n}^{\infty} \left\{ \frac{3-4\nu}{1-\nu} \left(\frac{1}{\sqrt{\frac{u^2}{2}+1}} - \frac{1}{\sqrt{\frac{u^2}{2}+2}} \right) + \frac{1}{1-\nu} \frac{1}{(u^2+1)^{3/2}} \right\} \\ + \frac{a}{32\pi} \left(\sum_{u=1}^{\infty} + \sum_{u=1}^n \right) \frac{3-4\nu}{1-\nu} \left(\frac{1}{u} - \frac{1}{\sqrt{\frac{u^2}{2}+1}} \right) + \frac{\mu a^2}{2C_2}, \quad (201)$$

and for a double kink of length $2Na$,

(a) All x_2 except $x_2 = 0$ and $-Na \leq x_1 \leq Na$

$$u'_{2(DK)}(x_1, x_2, \frac{a}{2}) = \frac{a}{32\pi} \sum_{p=-N}^N \left\{ \frac{3-4\nu}{(1-\nu)} \left[\frac{1}{\sqrt{(x_1-pa)^2 + (x_2+a)^2}} \right. \right. \\ \left. \left. - \frac{1}{\sqrt{(x_1-pa)^2 + (x_2+a)^2 + a^2}} + \frac{1}{\sqrt{(x_1-pa)^2 + x_2^2}} - \frac{1}{\sqrt{(x_1-pa)^2 + x_2^2 + a^2}} \right] \right. \\ \left. + \frac{1}{(1-\nu)} \left[\frac{(x_2+a)^2}{[(x_1-pa)^2 + (x_2+a)^2]^{3/2}} + \frac{x_2^2}{[(x_1-pa)^2 + x_2^2]^{3/2}} \right. \right. \\ \left. \left. - \frac{(x_2+a)(x_2+2a)}{[(x_1-pa)^2 + (x_2+a)^2 + a^2]^{3/2}} - \frac{x_2(x_2-a)}{[(x_1-pa)^2 + x_2^2 + a^2]^{3/2}} \right] \right\}; \quad (202)$$

(b) $x_2 = 0$ and $-Na \leq x_1 \leq Na$

$$u'_{2(DK)}(na, 0, \frac{a}{2}) = \frac{a}{32\pi} \sum_{p=-N}^N \left\{ -\frac{3-4\nu}{1-\nu} \frac{1}{\sqrt{(n-p)^2 + 1}} + \frac{1}{1-\nu} \left[\frac{1}{[(n-p)^2 + 1]^{3/2}} \right. \right. \\ \left. \left. - \frac{2}{[(n-p)^2 + 2a^2]^{3/2}} \right] \right\} + \frac{a}{32\pi} \left(\sum_{u=1}^{N+n} + \sum_{u=1}^{N-n} \right) \frac{3-4\nu}{1-\nu} \left(\frac{1}{u} \right) + \frac{\mu a^2}{2C_2}. \quad (203)$$

The force constant C_2 used here ought to be $C_2(0)$, computed from Equation (162). It can only be approximated, since $\Delta u_2(0)$ for the edge dislocation is only known approximately as $0.4a$. In any event, we shall use this value to obtain the general trend of the atomic configuration in the immediate vicinity of the kink. The atomic displacements are tabulated in Table 9 for the single kink, and in Tables 10 to 12 for the double kinks.

TABLE 9. Atomic Displacements for a Single Kink in an Edge Dislocation

x_1	$u'_{2(SK)}(x_1, x_2)$		
	$x_2 = 0$	$x_2 = -a$	$x_2 = -2a$
- 5	.1243	.0854	.471
- 4	.1242	.0852	.0468
- 3	.1239	.0850	.0464
- 2	.1224	.0834	.0442
- 1	.1145	.0764	.0355
0	.0622	.0428	.0223
1	.0090	.0090	.0116
2	.0020	.0020	.0029
3	.0004	.0004	.0007
4	.0002	.0002	.0003
5	.0001	.0001	.0001

TABLE 10. Atomic Displacements for a Double Kink of Length $2a$ in an Edge Dislocation

x_1/a	$u'_{2(DK)}(x_1, x_2)$			
	$x_2 = -2a$	$x_2 = -a$	$x_2 = 0$	$x_2 = a$
0	.0404	.0804	.1194	.0404
1	.0338	.0719	.1109	.0338
2	.0115	.0120	.0120	.0115
3	.0031	.0022	.0022	.0031
4	.0010	.0006	.0006	.0010
5	.0003	.0002	.0002	.0003

TABLE 11. Atomic Displacements for a Double Kink of Length $4a$ in an Edge Dislocation

x_1/a	$u'_{2(DK)}(x_1, x_2)/a$			
	$x_2 = -2a$	$x_2 = -a$	$x_2 = 0$	$x_2 = a$
0	.0446	.0835	.1225	.0446
1	.0432	.0824	.1214	.0432
2	.0348	.0725	.1115	.0348
3	.0118	.0122	.0122	.0118
4	.0031	.0022	.0022	.0031
5	.0010	.0006	.0006	.0010

TABLE 12. Atomic Displacements for a Double Kink of Length $6a$ in an Edge Dislocation

x_1/a	$u'_{2(DK)}(x_1, x_2)/a$			
	$x_2 = -2a$	$x_2 = -a$	$x_2 = 0$	$x_2 = a$
0	.0460	.0844	.1234	.0460
1	.0456	.0842	.1232	.0456
2	.0435	.0827	.1217	.0435
3	.0348	.0743	.1133	.0348
4	.0118	.0123	.0123	.0118
5	.0031	.0023	.0023	.0031

Figures 28 to 31 show the atomic configurations of the defects in the planes $x_3 = \pm a/2$, corresponding to the values listed in Tables 9 to 12 in the same order. The same comments made for kinks in the screw dislocation apply here, that is, particularly the localization of the distortion in the immediate vicinity of the defect.

B. Energy of the double and single kinks

The energy of a double kink will be defined as the difference between the energy of the modified rectangular array of forces and the unmodified rectangular dislocation loop. First, the energy difference between the two arrays of forces is equal to the self-energy of the extra double row of forces added to their interaction energies with the rest of the array. Their expressions are

$$\begin{aligned}
 E_{\text{Row}} = & (2N+1) \mu^2 a^4 \left[\frac{1}{c_2} - G_{22}(0,0,a) \right] \\
 & + \mu^2 a^4 \left[\sum_{p=1}^{2N+1} (4N+2-p) + \sum_{p=2N+2}^{R/2} (2N+1) \right] \left[G_{22}(pa,0,0) - G_{22}(pa,0,a) \right] \\
 & - \mu^2 a^4 \left[\sum_{p=1}^{2N+1} p + \sum_{p=2N+2}^{R/2} (2N+1) \right] \left[G_{33}(pa,0,0) + G_{33}(pa,0,a) \right], \quad (204)
 \end{aligned}$$

$$\begin{aligned}
 E_I = & 2(2N+1) \mu^2 a^4 \sum_{q=1}^L \left\{ \left[G_{22}(0,qa,0) - G_{22}(0,qa,a) \right] \right. \\
 & + 2 \sum_{p=1}^{R/2} \left[G_{22}(pa,qa,0) - G_{22}(pa,qa,a) \right] \left. \right\} \\
 & + \mu^2 a^4 \left[\sum_{p=1}^{2N+1} p + \sum_{p=2N+2}^{R/2} (2N+1) \right] \left[2G_{23}(pa,a,a) - G_{22}(pa,a,0) \right. \\
 & + G_{22}(pa,a,a) + G_{33}(pa,a,0) + G_{33}(pa,a,a) \left. \right], \quad (205)
 \end{aligned}$$

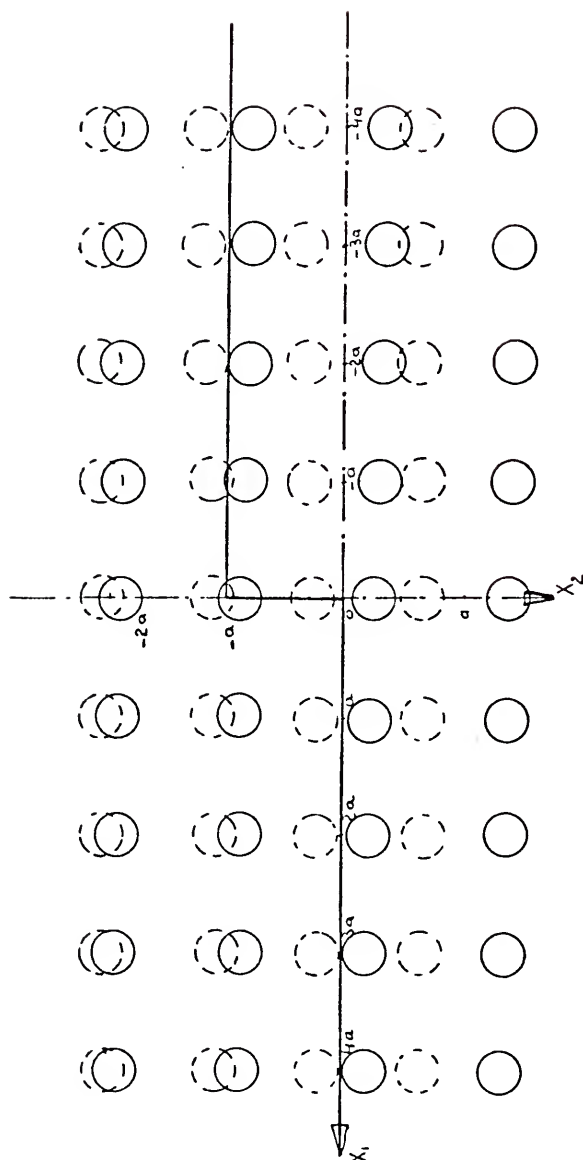


Figure 28. Atomic Arrangement for a Single Kink in an Edge Dislocation

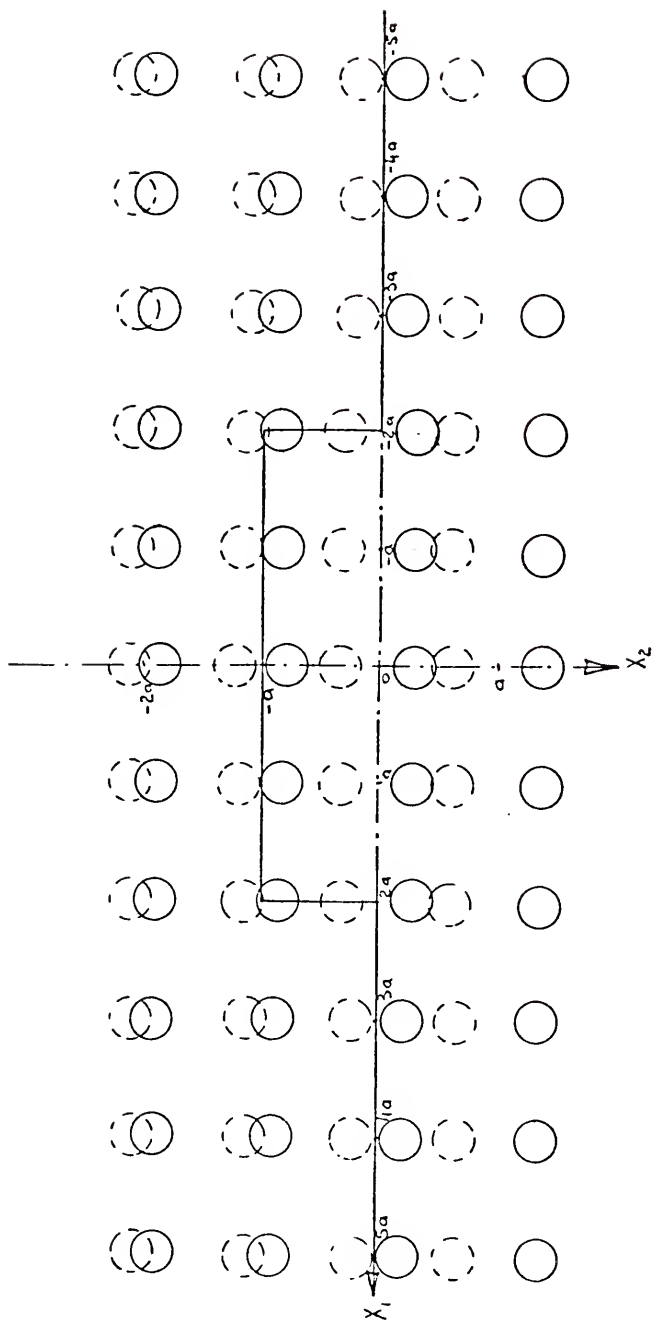


Figure 30. Atomic Arrangement for a Double Kink of Length 4a in an Edge Dislocation

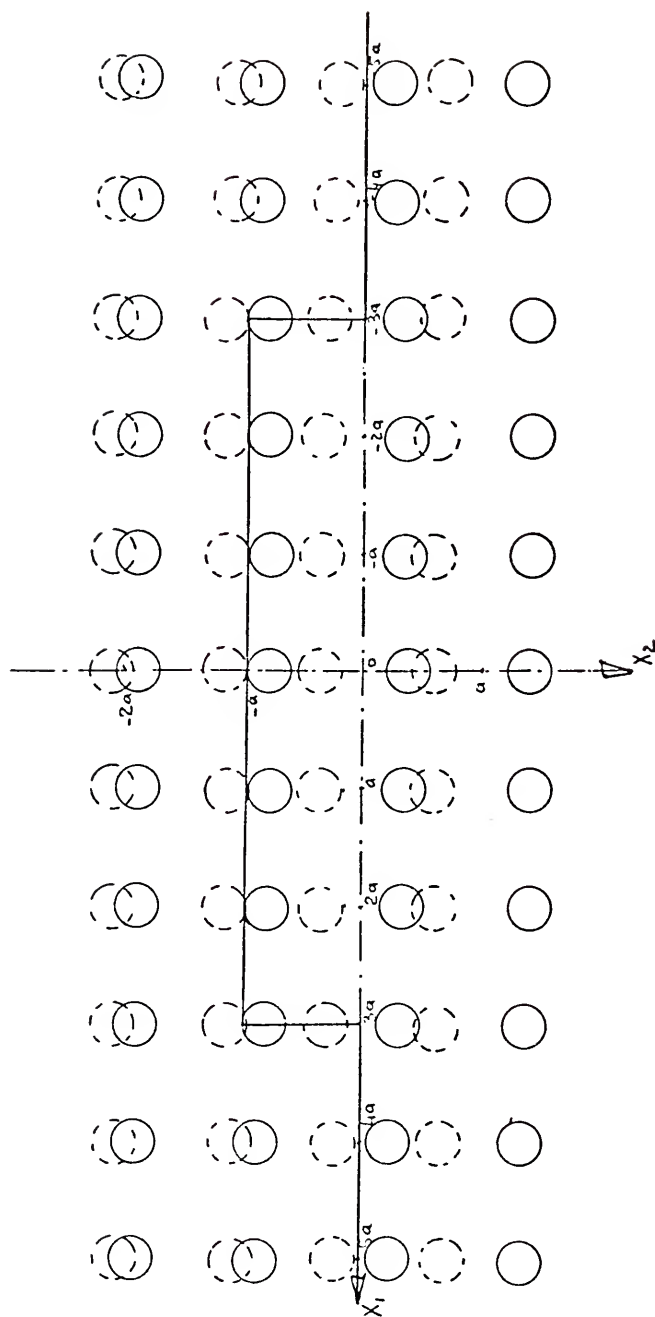


Figure 31. Atomic Arrangement for a Double Kink of Length $6a$ in an Edge Dislocation

with

$$W = E_{\text{Row}} + E_I. \quad (206)$$

In the expressions above, we always considered the length of the double kink to be much smaller than the length of the dislocation. Replacing the Green's functions by their explicit expressions leads to

$$\begin{aligned} W = & \frac{\mu a^3}{16\pi} (2N+1) \left\{ \sum_{q=1}^L \left[8 \left(\frac{1}{q} - \frac{1}{\sqrt{q^2+1}} \right) + \frac{1}{1-\nu} \frac{2}{(q^2+1)^{3/2}} \right] \right. \\ & + 4 \sum_{q=1}^L \sum_{p=1}^{R/2} \left[\frac{3-4\nu}{1-\nu} \left(\frac{1}{\sqrt{p^2+q^2}} - \frac{1}{\sqrt{p^2+q^2+1}} \right) + \frac{1}{1-\nu} \left(\frac{q^2}{(p^2+q^2)^{3/2}} \right. \right. \\ & \left. \left. - \frac{q^2}{(p^2+q^2+1)^{3/2}} \right) \right] + 2 \sum_{p=1}^R \frac{3-4\nu}{1-\nu} \left(\frac{1}{p} - \frac{1}{\sqrt{p^2+1}} \right) + 2 \sum_{p=1}^{R/2} \times \\ & \left[\frac{3-4\nu}{1-\nu} \left(\frac{1}{\sqrt{p^2+2}} - \frac{1}{p} \right) + \frac{1}{1-\nu} \left(\frac{2}{(p^2+2)^{3/2}} - \frac{1}{(p^2+1)^{3/2}} \right) \right] - \frac{3-4\nu}{1-\nu} \\ & + 16\pi \frac{\mu a}{C_2} \left. \right\} + \frac{\mu a^3}{8\pi} \sum_{p=1}^{2N+1} \left\{ \frac{3-4\nu}{1-\nu} \left(\frac{p}{\sqrt{p^2+2}} - 1 \right) + \frac{1}{1-\nu} \left(\frac{2p}{(p^2+2)^{3/2}} \right. \right. \\ & \left. \left. - \frac{p}{(p^2+1)^{3/2}} \right) \right\}. \quad (207) \end{aligned}$$

The term $\mu a/C_2$, depending on the force constant, can be replaced by its value, as defined in Equations (113) and (114). The final expression for the energy difference between the systems of forces becomes

$$W = \frac{\mu a^3}{8\pi} (2N+1) \left\{ 4\pi + \sum_{p=1}^{R/2} \left[\frac{3-4\nu}{1-\nu} \left(\frac{1}{\sqrt{p^2+2}} - \frac{1}{p} \right) + \right. \right.$$

$$\begin{aligned}
& + \frac{1}{1-\nu} \left(\frac{2}{(p+2)^{3/2}} - \frac{1}{(p+1)^{3/2}} \right) \Bigg] \Bigg\} \\
& + \frac{\mu a^3}{8\pi} \sum_{p=1}^{2N+1} \left\{ \frac{3-4\nu}{1-\nu} \left(\frac{p}{\sqrt{p+1}} - 1 \right) + \frac{1}{1-\nu} \left(\frac{2p}{(p+2)^{3/2}} - \frac{p}{(p+1)^{3/2}} \right) \right\} :
\end{aligned} \tag{208}$$

If N becomes large, but still smaller than the length of the edge dislocation, the double kink behaves like two separate single kinks. The corresponding energy of the system of forces for each single kink is the limit of $W/2$ when N increases:

$$\begin{aligned}
W_{SK} = & \frac{\mu a^3}{2} N + \frac{\mu a^3}{16\pi} \sum_{p=1}^{\infty} \left\{ \frac{3-4\nu}{1-\nu} \left(\frac{p}{\sqrt{p+1}} - 1 \right) \right. \\
& \left. + \frac{1}{1-\nu} \left(\frac{2p}{(p+2)^{3/2}} - \frac{p}{(p+1)^{3/2}} \right) \right\} .
\end{aligned} \tag{209}$$

The interaction energy between the two kinks is simply $(2W_{SK} - W)$.

As for the kinks in a screw dislocation, a correction energy term has to be introduced to remove the excess strain energy contained in the region between the planes of forces. Unfortunately, the same difficulties arise as before and we shall not be able to perform a complete analysis of the energy of a double kink. The computation of the strain energy can be done exactly in the same way as for the screw dislocation, and its development here would only be a repetition of the treatment of the correction energy for a double kink in a screw dislocation.

We anticipate that in the complete expression for the energy of the kink, the coefficient of N can be made to vanish, leaving only a pure number. It is interesting to point out that Equations (208) and

(209) have exactly the same form as Equations (115) and (116), except for the presence of the force constant C_3 . This is due mainly to the screw dislocation character of the kink segments. If a complete treatment of the correction energy can be achieved, the energy of a kink in an edge dislocation is thoroughly determined.

The results already obtained are very encouraging and a complete treatment should lead to a better understanding of kinks in edge dislocations.

CHAPTER 6

EDGE DISLOCATION IN SIMPLE CUBIC CRYSTAL CONSTRUCTED FROM AN ARRAY OF PRISMATIC LOOPS

A rectangular dislocation loop formed by four segments of edge dislocations can be simulated by an array of primitive prismatic loops as defined in the first chapter. This is equivalent to a rectangular plane of vacancies plus an extra contraction in a direction normal to this plane. The loop is shown in Figures 32 and 33. The forces F and G are those computed from Equations (15) and (16), and have the respective values:

$$F = \frac{\lambda a^2}{2} \quad (210)$$

and

$$G = \frac{\lambda + 2\mu}{2} a^2. \quad (211)$$

The same procedure as used in the previous chapters will be followed here to obtain the displacement field, width and self-energy of the pure edge dislocation.

Displacement Field

The loop considered will be rectangular, of dimensions La and Ra in directions parallel to x_2 and x_3 , respectively. This means that the loop is composed of $(R+1)(L+1)$ vacancies. The edge dislocation considered will have its line parallel to the \vec{x}_2 axis and located

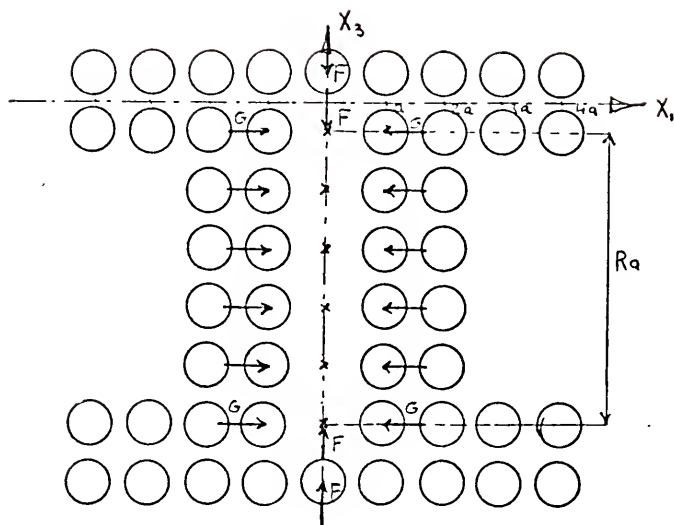


Figure 32. Array of Prismatic Loop in $x_2 = 0$ Plane

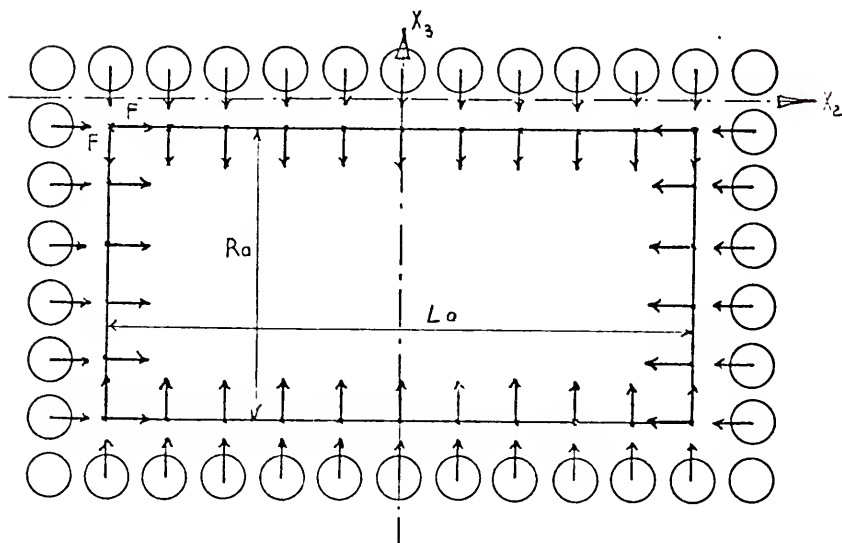


Figure 33. Array of Prismatic Loop in $x_1 = 0$ Plane

near $x_3 = 0$. So the coordinates x_2 and x_3 will always be considered small with respect to La and Ra , respectively.

Considering the displacement field in this region as the superposition of the displacement fields of all the point forces leads to the following formal expression in terms of Green's functions:

$$\begin{aligned}
 u_1(x_1, x_2, x_3) = & \frac{\lambda a^2}{2} \sum_{q=-L/2}^{L/2} \left\{ -G_{3i}(x_1, x_2 - qa, x_3 - \frac{a}{2}) \right. \\
 & - G_{3i}(x_1, x_2 - qa, x_3 + \frac{a}{2}) + G_{3i}(x_1, x_2 - qa, x_3 + \frac{a}{2} + Ra) \\
 & + G_{3i}(x_1, x_2 - qa, x_3 + \frac{3a}{2} + Ra) \left. \right\} + \frac{\lambda a^2}{2} \sum_{r=1}^{R+1} \left\{ G_{2i}(x_1, x_2 + \frac{La}{2}, x_3 - \frac{a}{2} + Ra) \right. \\
 & + G_{2i}(x_1, x_2 + \frac{La}{2} + a, x_3 - \frac{a}{2} + ra) - G_{2i}(x_1, x_2 - \frac{La}{2}, x_3 - \frac{a}{2} + ra) \\
 & - G_{2i}(x_1, x_2 - a - \frac{La}{2}, x_3 - \frac{a}{2} + ra) \left. \right\} + \frac{\lambda + 2\mu}{2} a^2 \sum_{r=1}^{R+1} \sum_{q=-L/2}^{L/2} x \\
 & \left\{ G_{1i}(x_1 + a, x_2 - qa, x_3 - \frac{a}{2} + ra) - G_{1i}(x_1 - a, x_1 - qa, x_3 - \frac{a}{2} + ra) \right\}, \quad (212)
 \end{aligned}$$

where $G_{ij}(X_1, X_2, X_3)$ is defined by Equation (3).

Again, Euler's formula, Equation (29), will be used to evaluate the discrete summations. The first summation considered will be along the line of the dislocation. This sum is found to be identical to the first term of Euler's approximation:

$$\sum_{q=-L/2}^{L/2} f(q) = \int_{-L/2}^{L/2} f(x) dx, \quad (213)$$

so an expression of $u_1(x_1, x_2, x_3)$ can be written as:

$$\begin{aligned}
u_1(x, x, x) = & - \frac{va}{8\pi(1-\nu)(1-2\nu)} \left[\frac{x_1(x_3 - \frac{a}{2})}{x_1^2 + (x_3 - \frac{a}{2})^2} + \frac{x_1(x_3 + \frac{a}{2})}{x_1^2 + (x_3 + \frac{a}{2})^2} \right] \\
& + \frac{a}{16\pi} \sum_{r=1}^{R+1} \left\{ \frac{3-4\nu}{1-2\nu} \ell n \frac{(x_1-a)^2 + (x_3 - \frac{a}{2} + ra)^2}{(x_1+a)^2 + (x_3 - \frac{a}{2} + ra)^2} \right. \\
& \left. + \frac{2}{1-2\nu} \left[\frac{(x_1+a)^2}{(x_1+a)^2 + (x_3 - \frac{a}{2} + ra)^2} - \frac{(x_1-a)^2}{(x_1-a)^2 + (x_3 - \frac{a}{2} + ra)^2} \right] \right\}, \quad (214)
\end{aligned}$$

$$u_2(x_1, x_2, x_3) = 0, \quad (215)$$

$$\begin{aligned}
u_3(x_1, x_2, x_3) = & \frac{va}{16\pi(1-\nu)} \left\{ 8 \ell n \frac{L/2 + \sqrt{L^2/4 + R^2}}{L} \right. \\
& + \frac{3-4\nu}{1-2\nu} \left[-4 \ell n R + \ell n \left[x_1^2 + (x_3 - \frac{a}{2})^2 \right] + \ell n \left[x_1^2 + (x_3 + \frac{a}{2})^2 \right] \right] \\
& + \frac{1}{1-2\nu} \left[\frac{x_1^2}{x_1^2 + (x_3 - \frac{a}{2})^2} + \frac{x_1^2}{x_1^2 + (x_3 + \frac{a}{2})^2} \right] \left. \right\} \\
& + \frac{a}{8\pi(1-2\nu)} \sum_{r=1}^{R+1} \left\{ \frac{(x_3 - \frac{a}{2} + ra)(x_1+a)}{(x_3 - \frac{a}{2} + ra)^2 + (x_1+a)^2} - \frac{(x_3 - \frac{a}{2} + ra)(x_1-a)}{(x_3 - \frac{a}{2} + ra)^2 + (x_1-a)^2} \right\}. \quad (216)
\end{aligned}$$

The second step of the computation consists of applying Euler's formula a second time, giving a series of expressions which represent successively higher approximations to the displacement field of the edge dislocation. The mathematical difficulties encountered when computing integrals over a region containing singular points are solved in the same manner as for the screw dislocation in Chapter 3. The final analytic expressions for u_1 and u_3 take the form

$$u_1 = u_1^0 + u_1^1 + u_2^2 + u_1^3 + \dots, \quad (217)$$

with

$$\begin{aligned} u_1^0(x_1, x_2, x_3) = & \frac{1}{4\pi} \left\{ \frac{-\pi a}{\pi a} + (x_1 + a) \tan^{-1} \frac{x_3 + \frac{a}{2}}{x_1 + a} - (x_1 - a) \tan^{-1} \frac{x_3 + \frac{a}{2}}{x_1 - a} \right\} \\ & + \frac{3-4\nu}{16\pi(1-2\nu)} (x_3 + \frac{a}{2}) \ln \frac{(x_1 + a)^2 + (x_3 + \frac{a}{2})^2}{(x_1 - a)^2 + (x_3 + \frac{a}{2})^2} \\ & - \frac{\nu a}{8\pi(1-\nu)(1-2\nu)} \left\{ \frac{x_1(x_3 - \frac{a}{2})}{x_1^2 + (x_3 - \frac{a}{2})^2} + \frac{x_1(x_3 + \frac{a}{2})}{x_1^2 + (x_3 + \frac{a}{2})^2} \right\}, \quad (218) \end{aligned}$$

The terms $-\pi a$, $-\pi x_1$ and πa in Equation (218) correspond to the regions $x_1 > a$, $-a < x_1 < a$ and $x_1 < -a$, respectively.

$$\begin{aligned} u_1^1(x_1, x_2, x_3) = & -\frac{a(3-4\nu)}{32\pi(1-2\nu)} \ln \frac{(x_1 + a)^2 + (x_3 + \frac{a}{2})^2}{(x_1 - a)^2 + (x_3 + \frac{a}{2})^2} \\ & - \frac{a}{16\pi(1-2\nu)} \left\{ \frac{(x_1 - a)^2}{(x_1 - a)^2 + (x_3 + \frac{a}{2})^2} - \frac{(x_1 + a)^2}{(x_1 + a)^2 + (x_3 + \frac{a}{2})^2} \right\}, \quad (219) \end{aligned}$$

$$\begin{aligned} u_1^2(x_1, x_2, x_3) = & -\frac{a^2(3-4\nu)}{96\pi(1-2\nu)} \left\{ \frac{x_3 + a/2}{(x_1 - a)^2 + (x_3 + \frac{a}{2})^2} - \frac{x_3 + a/2}{(x_1 + a)^2 + (x_3 + \frac{a}{2})^2} \right\} \\ & - \frac{a^2}{48\pi(1-2\nu)} (x_3 + \frac{a}{2}) \left\{ \frac{(x_1 - a)^2}{[(x_1 - a)^2 + (x_3 + \frac{a}{2})^2]^2} \right. \\ & \left. - \frac{(x_1 + a)^2}{[(x_1 + a)^2 + (x_3 + \frac{a}{2})^2]^2} \right\}, \quad (220) \end{aligned}$$

and

$$\begin{aligned}
 u_1^3(x_1, x_2, x_3) = & -\frac{a^4(3-4\nu)}{2880\pi(1-2\nu)} (x_3 + \frac{a}{2}) \left\{ \frac{3(x_1-a)^2 - (x_3 + \frac{a}{2})^2}{[(x_1-a)^2 + (x_3 + \frac{a}{2})^2]^3} \right. \\
 & - \frac{3(x_1+a)^2 - (x_3 + \frac{a}{2})^2}{[(x_1+a)^2 + (x_3 + \frac{a}{2})^2]^3} \left. - \frac{a^4}{240\pi(1-2\nu)} (x_3 + \frac{a}{2}) \left\{ \frac{(x_1-a)^2 [(x_1-a)^2 - (x_3 + \frac{a}{2})^2]}{[(x_1-a)^2 + (x_3 + \frac{a}{2})^2]^4} \right. \right. \\
 & \left. \left. - \frac{(x_1+a)^2 [(x_1+a)^2 - (x_3 + \frac{a}{2})^2]}{[(x_1+a)^2 + (x_3 + \frac{a}{2})^2]^4} \right\} \right\}. \quad (221)
 \end{aligned}$$

The other non-zero component of the displacement field is written similarly:

$$u_3 = u_3^0 + u_3^1 + u_3^2 + u_3^3 + \dots, \quad (222)$$

with

$$\begin{aligned}
 u_3^0(x_1, x_2, x_3) = & \frac{1-2\nu}{4\pi(1-\nu)} a \ell n \frac{RL}{L/2 + \sqrt{L^2/4 + R^2}} + \\
 & + \frac{\nu(3-4\nu)a}{16\pi(1-2\nu)(1-\nu)} \left\{ \ell n \frac{x_1^2 + (x_3 - \frac{a}{2})^2}{a^2} + \ell n \frac{x_1^2 + (x_3 + \frac{a}{2})^2}{a^2} \right\} \\
 & + \frac{\nu a}{8\pi(1-2\nu)(1-\nu)} \left\{ \frac{x_1^2}{x_1^2 + (x_3 - \frac{a}{2})^2} + \frac{x_1^2}{x_1^2 + (x_3 + \frac{a}{2})^2} \right\} \\
 & + \frac{1}{16\pi(1-2\nu)} \left\{ (x_1-a) \ell n \frac{(x_1-a)^2 + (x_3 + \frac{a}{2})^2}{a^2} \right. \\
 & \left. - (x_1+a) \ell n \frac{(x_1+a)^2 + (x_3 + \frac{a}{2})^2}{a^2} \right\}, \quad (223)
 \end{aligned}$$

$$u_3^1(x_1, x_2, x_3) = \frac{a}{16\pi(1-2\nu)} \left(x_3 + \frac{a}{2} \right) \left\{ \frac{x_1 + a}{(x_1 + a)^2 + (x_3 + \frac{a}{2})^2} - \frac{x_1 - a}{(x_1 - a)^2 + (x_3 + \frac{a}{2})^2} \right\}, \quad (224)$$

$$u_3^2(x_1, x_2, x_3) = - \frac{a^2}{96\pi(1-2\nu)} \left\{ \frac{(x_1 + a) \left[(x_1 + a)^2 - (x_3 + \frac{a}{2})^2 \right]}{\left[(x_1 + a)^2 + (x_3 + \frac{a}{2})^2 \right]^2} - \frac{(x_1 - a) \left[(x_1 - a)^2 - (x_3 + \frac{a}{2})^2 \right]}{\left[(x_1 - a)^2 + (x_3 + \frac{a}{2})^2 \right]^2} \right\}, \quad (225)$$

and

$$u_3^3(x_1, x_2, x_3) = - \frac{a^4}{960\pi(1-2\nu)} \left\{ \frac{(x_1 + a) \left[(x_1 + a)^4 - 6(x_1 + a)^2(x_3 + \frac{a}{2})^2 + (x_3 + \frac{a}{2})^4 \right]}{\left[(x_1 + a)^2 + (x_3 + \frac{a}{2})^2 \right]^4} - \frac{(x_1 - a) \left[(x_1 - a)^4 - 6(x_1 - a)^2(x_3 + \frac{a}{2})^2 + (x_3 + \frac{a}{2})^4 \right]}{\left[(x_1 - a)^2 + (x_3 + \frac{a}{2})^2 \right]^4} \right\}. \quad (226)$$

The consistency of this displacement field with results already obtained from the ordinary continuum model is checked by considering x_1 and x_3 to be far from the dislocation line, and by expanding u_1 and u_3 in a Taylor series,

$$f(x_1 + \epsilon_1, x_3 + \epsilon_3) = f(x_1, x_3) + \epsilon_1 \frac{\partial f}{\partial x_1}(x_1, x_3) + \epsilon_3 \frac{\partial f}{\partial x_3}(x_1, x_3), \quad (227)$$

where ϵ_1 and ϵ_3 are small with respect to x_1 and x_3 , respectively.

The following expressions are found:

$$u_1(x_1, x_2, x_3) = \frac{a}{2\pi} \left\{ \begin{matrix} -\pi/2 \\ \pi/2 \end{matrix} + \tan^{-1} \frac{x_3}{x_1} \right\} + \frac{1}{4\pi(1-\nu)} \frac{x_1 x_3}{x_1^2 + x_3^2}, \quad (228)$$

where $-\pi/2$ and $\pi/2$ correspond to $x_1 > 0$ and $x_1 < 0$, respectively.

Also

$$u_2(x_1, x_2, x_3) = 0; \quad (229)$$

$$u_3(x_1, x_2, x_3) = \frac{1-2\nu}{8\pi(1-\nu)} a \left\{ 2 \ln \frac{RL}{L/2 + \sqrt{L^2/4 + R^2}} - \ln \left(\frac{x_1^2 + x_3^2}{x_1^2 + x_3^2} \right) \right\} - \frac{a}{4\pi(1-\nu)} \frac{x_1^2}{x_1^2 + x_3^2}. \quad (230)$$

These equations match exactly with the ordinary continuum model, Equations (146), (147) and (148), when one realizes that $u_1(x_1, x_2, 0)$ is equal to $-a/4$ from the way the displacement field has been defined.

By contrast with the simulation of an edge dislocation by an array of shear loops, in the present case the displacement field is symmetrical with respect to the plane $x_1 = 0$. The only singular points occur for $x_1 = \pm a$ and $x_3 = -na + a/2$ ($n \geq 1$), and $x_1 = 0$ with $x_3 = a/2$. We shall demonstrate that the plane $x_3 = 0$ plays a unique role for the dislocation in the sense that the displacement of singular points will be shown from the displacement of the points symmetric with respect to $x_3 = 0$. We have the fundamental relations:

$$u_1(x_1, x_2, na + \frac{a}{2}) + u_1(x_1, x_2, -na - \frac{a}{2}) = -\frac{a}{2}, \quad (231)$$

and

$$u_3(x_1, x_2, na + \frac{a}{2}) = u_3(x_1, x_2, -na - \frac{a}{2}). \quad (232)$$

Let us first consider the special case of $n = 0$ for u_1 .

From Equation (214), we have

$$u_1(x_1, x_2, \frac{a}{2}) = \frac{va}{8\pi(1-\nu)(1-2\nu)} \frac{ax_1}{x_1+a} + \frac{a}{16\pi} \sum_{r=1}^{\infty} f(ra), \quad (233)$$

$$u_1(x, x, -\frac{a}{2}) = \frac{va}{8\pi(1-\nu)(1-2\nu)} \frac{ax_1}{x_1+a} + \frac{a}{16\pi} \sum_{r=1}^{\infty} f(ra-a), \quad (234)$$

with

$$f(ra) = \frac{3-4\nu}{1-2\nu} \ln \frac{(x_1-a)^2 + r^2 \frac{a^2}{2}}{(x_1+a)^2 + r^2 \frac{a^2}{2}} + \frac{2}{1-\nu} \left[\frac{(x_1+a)^2}{(x_1+a)^2 + r^2 \frac{a^2}{2}} - \frac{(x_1-a)^2}{(x_1-a)^2 + r^2 \frac{a^2}{2}} \right]. \quad (235)$$

Noticing that

$$\sum_{r=1}^{\infty} f(ra-a) = \sum_{r=1}^{\infty} f(ra) + f(0), \quad (236)$$

the two identities follow:

$$u_1(x_1, x_2, \frac{a}{2}) + u_1(x_1, x_2, -\frac{a}{2}) = \frac{a}{8\pi} \sum_{r=1}^{\infty} f(ra) + \frac{a}{16\pi} \frac{3-4\nu}{1-2\nu} \ln \frac{(x_1-a)^2}{(x_1+a)^2} \quad (237)$$

$$u_1(x_1, x_2, -\frac{a}{2}) - u_1(x_1, x_2, \frac{a}{2}) = \frac{a}{16\pi} \frac{3-4\nu}{1-2\nu} \ln \frac{(x_1-a)^2}{(x_1+a)^2}. \quad (238)$$

On another hand, from Equations (218) to (221), $u_1(x_1, x_2, -\frac{a}{2})$

has the exact value

$$u_1(x_1, x_2, -\frac{a}{2}) = \begin{vmatrix} -a/4 \\ -x_1/4 \\ a/4 \end{vmatrix} + \frac{va}{8\pi(1-\nu)(1-2\nu)} \frac{ax_1}{x_1+a} \\ + \frac{(3-4\nu)a}{32\pi(1-2\nu)} \ln \frac{(x_1-a)^2}{(x_1+a)^2}, \quad (239)$$

where the terms $-a/4$, $-x_1/4$ and $a/4$ correspond to the region $x_1 > a$, $-a < x_1 < a$, and $x_1 < -a$, respectively. Comparison with Equations (237) and (238) leads to

$$u_1(x_1, x_2, -\frac{a}{2}) + u_1(x_1, x_2, \frac{a}{2}) = \begin{vmatrix} -a/2 \\ -x_1/2 \\ a/2 \end{vmatrix}. \quad (240)$$

Accidentally, an interesting identity has been proved, that is,

$$\frac{1}{2} = \frac{1}{16\pi} \frac{3-4\nu}{1-2\nu} \ln \frac{(x_1+a)^2}{(x_1-a)^2} - \frac{1}{8\pi} \sum_{r=1}^{\infty} f(ra). \quad (241)$$

This result can easily be generalized to $x_3 = na + a/2$ and $x_3 = -(na + \frac{a}{2})$ for any value of n . The displacements in the x_2 direction for these points have the form

$$u_1(x_1, x_2, na + \frac{a}{2}) = - \frac{va}{8\pi(1-\nu)(1-2\nu)} \left\{ \frac{x_1 na}{\frac{x_1^2}{2} + \frac{n^2 a^2}{2}} \right. \\ \left. + \frac{x_1 (na+a)}{\frac{x_1^2}{2} + \frac{(na+a)^2}{2}} \right\} + \frac{a}{16\pi} \left(\sum_{r=1}^{\infty} - \sum_{r=1}^n \right) f(ra), \quad (242)$$

when it is noticed that

$$\sum_{r=1}^{\infty} f(ra+na) = \sum_{r=1}^{\infty} f(ra) - \sum_{r=1}^n f(ra), \quad (243)$$

and

$$u_1(x_1, x_2, -na - \frac{a}{2}) = + \frac{va}{8\pi(1-\nu)(1-2\nu)} \left\{ \frac{x_1 na}{x_1^2 + n^2 a^2} + \frac{x_1(na+a)}{x_1^2(na+a)^2} \right\} + \frac{a}{16\pi} \left(\sum_{r=1}^{\infty} + \sum_{r=0}^n \right) f(ra) . \quad (244)$$

So, by adding Equations (242) and (244), the same expression as Equation (237) is found, which leads to

$$u_1(x_1, x_2, na + \frac{a}{2}) + u_1(x_1, x_2, -na - \frac{a}{2}) = \begin{cases} -a/2 \\ -x_1/2 \\ a/2 \end{cases} . \quad (245)$$

The same line of reasoning applies to u_3 , leading to

$$u_3(x_1, x_2, na + \frac{a}{2}) = u_3(x_1, x_2, -na - \frac{a}{2}) . \quad (246)$$

Equation (245) will help us to find the atomic displacements of the singular points and the force constant C_1 . The latter can be obtained by expressing the displacement of these singular points in terms of Green's tensor:

$$u_1(a, -na - \frac{a}{2}) = -\frac{\lambda a^2}{2} \sum_{q=-L/2}^{L/2} \left\{ G_{31}(a, x_2 - qa, -na - a) + G_{31}(a, x_2 - qa, -na) \right\} + \frac{\lambda + 2\mu}{2} a^2 \sum_{r=1}^{R+1} \sum_{-L/2}^{L/2} \left\{ G_{11}(2a, x_2 - qa, -na - a + ra) - G_{11}(0, x_2 - qa, -na - a + ra) \right\} . \quad (247)$$

After summing on q , Equation (247) becomes

$$u_1(a, -na - \frac{a}{2}) = \frac{va}{8\pi(1-2\nu)(1-\nu)} \left[\frac{n+1}{(n+1)^2 + 1} + \frac{n}{n+1} \right] +$$

$$\begin{aligned}
& + \frac{a}{4\pi(1-2\nu)} \left\{ \left(\sum_{r=1}^n + \sum_{r=1}^{\infty} \right) \left[-\frac{3-4\nu}{4} \ln \frac{r^2+4}{r^2} + \frac{2}{r^2+4} \right] \right. \\
& + \sum_{r=1}^{\infty} \frac{3-4\nu}{2} \left[\frac{1}{\sqrt{r^2+4}} - \frac{1}{r} + \frac{2}{(r^2+4)^{3/2}} \right] + \frac{1}{2} \Bigg\} \\
& - \frac{\lambda+2\mu}{2} \frac{a^2}{C_1}.
\end{aligned} \tag{248}$$

By comparing the values of $u_1(a, -na, -a/2)$ from Equations (217) and (248), C_1 can be computed for each value of n . Several values are listed in Table 13.

TABLE 13. Displacements and Force Constants C_1 at Singular Points for an Edge Dislocation

n	$u_1(-\frac{a}{2} - na)/a$	$C_1 (\nu = 1/3)$
0	- .4100	4.692
1	- .4511	4.688
2	- .4731	4.679
3	- .4833	4.674
4	- .4882	4.672
5	- .4910	4.671
6	- .4928	4.669
7	- .4940	4.669
8	- .4948	4.669
9	- .4954	4.669
∞	- .5000	4.666

The relative displacement across the slip plane can be easily deduced and has the form

$$\Delta u_1(x_1) = u_1(x_1, \frac{a}{2}) - u_1(x_1, -\frac{a}{2}) = -\frac{a}{2} - 2u_1(x_1, -\frac{a}{2}). \tag{249}$$

Recalling Equation (239), Δu_1 has the final form

$$\Delta u_1(x_1) = \frac{a}{16\pi} \frac{3-4\nu}{1-2\nu} \frac{(x_1+a)^2}{(x_1-a)^2} - \frac{a}{4\pi} \frac{\nu}{(1-\nu)(1-2\nu)} \frac{ax_1}{x_1+a} \quad (250)$$

Values of Δu_1 are plotted in Figure 34. Finally, a mapping on the $x_3 = 0$ plane of the atomic arrangement is shown in Figure 35.

A direct comparison with Peierls' model can be attempted, since both models are symmetrical about $x_1 = 0$. From Peierls' model, the relative displacement has the form

$$\Delta u_1(x_1) = \frac{a}{2} - \frac{a}{\pi} \tan^{-1} \frac{x_1}{\xi} \quad (251)$$

where

$$\xi = \frac{a}{2(1-\nu)} \quad (252)$$

We shall expand Equations (249) and (250) in powers of $1/x_1$ and shall select ξ so that both expressions match at large values of x_1 . So first order this gives

$$\Delta u_1(x_1) \approx \frac{a}{4\pi} \frac{3-2\nu}{1-\nu} \frac{a}{x_1} \quad (253)$$

and for the Peierls' model

$$\Delta u_1(x_1) = \frac{a}{\pi} \frac{\xi}{x_1} \quad (254)$$

By matching Equations (252) and (253) Peierls' model is identical to ours for large x_1 , if

$$\xi = \frac{a}{4} \frac{3-2\nu}{1-\nu} \quad (255)$$

In contrast with the screw dislocation, this is not the value found by Peierls. Peierls' expressions for $\xi = a/2(1-\nu)$ and $\xi = (a/4)(3-2\nu)/(1-\nu)$

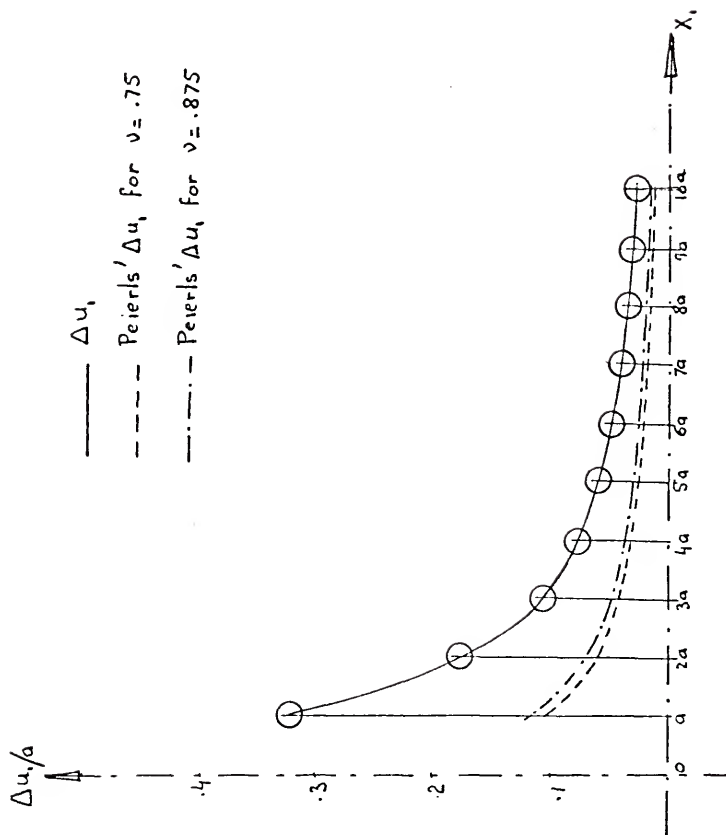


Figure 34. Relative Displacement of an Edge Dislocation

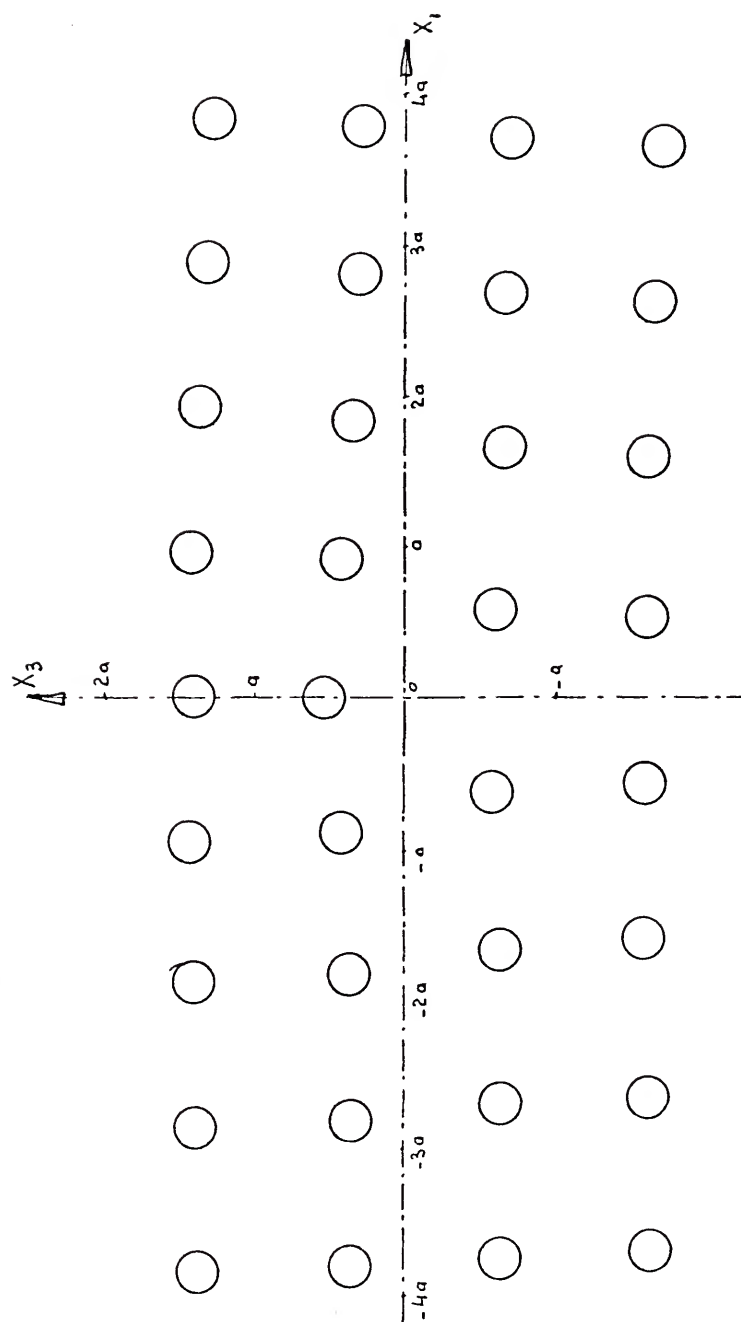


Figure 35. Atomic Arrangement in $x_2 = 0$ Plane of an Edge Dislocation

are plotted in Figure 34. For $\nu = 1/3$, the values of ξ are .75 and .875, respectively. So our model for the edge dislocation is wider than Peierls' model.

It is impossible to say which value is the actual one, since both models are completely different and involve different approximations. As a conclusion we would say that simulating edge dislocation by an array of prismatic loops gives a displacement field which exhibits the expected symmetry relative to the extra half-plane, in contrast to the result for the shear loops.

Self-Energy of the Edge Dislocation

The energy of the system of point forces is composed as usual of the sum of the self-energies of the point forces less the sum of their pairwise interaction energies. Because of the formidable length of the expression, we shall divide the whole equation into smaller subdivisions.

(a) Energy of the array of G forces:

$$\begin{aligned}
 W_G = & (R+1)(L+1)G^2 \left[\frac{1}{C_1} - G_{11}(2a, 0, 0) \right] \\
 & + 2G^2(R+1) \sum_{q=1}^L (L-1-q) \left[G_{11}(0, qa, 0) - G_{11}(2a, qa, 0) \right] \\
 & + 2G^2(L+1) \sum_{q=1}^R (R+1-q) \left[G_{11}(0, 0, pa) - G_{11}(2a, 0, pa) \right] \\
 & + 4G^2 \sum_{p=1}^R \sum_{q=1}^L (R+1-p)(L+1-q) \left[G_{11}(0, qa, pa) - G_{11}(2a, qa, pa) \right] .
 \end{aligned}
 \tag{256}$$

(b) Energy of the array of F forces:

$$\begin{aligned}
 W_F = & \frac{2F^2(L+1)}{C_3} + 2F^2(L+1) G_{33}(0,0,a) + 2F^2 \sum_{q=1}^L (L+1-q) \left[2G_{33}(0,qa,0) \right. \\
 & + 2G_{33}(0,qa,a) - G_{33}(0,qa,Ra) - G_{33}(0,qa,Ra+2a) \\
 & \left. - 2G_{33}(0,qa,Ra+a) \right] - (L+1) \left[2G_{33}(0,0,Ra+a) + G_{33}(0,0,Ra) \right. \\
 & \left. + G_{33}(0,0,Ra+2a) \right] + \frac{2F^2(R+1)}{C_2} + 2F^2(R+1) G_{22}(0,a,0) \\
 & + 2F^2 \sum_{p=1}^R (R+1-p) \left[2G_{22}(0,0,pa) + 2G_{22}(0,a,pa) \right. \\
 & \left. - G_{22}(0,La,pa) - G_{22}(0,La+2a,pa) - 2G_{22}(0,La+a,pa) \right] \\
 & - (R+1) \left[2G_{22}(0,La+a,0) + G_{22}(0,La,0) + G_{22}(0,La+2a,0) \right] \\
 & - 16 \sum_{q=1}^L \sum_{p=1}^R G_{23}(0,qa,pa) - 8 \sum_{p=1}^R G_{23}(0,La+a,pa) \\
 & - 8 \sum_{q=1}^L G_{23}(0,qa,Ra+a) - 4G_{23}(0,La+a,Ra+a); \tag{257}
 \end{aligned}$$

(c) Interaction energy between both arrays:

$$\begin{aligned}
 W_{FG} = & -8 \left[\sum_{p=1}^R (L+1) G_{13}(a,0,pa) + \sum_{q=1}^L (R+1) G_{12}(a,qa,0) \right] \\
 & - 8 \left[\sum_{q=1}^L (L+1-q) G_{13}(a,qa,Ra+a) + \sum_{p=1}^R (R+1-p) G_{12}(a,La+a,pa) \right] \\
 & - 4 \left[(L+1) G_{13}(a,0,Ra+a) + (R+a) G_{12}(a,La+a,0) \right] \\
 & - 16 \left[\sum_{p=1}^R \sum_{q=1}^L (L+1-q) G_{13}(a,qa,pa) \right. \\
 & \left. + \sum_{p=1}^R \sum_{q=1}^L (R+1-p) G_{12}(a,qa,pa) \right]. \tag{258}
 \end{aligned}$$

The total energy of the system of forces is the sum of these three equations. After computation of the various sums and collecting terms containing R and L, the following expression is found for the energy of the whole array of forces.

$$\begin{aligned}
 \frac{W}{\mu a} = & \frac{(R+1)(L+1)}{4\pi} \frac{(1-\nu)^2}{(1-2\nu)^2} \left[4\pi \frac{\mu a}{C_1} + \frac{3.3524 - 8.6586\nu}{1-\nu} \right] \\
 & - \frac{1}{2\pi} \frac{1}{1-\nu} (L+1) \ell\pi \frac{2RL}{L + \sqrt{R^2 + L^2}} - \frac{1}{2\pi} \frac{1}{1-\nu} (R+1) \ell\pi \frac{2RL}{R + \sqrt{R^2 + L^2}} \\
 & + \frac{1}{2\pi} \frac{\nu}{(1-2\nu)^2} \left[(L+1) \frac{R + \sqrt{R^2 + L^2}}{L} + (R+1) \ell\pi \frac{L + \sqrt{R^2 + L^2}}{R} \right] \\
 & + (R+1+L+1) \left\{ - \frac{1}{4\pi} \frac{(1-\nu)^2}{(1-2\nu)^2} \left[\frac{8.0325 - 5.5644\nu}{1-\nu} \right] \right. \\
 & \left. + \frac{1}{2\pi} \frac{\nu^2}{(1-2\nu)^2} \left[\frac{4\pi\mu a}{C_2} - \frac{7.4947 - 9.1180\nu}{1-\nu} \right] + \frac{1}{\pi} \frac{\nu}{(1-2\nu)^2} (2.2148) \right\} \\
 & - \frac{\sqrt{R^2 + L^2}}{\pi(1-\nu)} - \frac{1}{2\pi} \frac{5\nu^2 - 5\nu + 1}{(1-\nu)(1-2\nu)^2} \frac{R+L}{RL} \sqrt{R^2 + L^2} \\
 & + \frac{1}{\pi} \frac{(1-\nu)^2}{(1-2\nu)^2} \left[\frac{.2988 + 5.0463\nu}{1-\nu} \right] + \frac{1}{\pi} \frac{\nu^2}{(1-2\nu)^2} \left[\frac{5.5876 - 7.1780\nu}{1-\nu} \right] \\
 & - \frac{3}{\pi} \frac{\nu}{(1-2\nu)^2} . \tag{259}
 \end{aligned}$$

If the array is extended in the x_2 direction such that L is much larger than R, the system becomes two antiparallel straight edge dislocations separated by a distance Ra. The energy per unit length of this system is the limit of $W/(L+1)a$ when L becomes infinite:

$$\begin{aligned}
\frac{W}{(L+1)a} = & \frac{\mu a^2}{4\pi} \frac{(1-\nu)^2}{(1-2\nu)^2} (R+1) \left[\frac{4\pi\mu a}{C_1} + \frac{3.3524 - 8.6586\nu}{1-\nu} \right] \\
& - \frac{\mu a^2}{2\pi} \frac{1}{1-\nu} \ln R + \left\{ - \frac{\mu a^2}{4\pi} \frac{(1-\nu)^2}{(1-2\nu)^2} \frac{8.0325 - 5.5644\nu}{1-\nu} \right. \\
& + \frac{\mu a^2}{2\pi} \frac{\nu^2}{(1-2\nu)^2} \left[\frac{4\pi\mu a}{C_3} - \frac{7.4947 - 9.1180\nu}{1-\nu} \right] + \frac{\mu a^2}{\pi} \frac{\nu}{(1-2\nu)^2} (2.2148) \\
& \left. - \frac{\mu a^2}{\pi} \frac{1}{1-\nu} \right\}. \quad (260)
\end{aligned}$$

In the special case of $\nu = 1/3$, we have

$$\begin{aligned}
\frac{W}{(L+1)a} = & \frac{\mu a^2}{\pi} (R+1) \left[\frac{4\pi\mu a}{C_1} + .6993 \right] - \frac{\mu a^2}{2\pi} \frac{1}{1-\nu} \ln R \\
& + \frac{\mu a^2}{2\pi} \left[\frac{4\pi\mu a}{C_3} - 14.9274 \right]. \quad (261)
\end{aligned}$$

Both force constants C_1 and C_3 are unknown unless C_1 is taken to be the value found from the displacement field computations. However, C_3 will still remain unknown, and the same difficulty as was encountered in the simulation from shear loops is encountered here.

Furthermore, Equation (260) does not have the well-known form of the energy of such a system. This is due to the excess strain energy stored between the planes $x_1 = \pm a/2$ after deformation. All the material contained between the planes $x_1 = \pm a$ before the introduction of the defect is compressed into a slab less twice the original width. Unfortunately, it has not been possible to propose a displacement field in this region which would permit one to obtain the correction energy for this system. The problem is much less simple than for the simulation from shear loops. So further research has to be done in this direction.

CHAPTER 7

CONCLUSIONS

The new approach presented here has given us very satisfying results for the computations of the small range displacement field and the self-energy of the various dislocations, especially for the case of the screw dislocation where a complete treatment could be done. For the long range displacement field, this model is in agreement with ordinary continuum model in all cases. When compared to Peierls' model, the screw dislocation has a narrower width in our model, although the edge dislocation has a broader width.

The arrangement of atoms in the vicinity of the dislocation line is obtained for most of the cases and at distances closer to the dislocation line than the ordinary continuum model permits. It has not been possible to compare the atomic displacements with atomistic computations, since simple cubic structure is hypothetical. Its study, however, will be the guide of studies on real crystals.

At this time, there are two principal difficulties in applying this model: (a) the evaluation of the force constant corresponding to the forces normal to the slip plane, and (b) the computation of the excess strain energy between the planes of forces. One way to solve these problems would be to compare with computer simulation models.

Unfortunately, this can only be done on real crystal structures. So the next step for pursuing this study would be a direct application of the method employed here to reach the properties of dislocation and kinks in face centered cubic crystal, body centered cubic crystals or hexagonal compact crystals.

BIBLIOGRAPHY

1. J. D. Eshelby, Solid State Physics, 3, 79 (1956).
2. E. Kröner, "Kontinuumstheorie der Versetzungen und Eigenspannungen," Ergeb. der Angew. Math., 5, Springer-Verlag, Berlin (1958).
3. R. de Wit, Solid State Physics, 10, 249 (1960).
4. H. B. Huntington, J. E. Dickey, and R. Thompson, Phys. Rev., 100, 1117 (1955).
5. T. Kurosawa, J. Phys. Soc. Japan, 19, 2096 (1904).
6. F. Granzer, G. Wagner, and J. Eisenblätter, Phys. Status. Solidi, 30, 587 (1968).
7. R. M. J. Cotterill and M. Doyama, Phys. Rev., 145, 465 (1966).
8. M. Doyama and R. M. J. Cotterill, Phys. Rev., 150, 448 (1966).
9. R. Chang and L. T. Graham, Phys. Status. Solidi, 18, 99 (1966).
10. R. Chang, Phil. Mag., 16, 1021 (1967).
11. R. Bullough and R. C. Perrin, Atomic Energy Research Establishment, Harwell Report No. T-P-292, 1967 (unpublished).
12. R. Bullough and R. C. Perrin, in Dislocation Dynamics, edited by A. R. Rosenfield, G. T. Hahn, A. L. Bement, and R. I. Jaffee, McGraw-Hill, New York (1968).
13. P. C. Gehlen, A. R. Rosenfield, and G. T. Hahn, J. Appl. Phys., 39, 5246 (1968).
14. P. C. Gehlen, J. R. Beeler, and R. I. Jaffee, eds., Interatomic Potentials and Simulation of Lattice Defects, to be published by Plenum, Boston, 1972.
15. C. S. Hartley and R. B. Bullough, "On the Description of Crystal Defects by Point Force Arrays," AERE-TP-490, Harwell, U. K., July, 1972.
16. J. S. Koehler, J. Appl. Phys., 37, 435 (1966).

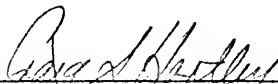
17. P. P. Groves and D. J. Bacon, J. Appl. Phys., 40, 4207 (1969).
18. F. Kroupa, Czech. J. Phys., B 12, 191 (1962).
19. J. B. Scarborough, Numerical Mathematical Analysis, The Johns Hopkins Press, Baltimore (1955).
20. J. P. Hirth and J. Lothe, Theory of Dislocations, McGraw-Hill, New York (1968).
21. R. E. Peierls, Proc. Phys. Soc., 52, 23 (1940).

BIOGRAPHICAL SKETCH

Jean-Pierre Georges was born in Les Lilas, France, on March 29, 1946. He completed his secondary education at the "Lycée Hoche" in Versailles; he passed the Baccalauréat in Mathematics in 1963; he attended the classes of "Mathématiques Supérieures" and "Mathématiques Spéciales" in the same college. He entered the "Ecole Centrale des Arts et Manufactures de la Ville de Paris" in 1966, and received the degree of "Ingénieur des Arts et Manufactures" in July, 1969. From September, 1969, to the present time, he has pursued his studies at the University of Florida. Working as a graduate assistant in the Department of Metallurgical and Materials Engineering, he received the degree of Master of Science in Engineering in December, 1970. Since then, he worked as a graduate assistant in the Department of Engineering Science and Mechanics toward the degree of Doctor of Philosophy.

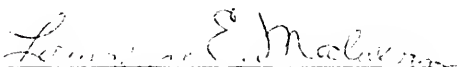
Jean-Pierre Georges is a member of the "Association des Anciens Elèves de l'Ecole Centrale de Paris."

I certify that I have read this study and that in my opinion it conforms to acceptable standards of scholarly presentation and is fully adequate, in scope and quality, as a dissertation for the degree of Doctor of Philosophy.



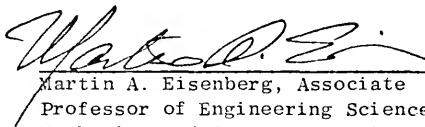
Craig S. Hartley, Chairman
Associate Professor of Engineering
Science, Mechanics and Aerospace
Engineering

I certify that I have read this study and that in my opinion it conforms to acceptable standards of scholarly presentation and is fully adequate, in scope and quality, as a dissertation for the degree of Doctor of Philosophy.



Lawrence E. Malvern, Professor of
Engineering Science, Mechanics and
Aerospace Engineering

I certify that I have read this study and that in my opinion it conforms to acceptable standards of scholarly presentation and is fully adequate, in scope and quality, as a dissertation for the degree of Doctor of Philosophy.



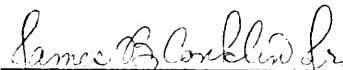
Martin A. Eisenberg, Associate
Professor of Engineering Science,
Mechanics and Aerospace Engineering

I certify that I have read this study and that in my opinion it conforms to acceptable standards of scholarly presentation and is fully adequate, in scope and quality, as a dissertation for the degree of Doctor of Philosophy.



John J. Hren, Professor of
Materials Science and Engineering

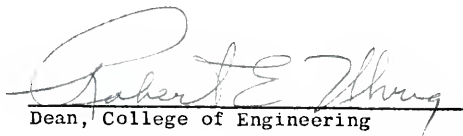
I certify that I have read this study and that in my opinion it conforms to acceptable standards of scholarly presentation and is fully adequate, in scope and quality, as a dissertation for the degree of Doctor of Philosophy.



James B. Conklin, Jr., Associate
Professor of Physics

This dissertation was submitted to the Dean of the College of Engineering and to the Graduate Council, and was accepted as partial fulfillment of the requirements for the degree of Doctor of Philosophy.

December, 1972



Dean, College of Engineering

Dean, Graduate School

